

Establishing tephrostratigraphic frameworks to aid the study of abrupt climatic and glacial transitions: a case study of the Last Glacial-Interglacial Transition in the British Isles (c. 16-8 ka BP)

Article

Accepted Version

Creative Commons: Attribution-Noncommercial-No Derivative Works 4.0

Timms, R. G. O., Matthews, I. P., Lowe, J. J., Palmer, A. P., Weston, D. J., MacLeod, A. and Blockley, S. P. E. (2019) Establishing tephrostratigraphic frameworks to aid the study of abrupt climatic and glacial transitions: a case study of the Last Glacial-Interglacial Transition in the British Isles (c. 16-8 ka BP). *Quaternary Science Reviews*, 192. pp. 34-64. ISSN 0277-3791 doi: <https://doi.org/10.1016/j.earscirev.2019.01.003> Available at <http://centaur.reading.ac.uk/86407/>

It is advisable to refer to the publisher's version if you intend to cite from the work. See [Guidance on citing](#).

To link to this article DOI: <http://dx.doi.org/10.1016/j.earscirev.2019.01.003>

Publisher: Elsevier

All outputs in CentAUR are protected by Intellectual Property Rights law, including copyright law. Copyright and IPR is retained by the creators or other copyright holders. Terms and conditions for use of this material are defined in the [End User Agreement](#).

www.reading.ac.uk/centaur

CentAUR

Central Archive at the University of Reading

Reading's research outputs online

1
2
3
4 1 ***Establishing tephrostratigraphic frameworks to aid the study of abrupt climatic and***
5 2 ***glacial transitions: a case study of the Last Glacial-Interglacial Transition in the***
6 3 ***British Isles (c. 16-8 ka BP)***
7
8 4

9 5 Rhys G.O. Timms^{a*}, Ian P. Matthews^a, J. John. Lowe^a, Adrian P. Palmer^a, Dorothy J.
10 6 Weston^a, Alison MacLeod^b, Simon P.E. Blockley^a
11 7

12 8
13 9 ^aCentre for Quaternary Research, Department of Geography, Royal Holloway University of
14 10 London, Egham, Surrey, UK

15 11 ^bDepartment of Geography and Environmental Science, University of Reading, Reading, UK.
16 12
17 13

18 14
19 15
20 16 *Corresponding author
21 17
22 18

23 19 ***Abstract***
24 20

25 21 Distally dispersed tephra layers have become an important tool in the investigation of
26 22 palaeoenvironmental and archaeological records across the globe. They offer possibilities
27 23 for the synchronisation and improved chronological control in those records to which they
28 24 can be traced and hence contribute to an improved understanding of the pattern and timing
29 25 of environmental and archaeological change during periods of rapid climatic adjustment.
30 26 However, their use as robust isochronous markers for synchronising records is frequently
31 27 compromised by uncertainties relating to stratigraphical context, precise chronology and
32 28 chemical composition. Here we collate and review the tephrostratigraphical information
33 29 dating to the Last Glacial-Interglacial Transition (LGIT; c. 16-8 ka BP) in the British Isles
34 30 based on published and unpublished records obtained from 54 sites. Based on details of
35 31 their stratigraphic position, chronology and chemical composition, we propose that 26
36 32 individual eruption events may be represented in this collective record which spans the
37 33 LGIT. The great majority of these eruptives can be traced in origin to Iceland, but we also
38 34 report on the recent discoveries of ultra-distal tephra from the North American Cascades
39 35 range, including for the first time the Mount St Helens J Tephra at a site in southern Ireland.
40 36 These particular ultra-distal discoveries have resulted from a reinterpretation of older data,
41 37 demonstrating the potential importance of ‘unknown’ analyses in older tephra datasets. The
42 38 outcome of this review is a comprehensive but provisional tephrostratigraphic framework for
43 39 the LGIT in the British Isles, which helps to focus future research on parts of the scheme
44 40 that are in need of further development or testing. The results, therefore, make an important
45 41 contribution to the wider European tephrostratigraphic framework, while adding new
46 42 discoveries of transcontinental isochronous tephra markers.
47 43
48 44
49 45
50 46
51 47
52 48
53 49
54 50
55 51
56 52
57 53
58 54
59 55

60
61
62
63
64
65
66
67
68
69
70
71
72
73
74
75
76
77
78
79
80
81
82
83
84
85
86
87
88
89
90
91
92
93
94
95
96
97
98
99
100
101
102
103
104
105
106
107
108
109
110
111
112
113
114
115
116
117
118

38
39
40
41
42
43
44
45
46
47
48
49
50
51
52
53
54
55
56
57
58
59
60
61
62
63
64
65
66
67
68
69
70
71
72
73
74
75
76
77
78
79
80
81
82
83
84
85
86
87
88
89
90
91
92
93
94
95
96
97
98
99
100
101
102
103
104
105
106
107
108
109
110
111
112
113
114
115
116
117
118

Keywords: Volcanic Ash layers, Cryptotephra, Tephrochronology, Europe, late Pleistocene, Holocene

1. Introduction

In the last three decades the adoption of (crypto-)tephrochronology as a technique for the dating and correlation of Quaternary environmental records has greatly increased (Lowe, 2008, 2011; Davies, 2015; Lane et al., 2017). This heightened interest, particularly in distal environments, reflects a wider appreciation of the unique combination of advantages that volcanic ash layers offer: (i) many have been shown to serve as precise isochrons that provide independent tests of stratigraphic correlations based on other approaches (see Davies et al., 2012; Blockley et al., 2014); (ii) where they can be dated directly, the results provide independent tests of age models based on alternative methods (e.g. Bourne et al., 2015a; Matthews et al., 2015); and (iii) where there is accordance between tephra-based and independently-derived age models, integration of the collective results leads to better-resolved chronologies (e.g. Blockley et al., 2008; Matthews et al., 2011; Lowe et al., 2013).

For the above applications to yield reliable results, however, secure chemical identification and robust dating of individual tephra layers are of paramount importance, but achieving these aims is frequently confounded by a number of practical obstructions. These include the difficulty of differentiating individual tephra layers that originate from volcanic sources with near-identical chemical signatures (e.g. Bourne et al., 2010; Bourne et al. 2015b; Lowe, D. et al., 2017), problems with distinguishing primary fall deposits from secondary reworked material (e.g. Guðmundsdóttir et al., 2011; Lowe, 2011; Griggs et al., 2015; Wulf et al., 2018), and the need for more robust universal standardisation procedures for the chemical fingerprinting of volcanic material (Pearce et al., 2014; Tomlinson et al., 2015; Lowe, D. et al., 2017). In an effort to overcome, or at least minimise, the effects of these complications, tephrochronologists are progressively developing regional schemes that integrate the stratigraphic, chemical and chronological information for all individual tephra layers within specified time intervals. These regionally focused initiatives aim to identify those tephra layers that best serve as reliable isochrons and the geographical ranges (or ‘footprints’) over which they can be traced; collectively these constitute a tephrochronological framework or ‘lattice’ (Lowe et al., 2015). Examples of Late Quaternary regional frameworks that are under construction include those for Europe and the Mediterranean (Blockley et al., 2014; Bronk Ramsey et al., 2015; Wulf et al., 2018), Greenland (Abbott and Davies, 2012; Bourne et al., 2015b), the North Atlantic Ocean (Davies et al., 2014; Abbott et al., 2018), North America

119
120
121 75 (Davies et al., 2016; Mackay et al., 2016; Pyne-O'Donnell et al., 2016), the Kamchatsky
122
123 76 Peninsula (Ponomareva et al., 2017), Japan and East Asia (Moriwakia et al., 2016; McLean
124
125 77 et al., 2018), southern Patagonia (Wastegård et al., 2013; Fontijn et al., 2016), East Africa
126
127 78 (Blegen et al., 2015; Lane et al., 2018), New Zealand (Lowe, D. et al., 2008) and East
128
129 80 Antarctica (Narcisi et al., 2010). Ultimately it may prove possible to link these regional
130
131 81 frameworks using common 'ultra-distal' tephra isochrons which, if successful, would provide
132
133 82 important markers for establishing or testing the alignment of palaeoenvironmental and
134
135 83 archaeological records at the continental and perhaps even global scale (Lane et al., 2017;
136
137 84 Plunkett and Pilcher, 2018).

136 85 In Europe tephra isochrons have proved especially valuable for highlighting the time-
137
138 86 transgressive nature of past environmental changes during the Last Termination and early
139
140 87 Holocene (also referred to as the Last Glacial-Interglacial Transition (LGIT), c. 16-8 ka BP),
141
142 88 particularly when associated with records that can be resolved at sub-centennial timescales
143
144 90 (e.g. Lane et al., 2013; Wulf et al., 2013; Rach et al., 2014). The framework for this region
145
146 91 currently includes approximately 60 different tephra layers, sourced primarily from Icelandic,
147
148 92 Eifel (Germany) and Italian volcanic sources (Figure 1), with overlapping envelopes
149
150 93 extending from Greenland (recorded in ice cores) to southern and eastern Europe (Davies et
151
152 94 al., 2002; Blockley et al., 2014; Bronk Ramsey et al., 2015; Lowe et al., 2015). Collectively,
153
154 95 they provide the potential for assessing environmental shifts across Europe over a refined
155
156 96 timescale and with a greater precision than has previously been attainable. However, the
157
158 97 majority of these tephra 'linkages' are based on the detection and analysis of glass shards
159
160 98 forming cryptotephra deposits, which can prove particularly challenging with respect to their
161
162 99 chemical analysis, precise dating and stratigraphic integrity.

158 100 Here, we evaluate the extent to which the aforementioned problems impact on the LGIT
159
160 101 tephrostratigraphic record of the British Isles, which afford a suitable case study for this
161
162 102 avenue of research for the following reasons: (i) the region is one of the most intensively
163
164 103 studied for cryptotephra deposition anywhere in the world; (ii) a large number of cryptotephra
165
166 104 layers have been traced across different depositional contexts (palaeoenvironmental and
167
168 105 archaeological) over the course of the last 30 years; (iii) many of the sites have been
169
170 106 forensically examined for cryptotephra content either through the analysis of multiple
171
172 107 sequences at a single site, or by the high-resolution contiguous sampling of an individual
173
174 108 record; (iv) the tephrostratigraphical sequences can be compared within a well-established
175
176 109 bio- and lithostratigraphical framework that spans the LGIT (see Walker and Lowe, 2017);
177
178 110 and (v) the British Isles are well positioned with respect to the dominant wind systems that

178
179
180
181
182
183
184
185
186
187
188
189
190
191
192
193
194
195
196
197
198
199
200
201
202
203
204
205
206
207
208
209
210
211
212
213
214
215
216
217
218
219
220
221
222
223
224
225
226
227
228
229
230
231
232
233
234
235
236

111 transport distal ash from volcanic centres in the Northern Hemisphere, as a number of sites
112 register multiple ashfall events within the comparatively short interval of the LGIT.

113
114 The main aim of this paper, therefore, is to provide a critical overview of the current potential
115 for building a robust tephrostratigraphical framework for the British Isles spanning the LGIT.
116 In the sections which follow we focus on (i) those tephra layers that can confidently be
117 assigned to the same eruption events and hence represent isochronous stratigraphic
118 markers; (ii) examples of proposed tephra correlations for which the evidence is presently
119 less certain, with proposals for more stringent tests of their credibility; and (iii) general
120 recommendations for advancing the construction of tephrostratigraphical frameworks in
121 distal and ultra-distal locations, where the available evidence consists entirely or
122 predominantly of cryptotephra deposits.

123
124 **2. Background: distal tephras detected in the British Isles**

125
126 The development of tephrochronology in Northern Europe can be traced to the seminal
127 works of (*inter alia*) Þórarinsson (1944), Noe-Nygaard (1951) and Persson (1966), who first
128 demonstrated the potential of Icelandic tephras to serve as isochronous markers in
129 Scandinavia. However, it wasn't until the late 1980s and early 1990s, following
130 methodological advances facilitating the routine identification and chemical characterisation
131 of invisible micro- or cryptotephra horizons, that the potential for (crypto-)tephrochronology in
132 distal locations was fully realised. In the British Isles, this potential was first demonstrated for
133 sites in mainland Scotland by Dugmore (1989), Blackford et al. (1992), Dugmore and
134 Newton (1992), extended to the Orkney and Shetland Isles by Bunting (1994) and Bennett et
135 al. (1992) and to Northern Ireland by Pilcher and Hall (1992). All of those studies were
136 focused on the investigation of Holocene sediments, from which the tephras could be
137 detected by combusting or dissolving the organic-rich or carbonate-rich substrate and
138 analysing the latent residues (cf. Gehrels et al., 2008). This procedure was not suitable,
139 however, for the processing of pre-Holocene sediments, because of their comparatively high
140 minerogenic content. It was therefore not until the application and further development of a
141 density-controlled sediment flotation procedure that the detection of cryptotephra layers in
142 Lateglacial sequences was made possible (Eden et al., 1992; Lowe and Turney, 1997;
143 Turney, 1998a; Blockley et al., 2005). The success of this relatively straightforward and
144 inexpensive laboratory method led to a rapid proliferation of the number of scientists
145 engaged in cryptotephra research, significantly increasing the number of tephras identified
146 across the British Isles and Europe, whilst simultaneously revising the eruptive history and

237
238
239
240
241
242
243
244
245
246
247
248
249
250
251
252
253
254
255
256
257
258
259
260
261
262
263
264
265
266
267
268
269
270
271
272
273
274
275
276
277
278
279
280
281
282
283
284
285
286
287
288
289
290
291
292
293
294
295

147 dispersal range of many volcanic centres at the global scale (e.g. Swindles et al., 2011; Lane
148 et al., 2017; Pilcher and Plunkett, 2018).

149
150 In the British Isles, the Quaternary tephrostratigraphic record is largely confined to the period
151 post-19 ka, because much of the region was still covered by the Late Devensian (last) ice
152 sheet until that time, while the ice did not retreat from Scotland and northern Ireland (where
153 most of the cryptotephra discoveries have been made) until after c. 16 ka (Clark et al., 2012;
154 Hughes et al., 2016). A brief and spatially-restricted resurgence of glaciers, locally termed
155 the Loch Lomond Readvance and dating approximately to the Younger Dryas cold phase,
156 occurred between c. 12.9 and 11.7 ka, which was followed by rapid and complete
157 deglaciation of the British Isles during the early Holocene (Ballantyne 2010, 2012; Walker
158 and Lowe, 2017; Bickerdike et al., 2018). The receding ice from these glacial episodes
159 uncovered large lake basins and many small kettle depressions that formed within
160 abandoned glacial deposits; these have subsequently infilled with lake sediments over
161 millennia, serving as archives for the accumulation of volcanic ash, whether delivered
162 directly by fallout from ash clouds, or washed in from surrounding catchment slopes.

163
164 At the time of writing, tephrostratigraphic investigations have been conducted on sediments
165 dating to the LGIT in 54 individual lake basins in the British Isles (e.g. Bennett et al., 1992;
166 Bunting, 1994; Lowe and Turney, 1997; Wastegård et al., 2000; Davies et al., 2001;
167 Bondevik et al., 2005; Ranner et al., 2005; Turney et al., 2006; Pyne-O'Donnell, 2007;
168 MacLeod 2008; Matthews et al., 2011; MacLeod et al., 2015; Jones et al., 2017; Kelly et al.,
169 2017; Timms et al., 2017, 2018; Housely et al., 2018; Figure 2) and it is this evidence that is
170 reviewed in this paper. The majority of the individual tephra layers have been traced in origin
171 to volcanic centres in Iceland, which reflects the position of the British Isles with respect to
172 the dominant cyclonic circulation in the North Atlantic, and the westerly storm tracks that it
173 promotes. Ejection of ash clouds into these systems means that the British Isles not only lay
174 within the likely dispersal envelope of a large proportion of eruptions derived from the
175 Icelandic province, but are also well within the dispersal envelope of 'ultra-distal' ashes
176 derived from volcanic centres across the Northern Hemisphere (Jensen et al., 2014; Plunkett
177 and Pilcher, 2018). Whilst the occurrence of ultra-distal ashes has been documented for
178 Holocene sequences across Europe (e.g. Van der Bilt et al., 2017; Watson et al., 2017;
179 Plunkett and Pilcher, 2018), the occurrence of ultra-distal ashes in records spanning the
180 LGIT are a more recent discovery and hence are less well researched, but nevertheless
181 promise exciting opportunities in the development of trans-continental tephra frameworks
182 (Pyne-O'Donnell and Jensen, 2018).

183

296
297
298
299
300
301
302
303
304
305
306
307
308
309
310
311
312
313
314
315
316
317
318
319
320
321
322
323
324
325
326
327
328
329
330
331
332
333
334
335
336
337
338
339
340
341
342
343
344
345
346
347
348
349
350
351
352
353
354

184 **3. Tephrostratigraphy of the British Isles, 16-8 ka BP**

185

186 **3.1. The nature of the tephra record**

187 The primary data that underpin tephrostratigraphic frameworks are robust chemical
188 signatures of the glass, crystal, pumice and lithic phases of an eruption, combined with
189 precise stratigraphic superposition, supported where possible, by independent dating of
190 individual tephra layers. In volcanically distal environments such as the British Isles,
191 however, the precise characterisation and correlation of tephra horizons presents a
192 significant technical challenge. The absence of crystal, pumice and lithic phases, owing to
193 the unfavourable transport of these components over longer distances, means that greater
194 emphasis is placed on the far travelled glass shard component. However, low glass shard
195 concentrations and small shard sizes in the distal environment hinder the application of
196 standard lithological methods, e.g. measures of physical properties such as grain-size,
197 colour, bed thickness etc., which are usually only feasible if the ash layer remains visible.
198 With few exceptions, tephra detected in the British Isles are ‘crypto’ in nature, which means
199 that the glass shards must first be extracted from their host sediments before
200 characterisation and correlation procedures can be adopted (see Lowe and Hunt, 2001).
201 Inevitably, because the data contributing to the British tephrostratigraphic framework have
202 been accrued over a period of approximately 25 years (see references in Supplementary
203 Table S1), sampling and analytical procedures have evolved and hence are not (at least in
204 raw format) fully standardised. Consequently, data comparisons should take into
205 consideration the following potential inconsistencies and limitations. Firstly, laboratory
206 procedures for cryptotephra (glass shard) extraction and separation have been progressively
207 refined. Early studies relied on destructive chemical procedures to eliminate non-tephra
208 particulate matter, but these were later shown to distort the chemical signatures of certain
209 compositions of tephra (Pollard et al., 2003; Blockley et al., 2005); as a result, the density
210 separation procedure of Turney (1998a) was modified to eliminate the need for chemical
211 digestion. Secondly, sieve sizes of a greater aperture range are now employed as routine,
212 usually 15-125 µm compared with the older and more restricted 25-80 µm range; this
213 change has assisted in the detection of shards that may have previously been missed (e.g.
214 Timms et al., 2017; 2018; Kearney et al., 2018). Thirdly, improvements to the spatial
215 resolution of characterisation techniques such as Electron Probe Microanalysis (EPMA) has
216 help facilitate the characterisation of smaller glass shards (Hayward, 2012). Fourthly,
217 although it is now common practice to sample sediment sequences contiguously, this has
218 not always been the case, for some studies have deliberately targeted specific stratigraphic
219 intervals in an effort to trace selected tephra layers (e.g. Roberts, 1997; Wastegard et al.,
220 2000; Pyne-O’Donnell et al., 2008; Bramham-Law et al., 2013). In these cases and

355
356
357
358
359
360
361
362
363
364
365
366
367
368
369
370
371
372
373
374
375
376
377
378
379
380
381
382
383
384
385
386
387
388
389
390
391
392
393
394
395
396
397
398
399
400
401
402
403
404
405
406
407
408
409
410
411
412
413

221 particularly in older studies employing ‘less-refined’ methods, absence of evidence is not
222 necessarily evidence of absence and hence the succession of cryptotephra layers in some
223 studies could be incomplete. Fifthly, most cryptotephra studies are based on one or a few
224 core sequences taken from the deepest part of a lake basin, where it is assumed that the
225 most complete sequence is to be found. So far as tephra layers are concerned, however,
226 this may not be the case, for comprehensive basin-wide studies have shown that not all
227 cryptotephra layers are evenly distributed and concentrated in the same part of a basin, possibly
228 due to variations in lake level and/or point of sediment focussing, or other taphonomic
229 complications (e.g. Boyle, 1999; Pyne-O’Donnell, 2011; Bertrand et al., 2014). Hence it
230 cannot be assumed that single-core studies have captured the full tephrostratigraphic
231 sequence that is preserved in a lake basin infill. Finally, studies in the British Isles and NW
232 Europe have historically relied on the analysis of major and minor elements for the
233 fingerprinting of glass shards from cryptotephra layers. There is now, however, an increasing
234 realisation of the potential of trace and rare earth element analyses, particularly in
235 circumstances when major and minor element ratios prove equivocal (Tomlinson et al.,
236 2015; Lowe, D. et al., 2017). In the British Isles and NW Europe, initial applications are
237 yielding results of varying success (e.g. Lane et al., 2012a; Lind et al., 2016; Cook et al.,
238 2018a), but may return dividends if more widely adopted.

239
240 In the following section we review the evidence for the tephrostratigraphy of the British Isles
241 for the period c. 16-8 ka BP, taking into account the difficulties summarised above. Sediment
242 records from the British Isles that span this interval often show a clear demarcation of
243 lithostratigraphic units that date to the Dimlington Stadial (DS), Windermere Interstadial (WI),
244 Loch Lomond Stadial (LLS) and early Holocene (Figure 3), a structure which is similarly
245 expressed in the bio-stratigraphic record (see Walker and Lowe, 2017). This pattern can also
246 be observed in climate records spanning the same interval in Europe and Greenland,
247 however, caution must be exercised in declaring synchronicity between these regions, as it
248 remains to be established whether these changes were genuinely time-parallel or offset
249 temporally (Björck et al., 1998; Walker et al., 1999; Walker and Lowe, 2017). With this in
250 mind, the DS can be roughly equated with the Late Weichselian/Late Wisconsinan or
251 Greenland Stadial 2 (GS-2), the WI corresponds to the Bölling-Alleröd period, or Greenland
252 Interstadial 1 (GI-1), and the LLS equates approximately with the Younger Dryas or GS-1
253 cold episode (Björck et al., 1998; Walker et al., 1999; Rasmussen et al., 2006). The
254 individual tephra layers detected in each of these stratigraphic intervals are presented in
255 chronological order in Table 1 and discussed in the same order below, together with
256 summaries of their key diagnostic data and any significant uncertainties that impact their
257 potential use as isochrons. Collectively these tephra are distributed across the 54 individual

414
415
416 258 sites located in Figure 2. A more detailed schematic which includes additional site
417
418 259 information is presented in Supplementary Figure S1, while Supplementary Table S1
419 260 provides a comprehensive overview of the sites investigated for glass-shard content, the
420 261 sampling strategies that were adopted and any caveats concerning their stratigraphic
422 262 context and use as isochronous markers.
423
424 263

425 264 *3.2 Tephra records of Dimlington Stadial (DS) age*

426 265 In the basal sediments of three basins in the Summer Isles, which lie off the NW coast of
427
428 266 Scotland and two sites on Orkney (Figure 1; 2; Supplementary Figure S1), cryptotephra
429 267 shards have been detected that date to the later part of the DS (Weston, 2012; Valentine,
430 268 2015; Timms, 2016; Timms et al., 2018). Although none of the layers has been dated
432 269 directly, their ages can be bracketed on the following grounds. First, they all lie within clastic
434 270 sediments that pre-date the deposition of WI organic-rich sediments, and although the age of
435 271 the base of these deposits is uncertain, they must pre-date c. 14.1 ka BP, the age of the
437 272 Borrobol Tephra, which is consistently found at the base of the organic sediments that
438 273 overlies them (see section 3.3.1). A maximum age for the basal tephras in the Summer Isles
439 274 sites is c. 16 ka BP, the age estimate for the retreat of the last ice sheet from this vicinity,
441 275 while deglaciation on Orkney may have been slightly earlier, by c. 17.0-16.5 ka BP (Phillips
442 276 et al., 2008; Ballantyne et al., 2009; Hughes et al., 2016; Ballantyne and Small, 2018).
444 277

445 278 At Tanera Mòr 2 in the Summer Isles (Figure 1), the tephra that pre-dates the WI has a sub-
446 279 alkaline rhyolitic glass signature similar to that of tephras produced by the Katla volcano in
448 280 Iceland. The Dimna Ash, discovered previously at a single site in Norway, also has this
450 281 chemical signature and has been dated to 15.1 ± 0.6 cal. ka BP (Koren et al., 2008). Given
451 282 the age constraints for the Tanera Mòr 2 basin outlined above, we tentatively correlated this
453 283 ash layer (TM2 504) with the Dimna Ash (Figure 4; Table 1). Glass shards with a similar
454 284 Katla-type chemistry and morphology have also been detected in the basal deposits of two
455 285 other Summer Isles sequences, at Tanera Mòr 1 (Timms, 2016) and at a site on the
457 286 neighbouring Priest Island (Valentine, 2015). However, these records are more complex. In
458 287 the Tanera Mòr 1 sequence, two tephra horizons were identified within the basal DS clays
460 288 (TM1 553 and TM1 546; Supplementary Figure S1), both yielding bi-modal glass chemical
462 289 data, one component matching the Dimna Ash, and the second showing a chemical affinity
463 290 to glass of the sub-alkaline Borrobol-type tephras (Figure 4). In the Priest Island record,
464 291 glass shards are spread diffusely through the basal DS clay deposits, but two shard peaks
466 292 were identified. The lowermost (PRI 811) did not yield sufficient glass shards for chemical
467 293 identification, but it is considered to correlate with the Dimna Ash on the basis of shard
469 294 morphology and stratigraphic position (Valentine, 2015; Supplementary Figure S1). An upper

473
474
475
476
477
478
479
480
481
482
483
484
485
486
487
488
489
490
491
492
493
494
495
496
497
498
499
500
501
502
503
504
505
506
507
508
509
510
511
512
513
514
515
516
517
518
519
520
521
522
523
524
525
526
527
528
529
530
531

295 peak, which lies closer to the transition between the DS and the WI (PRI-700), shows shard
296 morphological and chemical affinities with Borrobol-type tephras (Figure 4; Table 1). The
297 presence of a DS age Borrobol-type tephra has also been identified at Quoyloo Meadow on
298 Orkney (QM1 242; Timms, 2016; Supplementary Figure S1). In total, there are three sites in
299 the British Isles that show evidence for a Borrobol-type tephra of DS age and collectively
300 they are named here the ‘Tanera Tephra’ after the island where this tephra is presently most
301 clearly defined.

302
303 Cook et al. (2018a) have recently reported the discovery of glass shards with Borrobol-type
304 chemistry within the Greenland Stadial 2 (GS-2) interval in the Greenland ice-core record,
305 which is broadly equivalent to the DS (Rose, 1985; Walker, 1995; Björck et al. 1998; Figure
306 3), and thus suggestive of a match with records from the Summer Isles, and Quoyloo
307 Meadow. However, analyses from the British records are few in number and glass shards
308 exhibit consistently lower CaO wt % values than those identified in the ice cores, with the
309 former (British) tephras being more akin to the glass chemical signatures obtained from
310 Borrobol-type tephras dating to the WI (Figure 4). The current evidence is therefore
311 equivocal, as to whether a tephrostratigraphic correlation can be drawn between records in
312 the British Isles and the Greenland ice-core records during this interval, but the possibility
313 justifies further exploration of this layer.

314
315 Finally, a single glass shard dating to the Dimlington Stadial has also been recovered from
316 the site of Crudale Meadow on Orkney (CRUM1 676) although, in this instance, the chemical
317 results bear no consistent resemblance to any known Icelandic volcanic source and has
318 tentatively been matched to a source in Kamchatka (Timms et al., 2018). Hence the status of
319 this record and its potential as an isochron remain uncertain.

321 *3.3 Tephra records of Windermere Interstadial (WI) age*

323 *3.3.1 Borrobol-type tephras*

324 The number, climatostratigraphic position, age, source and glass chemical composition of
325 the Borrobol-type tephras have been a focus of research for more than 20 years (Turney et
326 al., 1997; Davies et al., 2004; Pyne-O’Donnell, 2007; Pyne-O’Donnell et al., 2008; Lind et al.,
327 2016; Cook et al., 2018a). Glasses of Borrobol-type tephras are sub-alkaline rhyolites with
328 high potassium values and characteristically low FeO (c. 1.5-1.3 wt %) and CaO (c. 0.7-0.6
329 wt %) totals (Table 1). The exact source of these Borrobol-type tephras has yet to be
330 established, but a growing body of evidence points toward an as yet unknown volcano in
331 Iceland (e.g. Pyne-O’Donnell, 2007; Lind et al., 2016; Cook et al., 2018a; Plunkett and

532
533
534
535
536
537
538
539
540
541
542
543
544
545
546
547
548
549
550
551
552
553
554
555
556
557
558
559
560
561
562
563
564
565
566
567
568
569
570
571
572
573
574
575
576
577
578
579
580
581
582
583
584
585
586
587
588
589
590

332 Pilcher, 2018). Current evidence suggests that there were two, or possibly three, eruption
333 events during the WI that delivered chemically indistinguishable Borrobol-type tephra to the
334 British Isles. In order of their date of discovery and stratigraphic superposition, these are
335 defined as the Borrobol Tephra, first reported from a site in NE Scotland (Lowe and Turney,
336 1997), the Penifiler Tephra, first reported from a site on the Isle of Skye (Pyne-O'Donnell,
337 2007) and the CRUM1 597 Tephra, first reported from, and presently unique to, Crudale
338 Meadow and the adjoining Spretta Meadow site on Orkney (Timms, 2016; Timms et al.,
339 2018; Supplementary Figure S1). Of the three, the Borrobol Tephra is recognised in the
340 largest number of sequences in the British Isles, and in the majority of sites it consistently
341 coincides with the onset of organic deposition that reflects the influence of the warmer
342 temperatures of the WI (Matthews et al., 2011; Cook et al., 2018a). The Penifiler Tephra, on
343 the other hand, appears mostly to coincide with a later short-lived phase of enhanced clastic
344 sediment deposition and reduced summer temperatures, thought to equate with the GI-1d
345 interval (cf. Older Dryas) in the Greenland stratotype sequence (Pyne-O'Donnell, 2007;
346 Matthews et al., 2011; Candy et al., 2016; Figure 3). The CRUM1 597 Tephra, dated to
347 $12,457 \pm 896$ cal. BP (Timms et al., 2018), falls close to the WI-LLS transition, but since it
348 has been detected only on Orkney Mainland, its potential to serve as an isochron has still to
349 be tested, although there is some tentative evidence to suggest that it could be represented
350 in other sequences (Table 2; Supplementary Figure S1).

351
352 These three tephtras are critically positioned with respect to important climatic transitions and
353 hence offer the potential for precise correlation of records that span the LGIT. However, their
354 overlapping glass chemical signature, can at times, make correlations problematic. This
355 difficulty has been exacerbated by inconsistent stratigraphic interpretations and terminology
356 in the literature reporting the British records, as illustrated by successive changes in
357 perspective concerning the WI tephrostratigraphic record in the Borrobol type-site (Figure 5).
358 Initially, Turney et al. (1997) proposed two stratigraphically distinct but chemically
359 indistinguishable WI tephra layers (Figure 5A), the lower considered a primary deposit and
360 named the Borrobol Tephra, but the upper not named because it was considered to be
361 reworked Borrobol material (Turney, 1998b). A reinvestigation of this sequence by Pyne-
362 O'Donnell et al. (2008) confirmed the two peaks near the base of the WI reported by Turney
363 et al. (1997), but additionally traced a third tephra layer at a higher level within the WI
364 sediments (Figure 5B), a sequence in accord with new WI tephra records from sites on the
365 Isle of Skye (Pyne-O'Donnell, 2005). These apparent consistent tephrostratigraphic series
366 were considered to indicate that all three chemically-identical layers represented primary
367 ash-fall events and so the two distinct tephra peaks originally reported by Turney et al.
368 (1997) were re-named the 'Borrobol A' and 'Borrobol B' tephtras, while the new younger peak

591
592
593
594
595
596
597
598
599
600
601
602
603
604
605
606
607
608
609
610
611
612
613
614
615
616
617
618
619
620
621
622
623
624
625
626
627
628
629
630
631
632
633
634
635
636
637
638
639
640
641
642
643
644
645
646
647
648
649

369 was considered the correlative of the Penifiler Tephra, a newly-discovered tephra detected in
370 the Druim Loch sequence on Skye (Figure 5B; Pyne-O'Donnell, 2007). A subsequent
371 reinvestigation of the Borrobol type site by Lind et al. (2016) led to a further revised scheme,
372 in which the upper tephra layer reported by Pyne-O'Donnell et al. (2008) was not
373 recognised, only the two basal layers originally reported by Turney et al. (1997). Lind et al.
374 (2016) opted to assign the 'Borrobol A' layer to the Borrobol Tephra, but the 'Borrobol B'
375 layer to the Penifiler Tephra (Figure 5C). It appears, therefore, that the Borrobol Tephra is
376 stratigraphically consistent, but the designation of a 'Penifiler Tephra' has proved more
377 contentious.

378
379 The above example illustrates the difficulty of resolving tephra layers with near-identical
380 glass chemical signatures which are in close stratigraphical and/or chronological occurrence:
381 it may not always be possible to resolve individual ash layers, which may represent separate
382 ash-fall events, if the rate of sedimentation is too low. But other factors may also obscure
383 matters, including one already alluded to, namely the possibility of secondary reworking of
384 volcanic ash. The stratigraphic inconsistency of tephra layers assigned to the Penifiler
385 Tephra, which often appear to merge with the underlying Borrobol Tephra (e.g. in the
386 Borrobol, Tynaspirit West and Whitrig Bog records; see Supplementary Figure S1), might
387 favour a reworking hypothesis to account for its origin. The Borrobol Tephra was deposited
388 relatively soon after the end of the DS during a phase of active paraglacial readjustment
389 when it is likely that slopes surrounding many newly formed lake basins were still sparsely
390 vegetated, supporting immature, loosely-bound materials at the land surface (Walker, 1984;
391 Ballantyne and Harris, 1994; Ballantyne, 2002). This setting could have promoted the
392 reworking of such materials containing glass shards, especially in high-altitude sites exposed
393 to flushing by melting snow and ice (Davies et al., 2007). Relevant in this context is that
394 layers assigned to the Penifiler Tephra generally coincide, or closely align, with a climatic
395 oscillation at c. 14.0 ka BP (broadly equivalent to GI-1d), a period that witnessed a cooling of
396 mean summer temperatures of c. 2-3°C in Scotland (Brooks and Birks, 2000; Brooks et al.,
397 2012, 2016); this could have provoked a resurgence of periglacial conditions and increased
398 disturbance of surface materials, resulting in continued or renewed reworking of glass
399 shards (cf. Boyle, 1999; Pyne-O'Donnell, 2011; Larsen, 2013).

400
401 On the other hand, reworking of Borrobol Tephra is a less probable explanation for tephra
402 layers assigned to the Penifiler Tephra in the following contexts: i) where there is a clear
403 stratigraphic separation between the Borrobol and Penifiler layers, as is the case of the
404 Abernethy Forest and Muir Park Reservoir profiles (Supplementary Figure S1); ii) where the
405 peak values in shard concentration for the Penifiler Tephra post-date the GI-1d interval, as in

650
651
652
653
654
655
656
657
658
659
660
661
662
663
664
665
666
667
668
669
670
671
672
673
674
675
676
677
678
679
680
681
682
683
684
685
686
687
688
689
690
691
692
693
694
695
696
697
698
699
700
701
702
703
704
705
706
707
708

406 the Pulpit Hill, Loch Ashik and Tanera Mòr 1 profiles; iii) where the basin catchment size is
407 restricted and the earliest sediments to accumulate in the basin post-date the Borrobol
408 Tephra, as is the case in the Druim Loch and Tirnie profiles; iv) where the glass shard
409 concentrations of the Penifiler Tephra are greater than those in the underlying Borrobol
410 Tephra as at Quoyloo Meadow and Muir Park Reservoir (Supplementary Figure S1). It would
411 therefore be premature to dismiss the possibility that at least two eruptive events are
412 represented in the sometimes diffuse Borrobol-type tephra record that is to be found in early
413 WI and GI-1d deposits in the British Isles (Davies et al., 2004).

414
415 On current evidence, therefore, the Borrobol Tephra appears stratigraphically secure and its
416 best estimated age is $14,098 \pm 94$ cal. BP, derived from a Bayesian age model based on
417 radiocarbon dates obtained from the Abernethy Forest sequence (Bronk Ramsey et al.,
418 2015). The Penifiler Tephra is less secure, except in those sites where it can be shown to be
419 stratigraphically distinct from the Borrobol Tephra; the two isochrons may only be resolvable
420 where sedimentation rates have been relatively high during the early WI. In cases where the
421 Penifiler Tephra is considered to be robustly represented, it can be assigned a provisional
422 age of $13,939 \pm 132$ cal. BP. This is considered provisional because (a) it has been derived
423 from an amalgamation of one age estimate based on the Abernethy Forest age model and
424 another based on what is assumed to be the correlative of the Penifiler Tephra in the
425 Hässeldala port sequence in Sweden (Bronk Ramsey et al., 2015); and (b) the layer
426 assigned to the Penifiler in the Abernethy Forest sequence extends over 20 cm, raising
427 doubts about the precision with which the isochron can be stratigraphically defined (Lind et
428 al., 2016). There is also some confusion over the interpretation of the Borrobol-type tephra
429 registered in the Hässeldala port sequence, since it has been ascribed to both the Borrobol
430 Tephra (Davies et al., 2003; Lind et al., 2016) and the Penifiler Tephra (Pyne-O'Donnell et
431 al., 2008; Bronk Ramsey et al., 2015), but the position of the layer near the end of the 'Older
432 Dryas' (GI-1d) interval and its age, as estimated by Davies et al. (2003) and Wohlfarth et al.
433 (2006), would seem to favour the latter. This confusion over a singular Borrobol-type tephra
434 at Hässeldala port also extends to other records across Europe, as it is only from sites in
435 Scotland and the Greenland ice-core records that multiple layers with identical Borrobol-
436 chemical signatures have been reported for the WI (see Lind et al., 2016; Cook et al.,
437 2018a). Elsewhere in Europe only a single Borrobol-type horizon is registered for this
438 interval, leading to some confusion as to which, if any, of the three potential British layers it
439 may be linked to (e.g. Davies et al., 2003; 2004; Pyne-O'Donnell et al., 2008; Koren et al.,
440 2008; Larsen, 2013; Lilja et al., 2013; Lind et al., 2016; Jones et al., 2018).

709
710
711
712
713
714
715
716
717
718
719
720
721
722
723
724
725
726
727
728
729
730
731
732
733
734
735
736
737
738
739
740
741
742
743
744
745
746
747
748
749
750
751
752
753
754
755
756
757
758
759
760
761
762
763
764
765
766
767

442 Stratigraphic and chronological issue with the Penifiler Tephra may be reduced if routine
443 application of magnetic separation procedures were applied to ‘Penifiler’ Intervals. The
444 rationale for this approach stems from the discovery of glass shards with basaltic chemistry
445 alongside the Penifiler Tephra at the site of Loch Ashik, Isle of Skye (Pyne-O’Donnell et al.,
446 2008; Table 1; Supplementary Figure S1). This basaltic component has a major and minor
447 element signature matching glass of the Katla volcanic system, and is indistinguishable from
448 the basaltic glass component of the Vedde Ash (Figure 6). In the NGRIP ice-core record, a
449 tephra of similar stratigraphic position and chemistry has been identified (Mortensen et al.,
450 2005; Figure 6). This tephra is clearly defined at a depth of 1573 m within NGRIP where it is
451 dated to $14,020 \pm 84$ a b2k (before the year 2000; Abbott and Davies, 2012), overlapping
452 with the accepted age of the Penifiler Tephra identified in the British Isles. The robustness of
453 this link and utility of this layer is difficult to assess as, at present, the basaltic component of
454 the Penifiler has only been recognised at Loch Ashik and attempts to trace this layer to other
455 sites has proved unsuccessful (e.g. Timms et al., 2017). It seems unlikely that the basaltic
456 component of the Penifiler Tephra is as widespread as the rhyolitic fraction, but the
457 opportunity this layer presents to reduce the stratigraphic and chronological uncertainties
458 associated with the Penifiler Tephra suggests that it warrants further systematic testing.

460 *3.3.2 Mount St Helens J and Glacier Peak G, B*

461 The site of Finglas River in SW Ireland is a 60 cm exposure of limnic organic muds which
462 date to the latter part of the WI (named the Woodgrange Interstadial in Ireland; Bryant,
463 1974). It was one of the early sites to be examined for cryptotephra using the experimental
464 density separation techniques (Turney 1998a,b). Those investigations revealed a tephra
465 layer toward the base of the sequence (c. 53 cm; Supplementary Figure S1), which, when
466 analysed, yielded four shards of a mixed chemical composition (Supplementary Table S2).
467 Two shards (group A) are defined by relatively low Al_2O_3 (c. 11.84 wt %), FeO (c. 0.95 wt %),
468 CaO (c. 1.12 wt %) values; one shard (shard B) has higher Al_2O_3 (12.82 wt %), FeO (1.15 wt
469 %), CaO (1.34 wt %) totals in comparison (Table 1); and a third shard (shard C) reveals
470 Al_2O_3 (11.82 wt %), FeO (1.44 wt %), CaO (0.75 wt %) totals. At the time of study these
471 shards with multiple compositions could not be correlated with any known tephra, being
472 chemically different from the Vedde Ash and the limited number of Borrobol Tephra analyses
473 available at the time (Turney 1998b; Figure 7). However, a re-examination of these results in
474 the present study has revealed similarities with eruptions of WI equivalent age from Glacier
475 Peak and Mount St Helens, two volcanic centres in the North American Cascades range
476 (Figure 1).

768
769
770
771
772
773
774
775
776
777
778
779
780
781
782
783
784
785
786
787
788
789
790
791
792
793
794
795
796
797
798
799
800
801
802
803
804
805
806
807
808
809
810
811
812
813
814
815
816
817
818
819
820
821
822
823
824
825
826

478 Mount St Helens is known to have erupted several times though the LGIT producing two
479 main tephra units, the older set S (c. 16.0 cal. ka BP) and the younger set J (c. 13.8-12.8 cal.
480 ka BP), with each set consisting of multiple tephra layers from separate eruptions (Clyne et
481 al., 2008; Pyne-O'Donnell et al., 2016). Cumulatively these tephra are referred to as the
482 'Swift Creek' stage, and at present there are no reliable means by which these tephra can
483 be separated chemically (Pyne-O'Donnell et al., 2016). Interstadial-age volcanic activity at
484 Glacier Peak followed that at Mount St Helens and consisted of a series of closely spaced
485 eruptions leading to the formation of at least three tephra sets (Porter, 1978). The most
486 widely dispersed are sets G and B, which have a current best age estimate of 13.71-13.41
487 cal. ka BP (Kuehn et al., 2009). These phases can be distinguished from one another using
488 abundance ratios of CaO and FeO, and can be further differentiated from the Mount St
489 Helens tephra using K₂O (Kuehn et al., 2009; Pyne-O'Donnell et al., 2016; Figure 7).

490
491 At Finglas River, group A shards compositionally match with those of the Glacier Peak set G,
492 the group B shard with those of Mount St Helens, and the group C shard with those of the
493 Borrobol-type series (Figure 7). The presence of both Glacier Peak and Mount St Helens in
494 the same 'single' layer is not unusual—across North America these tephra are frequently
495 reported as a visible tephra couplet (Kuehn et al., 2009), and in cryptotephra investigations
496 in south-eastern Canada these tephra have also been identified within the same mixed
497 horizon (Pyne-O'Donnell et al., 2016). At Finglas River, as in North America, the coeval
498 expression of these tephra can be explained by a low sedimentation rate at the site of
499 deposition and a conflation of these individual isochrons. Presently this is the only confirmed
500 incidence of a Mount St Helens tephra shard being identified in interstadial deposits outside
501 of North America, and only one of two reported occurrences of Glacier Peak shards
502 identified in an ultra-distal setting. The second finding has recently come from western
503 Scotland, where shards of Glacier Peak B and G sets have also been identified alongside
504 shards of the Borrobol-type tephra series, and specifically those correlated to the Penifiler
505 Tephra (Pyne-O'Donnell and Jensen, 2018; Supplementary Table S1; S2). Whether these
506 shards identified in Ireland and Scotland are of sufficient concentration to declare the
507 presence of an isochron is perhaps a contentious matter. Nevertheless the presence of
508 these ultra-distal glass shards at two sites does suggest that given thorough investigation it
509 may be possible to define and constrain these 'tephra' more precisely in the British Isles.

510
511 The interstadial eruptions from Mount St Helens and Glacier Peak are well documented in
512 North America and have become important regional marker horizons for the dating and
513 correlation of palaeoenvironmental and archaeological records (see Kuehn et al., 2009;
514 Pyne-O'Donnell et al., 2016). Their detection in the British Isles over 7000 km from source

827
828
829
830
831
832
833
834
835
836
837
838
839
840
841
842
843
844
845
846
847
848
849
850
851
852
853
854
855
856
857
858
859
860
861
862
863
864
865
866
867
868
869
870
871
872
873
874
875
876
877
878
879
880
881
882
883
884
885

515 raises the exciting potential for inter-continental correlation and synchronisation of records
516 dating to the LGIT. Focus must now be on refining their presence within the known records
517 in Ireland and Scotland, as well as searching for these ultra-distal tephras, and others, in
518 records across the British Isles and NW Europe, especially in sequences that can be
519 examined at a high temporal resolution. This aim, however, may prove difficult given the
520 prominence of other ash layers dating to around the same time and possible 'masking' by
521 recycled tephra shards (e.g. Davies et al., 2007; Timms et al., 2017). Trace amounts of the
522 Mount St Helens and Glacier Peak tephras are likely to be obscured by the similarly-aged
523 Penifiler Tephra in some sites (Pyne-O'Donnell and Jensen, 2018). Such difficulties might,
524 however, be overcome by a more thorough 'forensic' approach in the examination of shard
525 distributions, morphological properties and chemical compositions, with a higher sampling
526 resolution than has been the norm hitherto (e.g. Pyne-O'Donnell, 2011; Timms et al., 2017;
527 McLean et al., 2018; Pyne-O'Donnell and Jensen, 2018).

528

529 3.3.3 *Roddans Port Tephra*

530 Two tephra layers have been reported from sediments of WI age preserved at the site of
531 Roddans Port, an intertidal sequence that is intermittently exposed off the coast of County
532 Down, Northern Ireland (Turney et al., 2006). Labelled Roddans Port A and B, the precise
533 age of these tephra layers is uncertain, but they lie within the middle part of deposits
534 assigned to the WI. While their glass-derived chemical signatures have been suggested as
535 Icelandic in origin (Turney et al., 2006), they do not resemble those of either the Borrobol-
536 type or silicic Katla tephras known to have been deposited through this interval (Figure 8;
537 Table 1; see section 3.4), and Turney et al. (2006) were uncertain as to whether they
538 represent two closely-timed primary ash-fall events or a primary and reworked event. A
539 chemically similar distal volcanic ash has been reported from the site of Vallensgård Mose
540 on Bornholm Island, Denmark (Turney et al., 2006), but it lies within sediments assigned to
541 the Younger Dryas interval. Some similarity can be observed between the Roddans Port B
542 Tephra and the Glacier Peak G Tephra, but this similarity is not consistent across all major
543 and minor elements (Figure 8) and tephrostratigraphic studies across sites in the British Isles
544 have failed to reveal any ash layer with a comparable glass chemical signature. In view of
545 their uncertain origins, ages and geographical footprints, the potential of the Roddans Port
546 tephras to serve as isochrons remains limited.

547

548 3.3.4 *LAS-1*

549 At Loch an t'Suidhe on the Isle of Mull, a tephra layer has been identified at the WI-LLS
550 transition at a depth of 842 cm (Davies, 2003; Supplementary Figure 1). Termed the LAS-1,
551 chemical analysis of glass shards from this layer revealed six shards of a mixed chemical

886
887
888
889
890
891
892
893
894
895
896
897
898
899
900
901
902
903
904
905
906
907
908
909
910
911
912
913
914
915
916
917
918
919
920
921
922
923
924
925
926
927
928
929
930
931
932
933
934
935
936
937
938
939
940
941
942
943
944

552 composition (Supplementary Table S2); two shards (group A) are defined by relatively high
553 FeO (2.17-2.53 wt %) and TiO₂ (0.63-0.89 wt %) totals; two shards (group B) exhibit low
554 FeO values (1.05-1.17 wt %) and similar TiO₂ totals (0.67-0.69 wt %); a single shard (shard
555 C) is characterised by FeO values of (1.37 wt %) and lower TiO₂ (0.14 wt %) totals; and one
556 further shard (shard D) expresses comparatively low FeO (0.47 wt %) totals and
557 comparatively high TiO₂ (0.71 wt %) values. This mixed chemical assemblage and the
558 stratigraphic occurrence of the layer within sediments relating to an unstable landscape and
559 transitioning climate, might suggest a reworked origin, a hypothesis further supported by low
560 analytical totals of c. 93 wt %, which may indicate some degree of post-depositional
561 alteration. Whilst caution must therefore be expressed in interpreting these analyses, the
562 chemical signature of at least two of the groups bears some resemblance to known tephtras
563 of WI age. Group B shows some chemical similarity to eruptives of Mount St Helens,
564 particularly in plots of FeO, CaO and K₂O (Figure 8). However, this overlap is not consistent
565 across all major and minor elements, with TiO₂ in particular exhibiting significantly higher
566 values than those expected from the Cascades range (Figure 8). Shard C shows an affinity
567 with the Borrobol-type tephtras, whereas group A and shard D do not appear to overlap with
568 any rhyolitic tephtra analyses known to occupy this interval (Figure 8). During a
569 reinvestigation of the Loch an t'Suidhe site by Pyne-O'Donnell (2005), multiple cores were
570 investigated and several of these revealed comparable peaks in shard concentration at
571 similar stratigraphic intervals to those of the LAS-1 tephtra layer. However, no glass
572 compositional analyses were undertaken. At present therefore the significance of the LAS-1
573 analyses and the relationship these may have to known tephtras of Interstadial-Stadial age
574 cannot be resolved. However, the possible occurrence of the ultra-distal Mount St Helens J
575 Tephtra should be enough to warrant a re-investigation of the tephrostratigraphic record.

576

577 *3.4 Tephtra records of Loch Lomond Stadial (LLS) age*

578

579 *3.4.1 The Vedde Ash*

580 The Vedde Ash is one of the best documented, securely-dated and widely-distributed
581 volcanic ash layers dating to the LGIT. The source of the ash is generally believed to be
582 from the Katla volcanic system on Iceland (Mangerud et al., 1984; Lacasse et al., 1995;
583 Lane et al., 2012a; Tomlinson et al., 2012; Figure 1) and was first detected as a component
584 of the North Atlantic Ash Zone 1 (e.g. Ruddiman and McIntyre, 1981), and later as a
585 distinctive individual marker horizon by Mangerud et al. (1984) in several lake sequences
586 (including at the locality of Vedde) in the Ålesund area of western Norway. Since then, the
587 Vedde Ash has been detected in sites ranging from as far north as the Greenland ice sheet
588 to Italy and Slovenia in the south (Grönvold et al., 1995; Mortensen et al., 2005; Lane et al.,

945
946
947 589 2011a; Bronk Ramsey et al., 2015). Typically it is the rhyolitic glass fraction which is most far
948
949 590 travelled, however, the Vedde Ash also comprises less well-distributed basaltic glass (Table
950 591 1), and an intermediate dacitic glass component currently restricted to a number of sites in
951
952 592 western Norway (see Lane et al., 2012a).

953 593
954 594 The Vedde Ash has consistently been found in sediments of Younger Dryas age across
955 595 Europe, and was first identified in the British Isles as a cryptotephra by Lowe and Turney
956 596 (1997) in their experimental use of the now widely applied density separation procedure
957 597 (Turney, 1998a; Blockley et al., 2005). At present, glass shards of the Vedde Ash have been
960 598 detected and chemically analysed in a total of 23 sites in the British Isles, while a further six
961
962 599 occurrences have been proposed on stratigraphic grounds (Supplementary Figure S1;
963 600 Supplementary Table S1), making it the most frequently recognised tephra layer in British
964
965 601 LGIT records. It is generally only the rhyolitic end member of the Vedde Ash that is reported
966 602 from sites in the British Isles, which may in part reflect an inherent bias in density separation
967 603 protocols toward the lighter (felsic) fraction (Turney, 1998a). The basaltic component is
969 604 noticeable, however, in two sequences where the Vedde Ash forms a visible layer (Figure 2),
970
971 605 on the Isle of Skye (Davies et al., 2001) and on Orkney Mainland (Timms, 2016), and can
972 606 be detected in cryptotephra layers by the application of magnetic separation techniques
973
974 607 (Mackie et al., 2002; Timms et al., 2017, 2018).

975 608
976 609 The Vedde Ash has been detected in the Greenland ice cores, with an age estimated as
977
978 610 $12,171 \pm 114$ a b2k; Rasmussen et al., 2006), while radiocarbon dates are available from a
979 611 number of terrestrial sites (e.g. Lohne et al., 2014). The most widely employed estimate,
980
981 612 however, is $12,023 \pm 43$ cal. BP, derived using a composite Bayesian age model that
982 613 combines the radiocarbon evidence for the age of the Vedde Ash obtained from several
983
984 614 records (Bronk Ramsey et al., 2015). Thanks to its precise age and extensive distribution,
985 615 the Vedde Ash is a key isochron within the British and European tephrostratigraphic
986
987 616 frameworks, enabling the detection of regional time-transgressive environmental changes
988 617 during the Younger Dryas/LLS interval (e.g. Bakke et al., 2009; Lane et al., 2013;
989
990 618 Muschitiello and Wohlfarth, 2015; Brooks et al., 2016).

991 619
992 620 *3.4.2 The Abernethy Tephra*
993
994 621 A tephra layer that lies close to, or coincides with, the LLS/Holocene boundary has recently
995 622 been proposed, based on evidence from a number of Scottish, Swedish and Norwegian
996
997 623 records; it has been named the Abernethy Tephra, after the site in NE Scotland where it is
998 624 best represented (Matthews et al., 2011; MacLeod et al., 2015). Its dominant glass chemical
999
1000 625 signature suggests it originated from the Katla volcanic system, with a composition similar to

1004
1005
1006 626 that of the Vedde Ash and several other tephra layers dating to the LGIT (Table 1), including
1007
1008 627 the Dimna Ash (Koren et al., 2008), the R1 (Thornalley et al., 2011), the IA2 (Bond et al.,
1009 628 2001), and the Suduroy tephtras (Wastegård, 2002). With the exception of the Vedde Ash,
1010
1011 629 however, confusion of the Abernethy Tephra with these others can be resolved on
1012 630 stratigraphic grounds. The LLS is clearly marked in LGIT sequences in the British Isles by a
1013
1014 631 prominent minerogenic lithological unit (Figure 3); the Suduroy post-dates this unit and the
1015 632 Dimna, R1 and IA2 tephtras all pre-date it. The uncertain issue that remains is whether the
1016
1017 633 Abernethy Tephra represents a primary ash-fall event, or reworked material derived from
1018 634 older tephtras with similar chemical composition.

1019 635
1020
1021 636 The strongest evidence for primary airfall comes from the detection of the Abernethy Tephra
1022 637 in glaciolacustrine varve records from Lochaber, Scotland (MacLeod et al., 2015). In this
1023
1024 638 composite record two tephra horizons were detected, the lower exhibiting morphological
1025 639 properties typical of the Vedde Ash: i.e. platy featureless shards (see Mangerud et al., 1984;
1026
1027 640 Lane et al., 2012a), whilst the upper revealed a silicic Katla signature and was assigned to
1028 641 the Abernethy Tephra (MacLeod et al., 2015). Importantly, these tephra layers are separated
1029
1030 642 by a minimum of c. 300 years with no evidence of shard remobilisation in the intervening
1031 643 sediments. This paucity is despite sedimentological evidence indicating that the local
1032
1033 644 catchment was susceptible to erosion and remobilisation (Palmer et al., 2010). At several
1034 645 other sites in Scotland, a lower peak in shard concentration (the Vedde Ash) and an upper
1035
1036 646 peak (the Abernethy Tephra), are separated by an interval where no shards have been
1037 647 detected (see MacLeod et al., 2015). In these cases, the possibility of reworking of older
1038 648 Katla tephra layers (i.e. the Vedde Ash) into a discrete layer at the Holocene transition also
1039
1040 649 seems unlikely. At Kingshouse 2 on the Rannoch Plateau, sedimentation of the basin began
1041 650 only toward the latter phases of the LLS. This timing precludes reworking as a hypothesis to
1042
1043 651 explain the presence of the Abernethy Tephra because the basin was not in existence during
1044 652 the eruption of the Vedde Ash (Lowe et al., in prep). In these examples it is more likely that
1045
1046 653 the silicic Katla-type tephra identified, and assigned to the Abernethy Tephra, is derived from
1047 654 a separate eruption event dating to the latter stages of the LLS (cf. Younger Dryas). It is
1048
1049 655 worth noting that evidence from Iceland indicates that the Katla volcano erupted several
1050 656 times during the Younger Dryas (Van Vliet-Lanoë et al., 2007). Hence it is reasonable to
1051
1052 657 suggest multiple Katla-derived ash clouds may have crossed the British Isles and NW
1053 658 Europe during this period.

1054 659
1055
1056 660 In some cases, however, interpretation of the Abernethy Tephra as a primary deposition
1057 661 event is less certain. Shard concentrations of the Abernethy Tephra tend to be low, and in
1058
1059 662 the British Isles are always less than in the accompanying Vedde horizon where these

1063
1064
1065 663 tephra are found together (Supplementary Figure S1). In many cases there is also a
1066 664 background of shards spanning the interval between the Vedde and Abernethy tephtras,
1067 665 which suggests recycling of Vedde Ash shards may be responsible for the secondary
1068 666 'Abernethy' peak in these circumstances. Furthermore, the glass chemical signature of the
1069 667 Abernethy Tephra obtained from records in the British Isles, is in many instances, mixed
1070 668 (Table 3; Figure 9). Whilst this heterogeneous chemical signal may represent a coeval
1071 669 eruption of two or more volcanic centres, it may also be further evidence of shard
1072 670 remobilisation. The harsh climatic conditions that prevailed during the LLS are known to
1073 671 have resulted in the reworking of soils, pollen and other biological remains into lake basins
1074 672 (Lowe and Walker, 1986; Lowe and Lowe, 1989), and there is no reason why tephra would
1075 673 be exempt from these processes.
1076 674

1077 675 In view of the evidence presented by MacLeod et al. (2015) from sites where two well-
1078 676 defined and stratigraphically discrete peaks in shard concentrations have been identified, the
1079 677 possibility that the Abernethy Tephra reflects a primary fall event should be retained.
1080 678 However, it is important to be mindful of the impact of enhanced sediment remobilisation
1081 679 processes operating during periods of abrupt climatic change, and the interpretation of
1082 680 tephrostratigraphic records that span these intervals. There is also a need to refine the age
1083 681 of the Abernethy Tephra because the present estimate of $11,462 \pm 122$ cal. BP has a large
1084 682 error range and is based on interpolation of an age model in which investigation of the
1085 683 Abernethy Tephra was not the focus of the dating programme (Matthews et al., 2011; Bronk
1086 684 Ramsey et al., 2015).
1087 685

1088 686 *3.5 Tephra records of early Holocene age*

1089 687 *3.5.1 CRUM1 561 (Crudale Tephra)*

1090 688 In recent tephrostratigraphical investigations at Crudale Meadow, Timms et al. (2018)
1091 689 identified tentative evidence for an eruption of Tindfjallajökull, a volcano that lies within the
1092 690 Icelandic Eastern Volcanic Zone (Figure 1). Only a few analyses were obtained (Table 1),
1093 691 and these were from shards spread over a 26 cm interval spanning the LLS-early Holocene,
1094 692 and which were mixed with shards of a silicic Katla signature. Shards are defined by FeO
1095 693 values of (c. 2.55 wt %), and relatively low CaO (c. 0.38 wt %) and high K₂O (c. 4.09 wt %)
1096 694 totals. Timms et al. (2018) commented upon the similarity of the CRUM1 561 analyses with
1097 695 those of the Torfajökull volcano, but the overall glass chemical signature presented a
1098 696 stronger correlation to the Tindfjallajökull centre. This correlation was based principally on
1099 697 published glass and pumice data of the Thórsmörk Ignimbrite eruption believed to have
1100 698 originated from Tindfjallajökull c. 57,300 cal. BP (Jørgensen, 1980; Tomlinson et al., 2010).
1101 699

1122
1123
1124 700 However, new field survey and petrological data from Moles et al. (2018) and Moles et al. (in
1125 701 review) would suggest that this correlation requires revision and that the Thórs mörk
1126 702 Ignimbrite eruption instead originated from the Torfajökull complex.
1127
1128
1129 703

1130 704 In a re-examination of existing chemical data for this study, shards of a similar chemical
1131 705 composition to those of the CRUM1 561 analyses were identified amongst data correlated to
1132 706 the Vedde Ash at Tynaspirit West (Figure 10; Roberts, 1997). Accepting the proposal of
1133 707 Moles et al. (2018, in review), the tephra evidence from Crudale Meadow and Tynaspirit
1134 708 West would suggest that an eruption of Torfajökull occurred during the Pleistocene-
1135 709 Holocene transition and that it was large enough, or atmospheric conditions were suitably
1136 710 favourable, to disperse tephra over the British Isles. Presently, because of poor
1137 711 stratigraphical control, a precise age estimate for the Torfajökull-type tephra identified at
1138 712 Crudale Meadow and Tynaspirit West cannot be given, only that one or more eruptions
1139 713 occurred between c. 12,111 and 11,174 cal. BP (Timms et al., 2018). As tephra of this
1140 714 chemical composition can now be tentatively identified at two sites, we propose 'Crudale
1141 715 Tephra' as a formal name to refer to shards exhibiting this chemical signature, and which are
1142 716 positioned within the Pleistocene-Holocene transition.
1143
1144
1145
1146
1147
1148
1149 717

1150 718 Interestingly glass analyses of the Crudale Tephra bear a stronger chemical resemblance to
1151 719 the older Torfajökull rhyolites than those which erupted later in the Holocene (Figure 10).
1152 720 McGarvie et al. (1990) noted there are several temporal trends in the postglacial rhyolites
1153 721 originating from the Torfajökull complex (whole rock analyses), most notably a depletion in
1154 722 SiO₂ and an enrichment in TiO₂, Al₂O₃, MgO and CaO wt %. Accepting the limitations of
1155 723 comparing glass and whole-rock data, these trends potentially could explain some of the
1156 724 chemical differences observed in Figure 10 between the older Crudale Tephra and the
1157 725 younger Ashik, An Druim-Høv darhagi and LAN1-325 tephtras which are also thought to
1158 726 originate from the Torfajökull complex (Pyne-O'Donnell, 2007; Ranner et al., 2005; Lind and
1159 727 Wastegård, 2011; Matthews, 2008). Further work is needed to establish whether the Crudale
1160 728 Tephra extends to other sites in the British Isles and whether glass analyses for this tephra
1161 729 may offer a more chemically distinctive marker for the LLS-Holocene transition than those for
1162 730 the Abernethy Tephra.
1163
1164
1165
1166
1167
1168
1169
1170 731

1171 732 3.5.2 The Hässeldalen Tephra

1172 733 The Hässeldalen Tephra has become one of the most important early-Holocene tephra
1173 734 horizons for palaeoclimate records in NW Europe. First identified in southern Sweden
1174 735 (Davies et al., 2003), this rhyolitic tephra has been repeatedly found in close association with
1175 736 proxy responses to the onset of the Pre-Boreal Oscillation (PBO; Wohlfarth et al., 2006; Ott
1176
1177
1178
1179
1180

1181
1182
1183 737 et al., 2016). Several Icelandic sources have been proposed for the Hässeldalen Tephra
1184 738 including Snæfellsjökull in western Iceland (Davies et al., 2003; Figure 1). However, recent
1185 739 work by Wastegård et al. (2018) shows that glass shards of tephtras originating from this
1186 740 centre have distinctively high Al_2O_3 values (c. 15-16 wt %), which the Hässeldalen Tephra
1187 741 does not exhibit (Table 1). An alternative source proposed by Wastegård et al. (2018) is the
1188 742 Thórdarhryna volcano located under the Vatnajökull ice-cap (Figure 1); however, at present
1189 743 this correlation is based on whole-rock analyses, and an investigation of the vitreous phase
1190 744 of Thórdarhryna will be necessary to further test this hypothesis.
1191 745

1192 746 Extensive radiocarbon dating at the type-site, Hässeldala port, has generated an age
1193 747 estimate of $11,387 \pm 270$ cal. BP (Ott et al., 2016), although remodelling of the Høvdarhagi
1194 748 bog sequence in the Faroe Islands by Wastegård et al. (2018) has recently refined this
1195 749 estimate to $11,316 \pm 124$ cal. BP. The Hässeldalen Tephra has a frequent occurrence in
1196 750 Scandinavia and northern Europe (e.g. Davies et al., 2003; Lind and Wastegård, 2011; Lane
1197 751 et al., 2012b; Housley et al., 2013; Lilja et al., 2013; Larsen and Noe-Nygaard, 2014; Wulf et
1198 752 al., 2016), but at present a fairly limited distribution in the British Isles. Only tentative
1199 753 evidence is available from Rubha Port an t-Seilic on Islay (Mithen et al., 2015) and from
1200 754 Quoyloo Meadow on Orkney Mainland (Timms et al., 2017), with both records subject to
1201 755 stratigraphic uncertainties. A more robust record, however, has been obtained from Crudale
1202 756 Meadow on Orkney Mainland (Timms et al., 2018) and more recently from the central
1203 757 Scottish Highlands (Lowe et al., in prep). On present evidence it appears that the
1204 758 Hässeldalen ash plume had a narrow dispersal range over the northernmost part of the
1205 759 British Isles (Wastegård et al., 2018). However, this distribution pattern could be misleading,
1206 760 as its presence could be masked by remobilisation of more abundant Vedde Ash glass
1207 761 shards, a problem that complicates the refinement of many early Holocene
1208 762 tephrostratigraphies (e.g. Mangerud et al., 1984; MacLeod et al., 2015; Timms et al., 2017;
1209 763 2018).
1210 764

1224 765 *3.5.3 The Askja-S and CRUM1 510 tephtras*

1225 766 The Askja-S Tephra was first identified in a distal setting at Hässeldala port, south-eastern
1226 767 Sweden (Davies et al., 2003), and is thought to derive from the Askja-Dyngjufjöll system, a
1227 768 caldera in the central Highlands of Iceland (Sigvaldason, 2002; Figure 1). Also referred to as
1228 769 the Askja-10ka Tephra, it is one of the few LGIT distal tephra layers with a known proximal
1229 770 correlative (Sigvaldason, 2002; Jones et al., 2017) it is one of the most widely dispersed
1230 771 tephtras originating from Iceland during the LGIT, being found as far south as the Alps,
1231 772 Slovenia and east into Romania (Lane et al., 2011b; Kearney et al 2018). Characterised by
1232 773 distinctive FeO (c. 2.52 wt %) values and relatively low K_2O (2.49 wt %) totals (Table 1), the
1233
1234
1235
1236
1237
1238
1239

1240
1241
1242
1243
1244
1245
1246
1247
1248
1249
1250
1251
1252
1253
1254
1255
1256
1257
1258
1259
1260
1261
1262
1263
1264
1265
1266
1267
1268
1269
1270
1271
1272
1273
1274
1275
1276
1277
1278
1279
1280
1281
1282
1283
1284
1285
1286
1287
1288
1289
1290
1291
1292
1293
1294
1295
1296
1297
1298

774 Askja-S was first identified in the British Isles as a series of deposits in Northern Ireland
775 (Turney et al., 2006), but has more recently been traced to sites in central Scotland (Kelly et
776 al., 2017; Lowe et al., 2017; Lowe et al., in prep), Wales (Jones et al., 2017) and Orkney
777 Mainland (Timms et al., 2017, 2018; Figure 2). The widespread distribution of the Askja-S,
778 its glass compositional distinctiveness for the time period and its presence in a series of
779 high-resolution sedimentary records, has enabled a well-constrained age estimate of $10,824$
780 ± 97 cal. BP to be derived by composite or ‘multi-site’ Bayesian age-modelling (Kearney et
781 al., 2018; Bronk Ramsey et al., 2015). This age estimate has recently been challenged by
782 Ott et al. (2016), who suggested an estimate of $11,228 \pm 226$ cal. BP, based on the Askja-S’
783 occurrence within an annually resolved record in Lake Czechowskie, Poland. However, there
784 is some uncertainty as to how the age of the Askja-S Tephra was derived in this study, the
785 varve record is floating, but has been anchored in time by importing the age estimate for the
786 Hässeldalen Tephra, which is also present in the record. This is slightly problematic, as it is
787 unclear whether it is the age of the Hässeldalen, the age of the Askja-S, or both tephra age
788 estimates which may need revision. Thus although the results from Lake Czechowskie offer
789 an excellent opportunity to refine the age of early Holocene tephtras, it is evident that further
790 work is necessary to anchor the Czechowskie varve chronology at a point independent from
791 the two tephra isochrons that are under scrutiny. Hence until this point is cleared up, we
792 adopt the age estimate generated by Kearney et al. (2018).

793
794 At Crudale Meadow, Orkney Mainland, the Askja-S Tephra is identified alongside a basaltic
795 ash layer, provisionally named the CRUM1 510 Tephra, sourced from the Grímsvötn
796 volcano, which lies beneath the Vatnajökull ice cap (Timms et al., 2018; Figure 1). With an
797 estimated age of $10,837 \pm 148$ cal. BP, this is the oldest Grímsvötn eruptive to have been
798 detected in the British Isles during the Holocene, and this is the first record where the Askja-
799 S Tephra is found in association with a basaltic glass component. Like the earlier
800 Hässeldalen Tephra, the Askja-S and CRUM1 510 tephtras are closely associated with the
801 PBO, with the latter two tephtras appearing to coincide with the termination of this event
802 (Davies et al., 2003; Wohlfarth et al., 2006). This combination of the Hässeldalen, Askja-S
803 and CRUM1-510 tephtras all found in such close association will constitute a powerful tool for
804 testing the spatial and temporal variability of the environmental response to the PBO across
805 the British Isles and mainland Europe.

806 807 *3.5.4. The Ashik Tephra*

808 The Ashik Tephra, first identified at Loch Ashik on the Isle of Skye, has a bi-modal glass
809 chemistry with a rhyolitic component derived from Torfajökull in south-central Iceland (Figure
810 10), and a basaltic component from Grímsvötn (Pyne-O’Donnell 2005, 2007; Figure 1; Table

1299
1300
1301 811 1). The tephra has a limited spatial distribution, with the rhyolitic component being identified
1302 812 only in sequences from the Inner Hebrides and Orkney (Pyne-O'Donnell 2007; Timms et al.,
1303 813 2017; Figure 2). A possible rhyolitic correlative has also been described from Loch Laggan in
1304 814 the central Grampian Highlands, but it is unclear whether this ash layer relates to the Ashik
1305 815 Tephra or to one of the younger Torfajökull-derived tephtras (MacLeod, 2008; Supplementary
1306 816 Figure S1). The basaltic component has thus far been chemically analysed only at the site of
1307 817 Druim Loch, on the Isle of Skye, and correlated with the Loch Ashik tephra series on the
1308 818 basis of tephrostratigraphic superposition (Pyne-O'Donnell, 2005). The age of the Ashik
1309 819 Tephra was not well known, described as being "below the Saksunarvatn Ash" (Pyne-
1310 820 O'Donnell, 2007), until refined by a tephra-based Bayesian age model for the site of Quoyloo
1311 821 Meadow on Orkney, to $10,716 \pm 230$ cal. BP (Timms et al., 2017).

1312 822
1313 823 A key question concerning the Ashik Tephra is its tephrostratigraphic relationship with the
1314 824 Askja-S Tephra. These ash layers have a limited distribution in the British Isles, but occupy a
1315 825 very similar stratigraphic position within the early Holocene. This close association has
1316 826 recently been highlighted by the high-resolution work of Timms et al. (2017), who identified
1317 827 both tephra layers in consecutive 1 cm samples at Quoyloo Meadow (QM1 187, QM1 188
1318 828 respectively). In this case, it was only the contiguous chemical analyses of adjacent samples
1319 829 which facilitated a separation of these ash layers. As a result it is now known that the
1320 830 rhyolitic component of the Ashik Tephra lies stratigraphically above the Askja-S Tephra.
1321 831 What is not presently clear, however, is the relationship of these ash layers with the basaltic
1322 832 component of the Ashik Tephra and the CRUM1 510 Tephra. With the closely spaced nature
1323 833 of these tephtras, it could be that the CRUM1 510 Tephra identified at Crudale Meadow is the
1324 834 same as the 'basaltic Ashik Tephra' described elsewhere (i.e. at Loch Ashik, Druim Loch and
1325 835 Loch an t'Suidhe). Further investigations at finer sampling resolutions or in stratigraphically
1326 836 expanded sequences are required to establish the precise relationship between the rhyolitic
1327 837 Ashik Tephra, the rhyolitic Askja-S Tephra and the accompanying Grímsvötn basalt (i.e. the
1328 838 CRUM1 510 and/or the basaltic Ashik Tephra). Despite these uncertainties, the close
1329 839 association between the Ashik and Askja-S tephtras makes the former ash layer another
1330 840 potential marker for constraining the end of the PBO phase of climate instability (Pyne-
1331 841 O'Donnell 2007).

1342 842 1343 843 *3.5.5 The Hovsdalur Tephra*

1344 844 The Hovsdalur Tephra, like the Hässeldalen Tephra, is thought to originate from the
1345 845 Thórdarhyrna volcano in Iceland (Wastegård et al., 2018; Table 1; Figure 1). Only two sites
1346 846 in NW Europe are reported to host the Hovsdalur, the type-site of the same name located in
1347 847 the Faroe Islands (Wastegård, 2002) and Quoyloo Meadow located on Orkney Mainland

1358
1359
1360 848 (Timms et al., 2017). At the type-site, the Hovsdalur Tephra was discovered at the base of
1361
1362 849 the sequence and was dated by a simple linear extrapolation from a single radiocarbon date
1363 850 obtained from a higher level in the sequence, an approach which may have underestimated
1364
1365 851 the age of the ash layer (Wastegård et al., 2018). This potentially erroneous age has been
1366 852 used to argue that the Hovsdalur at the type-site is misidentified Hässeldalen Tephra
1367
1368 853 (Wastegård et al., 2018), a plausible proposition because they have overlapping glass
1369 854 compositions and both lie within early Holocene deposits (Lind and Wastegård, 2011). At
1370
1371 855 Quoyloo Meadow, however, the layers assigned to the Hovsdalur and Hässeldalen tephras
1372 856 are separated by 5 cm of sediment and by the Askja-S Tephra; crucially, no shards with a
1373 857 Hovsdalur/Hässeldalen signature were detected in the Askja-S layer (eight shards
1374
1375 858 analysed), making reworking from the Hässeldalen layer unlikely in this instance (Timms et
1376 859 al., 2017). While evidence for the Hovsdalur Tephra is currently limited, the Quoyloo
1377
1378 860 Meadow record does suggest the possibility of a younger (post-Askja-S) eruption event with
1379 861 a Hässeldalen-type signature, but corroborating evidence is needed to confirm this.
1380
1381 862

1382 863 *3.5.6 The Saksunarvatn Ash (Saksunarvatn 10-ka series)*

1383
1384 864 Originating from the Grímsvötn volcanic system, the basaltic Saksunarvatn Ash has long
1385 865 stood as an important marker horizon for the early Holocene in NW Europe (Jöhansen,
1386 866 1977; Mangerud et al., 1986; Birks et al., 1996; Björck et al., 2001). The widespread
1387 867 distribution of this tephra has allowed it to be traced to a number of high-resolution records
1388 868 where it has been dated precisely to $10,210 \pm 70$ cal. BP at Kråkenes in western Norway
1389
1390 869 (Lohne et al., 2014), and to $10,347 \pm 89$ GICC05 a b2k in the Greenland ice-core records
1391 870 (Rasmussen et al., 2006).
1392
1393 871

1394 872 In the British Isles, the Saksunarvatn Ash was first identified at Dallican Water in Shetland
1395
1396 873 (Bennett et al., 1992), but has since been traced to a number of other records including Loch
1397 874 of Benston on Shetland (Bondevik et al., 2005), Quoyloo Meadow (Bunting, 1994; Timms et
1398 875 al., 2017), Crudale Meadow (Bunting, 1994; Timms et al., 2018) and was initially thought to
1400 876 be present at Loch Ashik (Pyne-O'Donnell 2007; c.f. Kelly et al., 2017). Tentative
1401 877 correlations based on superposition have also been proposed for the Borrobol sequence
1402 878 (Turney, 1998b) and Loch an t'Suidhe, located on the Isle of Mull (Pyne-O'Donnell, 2005),
1403 879 although no chemical evidence is available to support these correlations (Figure 2;
1404 880 Supplementary Figure S1; Supplementary Table S1).
1405
1406 881

1407 882 Recent evidence has cast doubt over the use of the Saksunarvatn Ash as a single
1408
1409 883 isochronous marker, because several separate Grímsvötn ash layers appear to have been
1410 884 deposited around the time interval c. 10.4 – 9.9 ka BP that was originally assigned to the
1411
1412
1413
1414
1415
1416

1417
1418
1419 885 'Saksunarvatn Ash' (Jennings et al., 2002, 2014; Jóhannsdóttir et al., 2005; Kristjánisdóttir et
1420 al., 2007; Kylander et al., 2011; Thordarson, 2014; Neave et al., 2015; Harning et al., 2018;
1421 886 Wastegård et al., 2018). In total it is believed that as many as seven Grímsvötn tephra layers
1422 887 may have been produced during this 500-year interval, hence leading to the term the
1423 888 'Saksunarvatn 10-ka series', although it is not clear how many of these were dispersed
1424 889 towards mainland Europe (Jóhannsdóttir et al., 2005; Jennings et al., 2014; Neave et al.,
1425 890 2015; Wastegård et al., 2018). At Havnardalsmyren in the Faroe Islands, five Grímsvötn
1426 891 tephra layers have been reported within early Holocene sediments, and two of these, Havn-3
1427 892 and Havn-4, can be distinguished on the basis of lower glass-derived MgO values than
1428 893 found in other 'Saksunarvatn Ash' glass analyses (Wastegård et al., 2018). This distinction
1429 894 has significance for the British tephrostratigraphic framework because the basaltic layer in
1430 895 the Loch Ashik sequence assigned by Pyne-O'Donnell et al. (2007) to the 'Saksunarvatn
1431 896 Ash' also has this characteristically low MgO signal (Wastegård et al., 2018), being further
1432 897 reflected in additional glass analyses provided for this layer in Kelly et al. (2017; Figure 11).
1433 898 It is more likely therefore that the 'Saksunarvatn Ash' at Loch Ashik is a correlative of the
1434 899 Havn-3 or Havn-4 eruptions, which date to between c. 10.37 and 10.3 ka BP, and thus we
1435 900 have revised the tephra record for the Loch Ashik sequence accordingly (Figure 2;
1436 901 Supplementary Figure S1; Supplementary Table S1).
1437 902
1438 903

1444 904 Following this revision, we have reassessed the glass compositional evidence obtained from
1445 905 'Saksunarvatn Ash' layers in the British Isles (Figure 11). The analyses of the Saksunarvatn
1446 906 Ash at Crudale Meadow by Bunting (1994) clearly exhibit two glass populations, one
1447 907 correlating with the Grímsvötn series and the other plotting close to the compositional
1448 908 envelope of Veiðivötn- Bárðarbunga. Importantly, Veiðivötn- Bárðarbunga glass analyses
1449 909 are also reported from the Havn-0 horizon at Havnardalsmyren (Wastegård et al., 2018), and
1450 910 from Bæjarvötn, a lake-site of similar age in the NW of Iceland (Harning et al., 2018).
1451 911 Wastegård et al. (2018) consider the Havn-0 horizon to represent reworking due to their
1452 912 coeval presence with Grímsvötn analyses. However, at Bæjarvötn the Veiðivötn-
1453 913 Bárðarbunga analyses form a distinct 1 cm marker horizon layered between Grímsvötn
1454 914 tephra layers of the 10-ka Saksunarvatn series (Harning et al., 2018). This finding hints at
1455 915 the possible discovery of a new isochronous marker in the North Atlantic region and one
1456 916 independent of the issues associated with the Saksunarvatn series. However, reinvestigation
1457 917 of the Crudale Meadow sequence by Timms et al. (2018) failed to detect any glass shards
1458 918 with a Veiðivötn-Bárðarbunga signature despite 29 analyses being obtained. Presently it is
1459 919 not exactly clear why this may be, but a speculative reason might be a slight difference in
1460 920 core location at the Crudale Meadow basin between the studies conducted by Bunting
1461
1462
1463
1464
1465
1466
1467
1468
1469
1470
1471
1472
1473
1474
1475

1476
1477
1478
1479
1480
1481
1482
1483
1484
1485
1486
1487
1488
1489
1490
1491
1492
1493
1494
1495
1496
1497
1498
1499
1500
1501
1502
1503
1504
1505
1506
1507
1508
1509
1510
1511
1512
1513
1514
1515
1516
1517
1518
1519
1520
1521
1522
1523
1524
1525
1526
1527
1528
1529
1530
1531
1532
1533
1534

921 (1994) and Timms et al. (2018). On current evidence therefore, the significance of the
922 Veiðivötn-Bárðarbunga analyses from Crudale Meadow is not yet substantiated.

923
924 All other ‘Saksunarvatn’ Ash analyses obtained from records in the British Isles plot within
925 the main Grímsvötn envelope, suggesting these probably correlate to either the Havn-2 or
926 Havn-1 tephras described from the Faroe Islands (Wastegård et al., 2018). The recent
927 findings of Harning et al. (2018) and Wastegård et al. (2018) with regard to the 10-ka
928 Saksunarvatn series go some way to resolving, or at the very least circumnavigating, the
929 complex issue of repeated Grímsvötn activity and the associated tephras recorded in early
930 Holocene sedimentary deposits in the North Atlantic region.

931

932 *3.5.7 The Fosen Tephra*

933 The Fosen Tephra has a chemical composition similar to that of the Borrobol-type tephras of
934 the Late Pleistocene (Table 1) and has been described from sites in western Norway (Lind et
935 al., 2013), Denmark (Larsen, 2013), eastern Iceland (Gudmundsdóttir et al., 2016) and
936 Orkney, where it has been dated indirectly using a tephra-based Bayesian age model to
937 $10,139 \pm 116$ cal. BP (Timms et al., 2017). A tentative correlative of this eruptive has also
938 been proposed from a sediment sequence in Loch Laggan in the central Grampian
939 Highlands (MacLeod, 2008; Supplementary Table S1). In the early Holocene, analyses of
940 glass from four other ash layers bear some chemical resemblance to that of the Fosen: the
941 Högstorpsmossen Tephra in Sweden, dated to c. 10,200 cal. BP (Björck and Wastegård,
942 1999); a component of the L-274 Tephra on the Faroe Islands, dated to c. 10,200 cal. BP
943 (Lind and Wastegård, 2011); population 3 of the QUB-608 Tephra on the Lofoten Islands,
944 dated to c. 9500 cal. BP (Pilcher et al., 2005); and the SSn Tephra c. 7300 cal. BP (Boyle,
945 1999). All of these ash layers can be described as ‘Borrobol-type’ in terms of their
946 composition, and there is a strong possibility that at least the first three could represent the
947 same eruptive event (Lind et al., 2013; 2016). At present, poor age control for these records
948 prevents more definitive conclusions, though it seems quite possible that the ‘Fosen Tephra’
949 could have a much wider dispersal range than is currently acknowledged.

950

951 In Norway and Orkney, the Fosen Tephra has been recognised as occurring just above the
952 Saksunarvatn Ash (Lind et al., 2013; Timms et al., 2017). Therefore the Fosen may form a
953 more useful stratigraphic marker in delineating the 10.3 ka event (Björck et al., 2001),
954 especially given the uncertainties of the Saksunarvatn 10-ka series discussed above
955 (section 3.5.6). The stratigraphic position of the Fosen Tephra may also make it a useful
956 isochron for marking the onset of the ‘Erdalen Events’ (c. 10.10-10.05 ka BP and 9.7 ka BP),
957 a series of glacier advances in Norway thought to have been triggered by a phase of climatic

1535
1536
1537 958 instability (Dahl et al., 2002). These Erdalen Events are relatively understudied in NW
1538
1539 959 Europe, but their effects may have been felt elsewhere around the periphery of Scandinavia,
1540 960 including in the British Isles. Tracing of the Fosen Tephra beyond its current known limits
1541
1542 961 may therefore help focus research into understanding their wider geographical impacts.
1543 962

1544 963 *3.5.8 The An Druim-Høvdarhagi Tephra*

1546 964 The An Druim Tephra is the third of four early Holocene rhyolitic ash layers thought to
1547 965 originate from the Torfajökull volcanic centre (Figure 10) and, like its predecessors, the
1548 966 Crudale Tephra and the Ashik Tephra, has a limited distribution (Figure 2; Table 1). The
1550 967 tephra was originally described from Lochan An Druim on the north coast of Scotland
1551 968 (Ranner et al., 2005), but recent work by Kelly et al. (2017) and Timms et al. (2017) have
1553 969 confirmed the occurrence of this tephra in sites in the Grampian Highlands and in Orkney.
1554
1555 970 These studies also present a strong case for linking the An Druim Tephra with the
1556 971 Høvdarhagi Tephra identified in the Faroe Islands and for both being representative of the
1557
1558 972 same eruption. Lind and Wastegård (2011) on the other hand have argued for a separation
1559 973 of these tephras based on marginally higher CaO and MgO wt % values in analyses of glass
1560 974 of the Høvdarhagi Tephra (Figure 10). This small chemical variance could result from the
1561 975 delivery of shards with a narrower chemical range to Scottish sequences and/or as an
1562 976 artefact of smaller sample sizes used in the Scottish studies (Kelly et al., 2017; Timms et al.,
1563
1564 977 2017; Wastegård et al., 2018), or through analytical imprecision (e.g. Lowe, D. et al. 2017).
1566 978 A re-run of the Lochan An Druim and Høvdarhagi age-depth models using the updated
1567
1568 979 OxCal parameters of Bronk Ramsey (2008; 2009), Bronk Ramsey and Lee (2013), and
1569 980 utilising the IntCal13 calibration curve (Reimer et al., 2013), indicates that these tephras
1570
1571 981 overlap chronologically (Timms, 2016), adding weight to the argument that they share the
1572 982 same source. We propose on current evidence that the best-estimate age for the An Druim-
1573
1574 983 Høvdarhagi Tephra is 9648 ± 158 cal. BP, based on the remodelled An Druim chronology,
1575 984 and therefore provisionally offers an additional marker horizon for establishing the wider
1576
1577 985 impacts of the early Holocene Erdalen Events (Timms, 2016).

1578 986 1579 1580 987 *3.5.9 The LAN1-325 Tephra*

1581 988 Within the current British tephrostratigraphic framework, the LAN1-325 Tephra is the fourth
1582 989 and youngest ash layer thought to originate from the Torfajökull volcanic centre (Table 1;
1583
1584 990 Figure 10; Matthews, 2008). The tephra's glass shards are characterised chemically by
1585 991 seven analyses and at present the tephra has only been detected at the type-site,
1586
1587 992 Loughanascaddy Crannog, Ireland (Figure 2). It is, however, well constrained
1588 993 stratigraphically, occurring just below the Lairg A Tephra (6903 ± 94 cal. BP), and 13 cm
1589
1590 994 above sediment with a radiocarbon date of 7620 ± 50 ^{14}C yrs. Bayesian age modelling

1594
1595
1596 995 suggests an age for this tephra of 8434 ± 96 cal. BP. There is some possibility therefore that
1597
1598 996 the LAN1-325 Tephra may correlate with the proximal Slettahraun deposit in Iceland, which
1599 997 has been dated to c. 8000 yr BP (MacDonald et al., 1990; McGarvie et al., 1990). At present,
1600
1601 998 however, the available chemical data for comparing the two are limited. Glass analyses for
1602 999 the LAN1-325 tephra are based on EPMA, and are published here for the first time
1603
1604 1000 (Supplementary Table S2), whereas the proximal analyses are based on whole-rock X-ray
1605 1001 Fluorescence (XRF). Single grain glass analysis of the latter will be needed to provide more
1606
1607 1002 directly comparable data. Nonetheless, the age of the tephra means that it is has the
1608 1003 potential to become a regionally valuable horizon for marking environmental responses to
1609
1610 1004 the 8.2 ka event.

1611 1005 1612 1006 *3.5.10 The Suduroy Tephra*

1614 1007 The Suduroy Tephra is a rhyolitic ash layer with a silicic Katla chemical signature (Table 1;
1615 1008 Wastegård, 2002; Lane et al., 2012a). It was first identified at Hovsdalur on the Faroe
1616
1617 1009 Islands where it was dated to 8073 ± 192 cal. BP (Wastegård, 2002). In the British Isles, this
1618 1010 tephra has been identified at two sites: Loch Laggan in the central Grampian Highlands
1619
1620 1011 (MacLeod, 2008) and Rubha Port an t-Seilich on Islay (Mithen et al., 2015; Figure 2). The
1621 1012 tephra has also been identified in a series of North Atlantic marine deposits (Kristjánsdóttir et
1622
1623 1013 al., 2007; Gudmundsdóttir et al., 2012) as well as in sites in mainland Europe (Pilcher et al.,
1624 1014 2005; Housley et al., 2012). There is some concern, however, that the Suduroy may
1625
1626 1015 represent reworked material from antecedent Vedde Ash deposits in some sites (Wastegård
1627 1016 et al., 2018). However, this seems unlikely at Loch Laggan as a number of discrete tephras
1628
1629 1017 lie between what is hypothesised to represent the Vedde Ash based on stratigraphic
1630 1018 superposition, and the glass-shard based chemically correlated Suduroy Tephra (MacLeod,
1631 1019 2008). At Rubha Port an t-Seilich the correlation is slightly more tentative as low
1632
1633 1020 concentrations of glass shards occur throughout the stratigraphic column suggesting a
1634 1021 problem of reworked shards. Despite these concerns, if the Suduroy Tephra can be shown
1635
1636 1022 to represent primary fallout at sites to which it is traced, the age of the isochron means that
1637 1023 like the LAN1-325 Tephra, the Suduroy Tephra may be particular useful in marking
1638
1639 1024 environmental response to the 8.2 ka event.

1640 1025 1641 1026 *3.5.11 The Breakish Tephra*

1643 1027 This is a rhyolitic ash layer which may originate from the Askja volcanic centre and its glass
1644
1645 1028 components exhibit distinctly high TiO_2 (c. 0.49 wt %) and FeO (c. 3.59 wt %) values (Table
1646 1029 1). So far, it has been detected in the Loch Ashik sequence on Skye only, where it was
1647
1648 1030 reported as lying stratigraphically above the Saksunarvatn Ash (now considered to be the
1649 1031 Havn-3 or 4 eruption, see section 3.5.6; Pyne-O'Donnell, 2007). At present the ash layer has

1653
 1654
 1655 1032 not been dated directly, while the nearest match on the basis of glass composition is the
 1656 1033 Glen Garry Tephra (Pyne-O'Donnell, 2007; Lowe et al., 2016) which, being dated to $2176 \pm$
 1658 1034 164 cal. BP (Barber et al., 2008), is hence too young to be a viable correlative. Recently a
 1659 1035 number of other Askja-derived tephras have been identified in early-Holocene sequences,
 1661 1036 the Askja-L (c. 9400 cal. BP), and the Askja-H (c. 8850 cal. BP; Gudmundsdóttir et al.,
 1662 1037 2016). These are unlikely correlatives for the Breakish Tephra, however, as both exhibit
 1664 1038 glass chemical signatures very similar to those of the Askja-S, which the Breakish Tephra
 1665 1039 does not consistently match (Pyne-O'Donnell, 2007). Presently the potential usefulness of
 1667 1040 this ash layer within the British tephrostratigraphic framework is uncertain, and hence it has
 1668 1041 limited value until corroborative records can be found.

1670 1042
 1671 1043 **4. Synthesis: an emerging tephrostratigraphic framework for the British Isles (16-8.0**
 1672 1044 **ka BP) and its validation**

1674 1045
 1675 1046 The previous section presented, in order of stratigraphic superposition from oldest to
 1677 1047 youngest, the record of tephra layers detected in the British Isles for the period 16-8 ka BP.
 1678 1048 Establishing this order was guided initially by the relative positions of individual tephra layers
 1679 1049 with respect to the boundaries for the DS, WI, LLS and early Holocene stratigraphic units,
 1681 1050 while additional order could be imposed where two or more tephra layers are co-registered
 1683 1051 within the same sequence and stratigraphic unit, as in the case of the Borrobol and Penifiler
 1684 1052 Tephras, both of which are detected in a number of sediment records dating to the early WI
 1686 1053 (Supplementary Figure S1; Supplementary Table S1). Integration of the complete
 1687 1054 tephrostratigraphic dataset using common marker tephras leads to the regional
 1689 1055 tephrostratigraphic scheme presented in row F of Figure 12. Parts of this scheme should,
 1690 1056 however, be considered provisional in view of the points raised in section 3 over the origins
 1691 1057 of some layers, whether they represent primary fall events or, in the cases of those detected
 1693 1058 at a single site only, whether they have the potential to serve as regional isochrons. For
 1694 1059 these reasons, the tephras are coded in row F, Figure 12, to signify: (i) those considered to
 1696 1060 be based on the most robust glass analytical data, with consistent stratigraphic positions and
 1697 1061 well-defined ages (n=6); (ii) those for which reasonably robust glass analytical data are
 1699 1062 available, but questions remain about their precise origins, stratigraphic integrity or age
 1700 1063 (n=9); and (iii) those most in need of further investigation to test their potential to serve as
 1702 1064 regional isochrons in the British Isles (n=11). It is tephras from these first two categories
 1703 1065 which we provisionally include within the formalised tephrostratigraphic framework (Table 4).

1705 1066
 1706 1067 To validate and extend this regional framework, a number of stratigraphic constraints need
 1707 1068 to be taken into account. First, very few sites with tephra layers dating to the DS or to the

1712
1713
1714 1069 DS-WI transition have been discovered in the British Isles so far, a reflection perhaps of the
1715 1070 geographical bias of recent tephrostratigraphical research, which has predominantly focused
1716 1071 on sites in the Scottish Highlands. While parts of Scotland were deglaciated by c. 16.0 ka BP
1717 1072 (Clark et al., 2012; Hughes et al., 2016; Ballantyne and Small, 2018), the current tephra
1718 1073 record suggests that much of the Scottish Highlands did not become ice-free until, or
1719 1074 marginally before, c. 14.0 ka BP. This inference is indicated by the frequency with which the
1720 1075 Borrobol Tephra is found close to the base of the earliest sediments to have accumulated in
1721 1076 a number of lake basins (Walker and Lowe, 2017; Supplementary Figure S1), whereas in the
1722 1077 Tirinie basin located in the Grampian Highlands, the younger Penifiler Tephra occupies this
1723 1078 position (Candy et al., 2016). Thus far, the only terrestrial sites in the British Isles in which
1724 1079 pre-WI tephra layers have been discovered are located on the Summer Isles in The Minch,
1725 1080 off the north-west coast of Scotland, and on Orkney, north of the Scottish mainland, i.e. in
1726 1081 parts of Scotland for which independent evidence indicates retreat of ice-sheet margins by or
1727 1082 before 16.0 ka BP (e.g. Phillips et al., 2008; Ballantyne et al., 2012; Hughes et al., 2016).
1728 1083 Hence the search for possible additional tephra records of pre-WI age in the British Isles
1729 1084 may prove more profitable if focused on sites located in areas outside of the Scottish
1730 1085 Highlands.
1731 1086
1732 1087 Only two tephra layers that date to within the WI have been proposed as viable regional
1733 1088 isochrons: the Borrobol and Penifiler tephras which both date to between c. 14.19 and 13.9
1734 1089 ka BP. Whilst uncertainty surrounds the origin of the Penifiler tephra (section 3.3.1), there is
1735 1090 nevertheless a degree of stratigraphic consistency in tephra records showing at least two
1736 1091 shard peaks of Borrobol chemistry in the lower part of the WI. Additional stratigraphic
1737 1092 markers help to constrain the age of these tephra layers for proxy environmental records
1738 1093 from the British Isles are increasingly indicating evidence for two short-lived oscillations
1739 1094 during the WI, which are assumed to equate with the GI-1d and GI-1b events (column A,
1740 1095 Figure 12) in the Greenland stratotype record (e.g. Brooks and Birks, 2000; Marshall et al.,
1741 1096 2002; Lang et al., 2010; Watson et al., 2010; van Asch et al., 2012; Whittington et al., 2015;
1742 1097 Brooks et al., 2012; 2016). In a number of tephra records, one of the peaks (usually the
1743 1098 more prominent) clearly pre-dates the oscillation equated with GI-1d, while the younger, less
1744 1099 prominent peak lies within this interval (Matthews et al., 2011; Brooks et al., 2012; 2016).
1745 1100
1746 1101 Some of the evidence on which these stratigraphic relationships are based has, however,
1747 1102 relied on correlations resting entirely on lithostratigraphic criteria, represented by loss-on-
1748 1103 ignition (LOI) data (e.g. Lowe et al., 1999; Turney et al., 2006; Pyne-O'Donnell, 2007; Pyne-
1749 1104 O'Donnell et al., 2008). Although the lithostratigraphic changes within the WI are clearly
1750 1105 evident in some sequences, they are poorly developed in others (cf. columns B and C,
1751
1752
1753
1754
1755
1756
1757
1758
1759
1760
1761
1762
1763
1764
1765
1766
1767
1768
1769
1770

1771
1772
1773 1106 Figure 12). This inconsistency could reflect the influence of local factors that acted to
1774 1107 dampen or enhance the impacts of the environmental conditions that caused these
1775 1108 lithostratigraphic changes, for example, the degree of shelter or exposure afforded to
1776 1109 different catchments, or poor resolution of these sedimentary features due to very low rates
1777 1110 of sedimentation. To complicate matters further, some sequences show evidence for at least
1780 1111 six lithological sub-units within the WI interval (e.g. column B, Figure 12 in which the more
1782 1112 minerogenic layers are numbered 1-3), and hence the possible occurrence of three short-
1783 1113 lived climatic oscillations rather than two (see Whittington et al., 2015; Candy et al., 2016;
1784 1114 Walker and Lowe, 2017). Finally, it cannot be assumed that these lithological changes
1785 1115 necessarily reflect climatic impacts. Short-lived increases in the rate of minerogenic
1786 1116 sediment supply to lake basins could reflect localised soil or land disturbance caused, for
1787 1117 example, by sediment or rock failures. A more secure basis, therefore, for assessing the
1789 1118 significance of these lithological changes would be by inclusion of palaeoclimate proxies in
1790 1119 site investigations, for example the analysis of stable oxygen isotope variations (column D,
1791 1120 Figure 12) or chironomid assemblages (column E, Figure 12), but detailed records of this
1792 1121 type that extend through the Lateglacial and early Holocene are presently available for only
1793 1122 a handful of records in the British Isles (e.g. Marshall et al., 2002; Brooks et al., 2012;
1794 1123 Whittington et al., 2015; Candy et al., 2016). Nevertheless, the few lake records that are
1795 1124 presently available that combine tephrostratigraphic with palaeoclimatic data do support the
1796 1125 view that two Borrobol-type tephra peaks dating to the early WI are distinguishable by
1797 1126 stratigraphic position relative to a short-lived climatic oscillation provisionally equated with
1798 1127 the GI-1d event (Brooks et al., 2016).
1800 1128
1801 1129 One of the main challenges facing the tephrostratigraphic scheme is the further refinement
1802 1130 and validation of tephras located between the LLS-Holocene transition and c. 8.0 ka BP.
1803 1131 Fifteen tephra layers have been proposed for this interval so far (section 3.5; Figure 12;
1804 1132 Table 4), some with very similar major and minor element glass compositions, some in close
1805 1133 stratigraphic proximity, and some sharing overlapping age ranges. In addition, there is a
1806 1134 likelihood that a proportion of these tephra layers, where present, will be conflated together
1807 1135 in a single horizon. This is due to the marked warming at the start of the Holocene, the
1808 1136 expansion of higher plant communities and the consequential stabilisation of catchment
1809 1137 soils, all of which would have led to a reduction in the sediment supply rate to lake basins
1810 1138 compared with the preceding Lateglacial period (e.g. Brauer et al., 1999). Furthermore, in
1811 1139 most lake basin sites in the British Isles, the early Holocene deposits lack the clear
1812 1140 lithostratigraphic markers that characterise Lateglacial sediment sequences (Column B and
1813 1141 C, Figure 12). This means that other indicators must play a more prominent role in refining the
1814 1142 stratigraphic superposition of tephra layers. For example, greater reliance may be placed

1830
1831
1832 1143 upon those tephras with distinctive glass chemical compositions or shard morphology as key
1833 1144 markers, such as the Håsseldalen, Askja-S and traditionally the Saksunarvatn Ash, although
1834 1145 the robustness of the latter is now doubtful. Recourse can also be made to other 'proxy'
1835 1146 stratigraphical information—for example, pollen-stratigraphic records for the early Holocene
1836 1147 throughout much of the British Isles reflect a characteristic plant colonisation sequence
1837 1148 dominated successively by *Empetrum*, *Juniperus*, *Betula* and *Betula-Corylus* (Walker, 1984;
1838 1149 Birks, 1989). In records obtained from sites in the Scottish Highlands, the Askja-S Tephra is
1839 1150 consistently found within the upper part of the *Juniperus* phase, whereas deposition of the
1840 1151 An Druim Tephra post-dates the local establishment of *Betula-Corylus* woodland (Ranner et
1841 1152 al., 2005; Kelly et al., 2017; Lowe et al., 2017). Whether these relationships hold for other
1842 1153 parts of the British Isles is unclear, however, as the process of plant colonisation over a
1843 1154 wider area is likely to have been time-transgressive (Tipping, 1987; Birks, 1989; Huntley,
1844 1155 1993; Normand et al., 2011).

1851 1156
1852 1157 The British Isles represent the most intensively studied area for LGIT-aged cryptotephra
1853 1158 anywhere, but it is clear from the above sections that the tephrostratigraphic scheme
1854 1159 presented here is still in need of further refinement (Figure 12; Table 4). Even though future
1855 1160 tephra studies will have a variety of specific goals, those offering the greater potential for
1856 1161 improving the tephrostratigraphic scheme presented here are likely to be those based on
1857 1162 sedimentary records that are: (i) capable of analysis at high stratigraphic and temporal
1858 1163 resolution, allowing closely timed ash-falls to be clearly separated and sequenced, such as
1859 1164 the Askja-S and Ashik tephras; and (ii) part of multi-proxy programmes of research, which
1860 1165 allow the local and wider climatic and environmental context at the time of deposition to be
1861 1166 assessed. Critical to this is the inclusion of palaeoclimatic reconstructions, enabling the
1862 1167 alignment of tephra layers with local or regional climatostratigraphic events to be established
1863 1168 (Figure 12). It should not be assumed, however, that these records need to be located within
1864 1169 the British Isles as sites with better resolution and more secure stratigraphic settings may be
1865 1170 available elsewhere in Northern Europe. A possible weakness that needs to be noted,
1866 1171 however, is that of circular argument where, on the one hand, tephra layers are used as
1867 1172 stable marker horizons to test for asynchronous climatic behaviour, while
1868 1173 climatostratigraphic boundaries are used to judge the isochronous nature of tephra layers,
1869 1174 an example being that of the Borrobol and Penifiler tephras (see section 3.3.1; see also
1870 1175 studies on this topic by Newnham and Lowe, 1999). In view of the growing evidence from
1871 1176 Europe that suggests climatic changes during the period c.16-8 ka were time-transgressive
1872 1177 (e.g. Lane et al., 2013; Rach et al., 2014; Muschitiello and Wohlfarth, 2015), care needs to
1873 1178 be exercised when adopting this approach. Likewise the use of local pollen-stratigraphic
1874 1179 boundaries for correlation purposes, as in the example given above of the Askja-S Tephra, is

1889
1890
1891 1180 also potentially problematic. This dilemma could be avoided if all tephra layers were
1892
1893 1181 chemically distinct, stratigraphically separable and reliably dated with narrow age ranges,
1894 1182 but, as illustrated in section 3, such an ideal scenario is far from the case. Thus the process
1895
1896 1183 of establishing the consistent stratigraphic context and isochronous nature of cryptotephra
1897 1184 layers will continue to be an iterative one.
1898
1899 1185

1900 1186 **5. Future targets and prospects**

1901 1187
1902
1903 1188 The tephrostratigraphic scheme outlined in Figure 12 reflects the current available evidence
1904 1189 in the British Isles, but aspects of the scheme require further refinement and to aid this we
1905
1906 1190 identify *reference records* for each proposed tephra isochron, including those that cannot yet
1907 1191 be integrated confidently into the framework (Table 4). Most of these reference records are
1908
1909 1192 provisional and were selected using a combination of criteria, notably the resolution and
1910 1193 magnitude of peak shard concentrations, the robustness of supporting glass analytical data,
1911
1912 1194 and the precision and reliability of associated age estimates. Note that an individual
1913 1195 reference record is not necessarily that from which the proposed isochron or tephra layer
1914
1915 1196 was first recognised in the British Isles, because later discoveries may be considered
1916 1197 superior. For example, the Tirinie sequence is selected as the reference record for the
1917
1918 1198 Penifiler Tephra in the British Isles for two main reasons: (i) it has a better resolved shard
1919 1199 peak than is the case for the Druim Loch record from Skye, which is located close to the
1920
1921 1200 village of Penifiler, after which the tephra is named; (ii) the site has robust palaeoclimatic
1922 1201 data available; and (iii) the collective stratigraphic evidence for the Tirinie sequence provides
1923 1202 the strongest argument against the Penifiler Tephra being derived by reworking of the
1924
1925 1203 Borrobol Tephra (see section 3.3.1), at least in this instance, since the onset of sediment
1926 1204 accumulation in the Tirinie basin post-dates deposition of the Borrobol Tephra (Candy et al.,
1927
1928 1205 2016). In due course, more secure reference records may emerge from investigations of
1929 1206 new sites, or through more rigorous re-examination of previously studied sequences that, for
1930
1931 1207 example, are in need of analysis at a higher stratigraphic or temporal resolution, or for which
1932 1208 glass shards are currently weakly characterised. To this end, development of reference
1933
1934 1209 records and the tephrostratigraphic framework as a whole will be enhanced by addressing
1935 1210 the following issues: (i) spatial and stratigraphic sampling biases; (ii) glass-shard analytical
1936 1211 data, both for major and trace elements, and the need for improved resolution and scrutiny
1937
1938 1212 of existing compositional data, and (iii) ongoing refinement of tephra age estimates.
1939
1940 1213

1941 1214 Studies over the past 25 years have revealed a wealth of tephrostratigraphic data for British
1942 1215 LGIT sediment sequences, but knowledge gaps remain. These include finding additional
1943
1944 1216 isochrons and establishing the full geographic ranges over which they are traced. In this

1948
1949
1950 1217 context, Scotland has been the most intensely studied area in the British Isles for tephra
1951 1218 layers dating to this interval, yet fewer than 20% of known sites containing suitable deposits
1952 1219 have so far been explored for their tephra content (Walker and Lowe, 2017), while the
1953 1220 comparable ratios for sites in England, Wales and Ireland are much lower (Figure 2;
1954 1221 Supplementary Figure S1). Given the relative abundance of mid-late Holocene tephra
1955 1222 detected in other areas of the British Isles (Swindles et al., 2011; Plunkett and Pilcher,
1956 1223 2018), it is probable that more tephra layers await discovery, including those dating to the
1957 1224 LGIT. Particularly intriguing in this respect are tephra that have been detected in a single
1958 1225 site only, such as the Roddans Port and LAN1-325 tephra in Ireland and the recent
1959 1226 discovery of 'ultra-distal' tephra from North American centres. It is not clear whether these
1960 1227 sparse records reflect a very limited impact of the corresponding ash clouds in the British
1961 1228 Isles, a failure to detect these layers in other records, or both.
1962 1229
1963 1230 Pertinent to this point is the strategy adopted when investigating the glass shard content of
1964 1231 sediment sequences. In some cases records have not been investigated in full, either
1965 1232 because research questions were focused on specific age intervals, or because certain
1966 1233 tephra were seen as more important than others and were preferentially targeted, or
1967 1234 because sampling resolution or methods were not sufficient to detect cryptotephra.
1968 1235 Understanding the purpose and sampling limitations behind individual tephrostratigraphic
1969 1236 studies is therefore important when synthesising records to construct a regional
1970 1237 tephrostratigraphic framework. In some previous records there has been a tendency to focus
1971 1238 attention on selected key marker horizons, such as the Vedde and Saksunarvatn ash layers
1972 1239 (e.g. Wastegård 2000; Bramham-Law et al., 2013). These tephra are understood to
1973 1240 represent the most explosive and voluminous eruptive events that occurred during the period
1974 1241 16-8 ka, but other tephra which have been explored less assiduously may prove to serve as
1975 1242 equally important isochrons, with dispersal ranges possibly just or as nearly widespread. The
1976 1243 recent eruptions of Eyjafjallajökull and Grímsvötn in Iceland (Davies et al., 2010; Stevenson
1977 1244 et al., 2012; 2013) have demonstrated that relatively small to moderate eruptions can have
1978 1245 much greater dispersal ranges than those presently recognised in the palaeo-tephra record.
1979 1246 This raises the question as to whether important ash layers are being overlooked by
1980 1247 selective low resolution sampling methods and the over emphasis and exploration of 'key
1981 1248 marker' horizons (Timms et al., 2017). Given this concern, more studies are now adopting
1982 1249 contiguous high resolution sampling strategies as routine practice, most being rewarded with
1983 1250 improved tephrostratigraphic resolution and discrimination, and more secure tephra-linkages
1984 1251 than coarse sampling strategies tend to yield (e.g. MacLeod 2008; Matthews et al., 2011;
1985 1252 Timms et al., 2017; 2018). It follows that if the tephrostratigraphic scheme and its
1986 1253 applications are to be optimised, this practice needs to be more commonly applied.
1987
1988
1989
1990
1991
1992
1993
1994
1995
1996
1997
1998
1999
2000
2001
2002
2003
2004
2005
2006

2007
2008
2009 1254
2010
2011 1255 In other cases the nature of negative information (the absence of glass shards) is not always
2012 1256 made clear. Gaps in the tephra record could reflect unsampled intervals, or cases where
2013 1257 investigations have been carried out but no tephra (glass) was found. In times of the latter, it
2014 1258 is recommended that such negative findings are always reported, as they are particularly
2015 1259 valuable for: (i) assessing the efficiency of different approaches employed for tephra
2016 1260 detection and extraction; (ii) reconstructing the geographical distribution ('footprints') of
2017 1261 individual tephra isochrons, and (iii) evaluating the taphonomic and other factors that
2018 1262 influence the deposition and preservation of volcanic glass shards. Negative results, where
2019 1263 known, have been compiled for this review (Supplementary Figure 1; Supplementary Table
2020 1264 1), and are beginning to be reported more routinely (e.g. Wastegård et al., 2000; van Asch et
2021 1265 al., 2012; Jones et al., 2017).
2022 1266
2023
2024 1267 Thorough tephrostratigraphic investigations should be coupled with robust chemical
2025 1268 determinations conducted at a comparable stratigraphic resolution (see Lowe, D. et al.,
2026 1269 2017). However, the greater scrutiny this enables will inevitably result in exposing further
2027 1270 levels of complexity for, as outlined in earlier sections of this paper, the LGIT
2028 1271 tephrostratigraphic record is already populated with tephra layers that share closely similar
2029 1272 or indistinguishable major element signatures. Whether this similarity extends to trace
2030 1273 element compositions remains to be widely tested, but as recommended elsewhere, when
2031 1274 major elements prove equivocal trace elemental analyses should be prioritised (e.g. Lowe
2032 1275 2011, Lowe, D. et al., 2017). This contribution has also shown the frequency with which a
2033 1276 single shard concentration peak may include shards with a range of different chemical
2034 1277 (major element) compositions (Supplementary Table S2), raising the question of whether
2035 1278 even finer resolution studies are required to resolve such complexities, including, for
2036 1279 example, high-resolution imaging techniques to better understand the local depositional
2037 1280 context (see Griggs et al., 2015). However, this greater scrutiny may only serve to highlight
2038 1281 the scales at which mixing processes occur, if shards are already known to be spread over
2039 1282 cm's, further examination at mm scales, or finer, may not yield further useful information. It
2040 1283 may be required, therefore, that future studies focusing on resolving regional
2041 1284 tephrostratigraphies be conducted in records that are less susceptible to taphonomic
2042 1285 processes, or in records where stratigraphic integrity can be reliably demonstrated e.g.
2043 1286 annually laminated records. Whatever the cause, repeating chemical signatures are
2044 1287 probably the greatest challenge to the refinement of any tephrostratigraphic scheme, and
2045 1288 may only be resolved by more comprehensive assays of the major, minor and trace element
2046 1289 compositions of the glass components of each tephra layer, coupled with a detailed
2047 1290 understanding of the stratigraphic context (Lowe, 2011; Lowe, D. et al., 2017).
2048
2049
2050
2051
2052
2053
2054
2055
2056
2057
2058
2059
2060
2061
2062
2063
2064
2065

2066
2067
2068
2069 1291
2070 1292 A further target for future research will be refinement of the age estimates assigned to each
2071 1293 tephra isochron, for a number of those included in the tephrostratigraphic framework outlined
2072 1294 here presently have wide ranges or conflicting age estimates. Examples include the Penifiler
2073 1295 Tephra (see section 3.3.1), the Askja-S Tephra (section 3.5.3) and the Saksunarvatn Ash,
2074 1296 this last example made more complicated by the likelihood that several closely-spaced
2075 1297 eruptions have become conflated under the single name (section 3.5.6). Since these age
2076 1298 uncertainties compromise the use of tephra isochrons for the development or testing of age
2077 1299 models based on other methods, the search for new sites which offer opportunities for
2078 1300 significantly reducing the uncertainties must be a priority. In this regard we advocate the
2079 1301 RESET approach (Bronk Ramsey et al., 2015; Lowe et al., 2015), where all the
2080 1302 chronological information associated with an individual tephra isochron is evaluated using
2081 1303 Bayesian probabilistic modelling to generate an optimised age estimate. This has the
2082 1304 potential advantage, depending on the number and uncertainty ranges of the dates
2083 1305 available, that no single erroneous estimate will heavily bias the outcome, although it is
2084 1306 recommended that this is only applied to sequences where correlations are robust and
2085 1307 unequivocal.
2086 1308
2087 1309 Finally, a more fully developed and secure tephrostratigraphic scheme potentially can yield a
2088 1310 number of dividends, not only in terms of improved dating and correlation of sedimentary
2089 1311 sequences, but also with respect to important palaeoenvironmental questions. For example,
2090 1312 it is noticeable that for the period 16-11.7 ka, only four clearly-defined tephras have been
2091 1313 detected in sites in the British Isles (the Dimna, Borrobol, Penifiler and Vedde), although
2092 1314 there are tentative signs that others may be added in due course. This record contrasts
2093 1315 starkly, however, with the much higher number of tephra layers detected in the shorter
2094 1316 period between 11.7 and 8 ka (Figure 12). The question that arises is what may have
2095 1317 caused this difference. One possibility is an increased frequency and perhaps magnitude of
2096 1318 volcanic eruptions in Iceland during the early Holocene. Tephrochronological research in
2097 1319 Iceland is increasingly pointing to a connection between the frequency and magnitude of
2098 1320 volcanic activity on the one hand, and glacial unloading due to a warming climate on the
2099 1321 other (e.g. Maclennan et al., 2002; Carrivick et al., 2009; Sigmundsson et al., 2010).
2100 1322 However, an alternative explanation for this contrast in the British tephrostratigraphical
2101 1323 record would be a major change in climatic regime in the North Atlantic region between the
2102 1324 end of the Pleistocene and start of the Holocene, which resulted in more ash plumes being
2103 1325 driven from Iceland towards the British Isles in the latter period. It is difficult on present
2104 1326 evidence to support either argument. There are also apparent notable differences in the
2105 1327 trajectories and dispersal limits of individual tephra layers, but these may be misleading due

2125
2126
2127 1328 to geographical bias in the distribution of sites from which detailed tephrostratigraphic
2128 records have been obtained and the degree to which some tephra layers have been
2129 1329 preferentially targeted. Hence caution should be exercised when drawing conclusions about
2130 1330 the factors that influenced tephra dispersal patterns (e.g. magnitude of eruption; wind
2131 strength and direction; seasonal climatic conditions) until more robust tephra 'footprints' over
2132 1331 Europe become available.
2133 1332
2134 1333
2135 1334

2136 1334
2137 1335 **6. Conclusions and recommendations**
2138 1336

2139 1336
2140 1337 The synthesis presented here, obtained from 54 sites and including 26 well established or
2141 potential eruptives, indicates the British Isles to be one of the most intensely studied regions
2142 1338 in the world for cryptotephra deposition. This network of sites offers an exceptional
2143 1339 opportunity for testing the timing of abrupt climatic transitions and their environmental,
2144 1340 archaeological and geological impacts during the LGIT. It is hoped that the tephra framework
2145 1341 presented here will, in time, help to resolve some of the long standing debates concerning
2146 1342 the precise chronology of events in the British Isles and Europe during the LGIT (e.g. Lowe,
2147 1343 2001; Palmer and Lowe, 2017; Peacock and Rose, 2017). Tephrochronology has the
2148 1344 potential to emerge as a ubiquitous connecting and dating method to support late
2149 1345 Quaternary palaeoenvironmental investigations, and is capable of enhancing and testing
2150 1346 more traditional geochronological techniques, given sufficient integration and development.
2151 1347 A systematic search for tephra in many more European palaeoclimate investigations should
2152 1348 foster more robust correlations, and allow the reconstruction of environmental changes with
2153 1349 a greater degree of finesse than has been achieved hitherto. It is essential therefore that
2154 1350 local tephra frameworks are developed in new regions, and particularly in areas where little
2155 1351 tephra exploration has been undertaken to date. As previously noted, very few tephras of
2156 1352 LGIT age have been identified in England, Wales and Ireland, while the level of such enquiry
2157 1353 is even lower for many other European countries.
2158 1354
2159 1355

2160 1355
2161 1356 Whilst it is now possible to precisely link sequences from the British Isles to Greenland,
2162 1357 Scandinavia, continental Europe and the Mediterranean region, with further development,
2163 1358 the potential for much wider trans-continental synchronisation appears to be within grasp.
2164 1359 The recent discovery of the Glacier Peak B Tephra in Scotland (Pyne-O'Donnell and Jensen,
2165 1360 2018) and the coeval discovery of the Glacier Peak and Mount St Helens J eruptions at
2166 1361 Finglas River (reported here) are significant finds which adds to the growing body of
2167 1362 literature describing ultra-distal tephras in the British Isles (Jensen et al. 2014; Plunkett and
2168 1363 Pilcher, 2018). Studies focused on mid to late Holocene records in Europe and the North
2169 1364 Atlantic margin are already reporting the discovery of multiple trans-continental ashes from a

2184
2185
2186
2187
2188
2189
2190
2191
2192
2193
2194
2195
2196
2197
2198
2199
2200
2201
2202
2203
2204
2205
2206
2207
2208
2209
2210
2211
2212
2213
2214
2215
2216
2217
2218
2219
2220
2221
2222
2223
2224
2225
2226
2227
2228
2229
2230
2231
2232
2233
2234
2235
2236
2237
2238
2239
2240
2241
2242

1365 variety of volcanic centres (Van der Bilt et al. 2017; Watson et al., 2017; Cook et al., 2018b);
1366 there is no good reason, therefore, why tephra from these centres should remain
1367 unregistered in records spanning the LGIT.

1368
1369 The challenges summarised above are not unique to the LGIT, or to the British Isles, but
1370 serve to highlight some important considerations for optimising tephrostratigraphic
1371 investigations and the construction of regional tephrostratigraphic frameworks, especially
1372 where the evidence comprises or includes cryptotephra layers with very low shard
1373 concentrations. Key recommendations for adoption are some or preferably all of the
1374 following:

- 1375
1376 • Contiguous sampling of sedimentary records at a coarse stratigraphic resolution,
1377 followed by more intensive re-sampling at a finer resolution, is an efficient approach
1378 for achieving a thorough assessment of a sites (crypto-)tephra content; this
1379 approach, however, promotes coverage over detail, with the potential result that
1380 eruptions represented by trace amounts of cryptotephra could be overlooked; this is
1381 particularly evident where more ‘minor’ (crypto-)tephras coincide with eruptions that
1382 produce more copious ash-fall; refined contiguous sampling at high stratigraphic
1383 resolution may therefore be required to detect and resolve these instances of
1384 conflated tephra layers (see Timms et al., 2017, 2018);
- 1385
1386 • The chemical classification of tephra layers has traditionally relied on the
1387 measurement of major and minor element ratios, an approach which has often
1388 proved inadequate as a discriminatory tool, especially for distinguishing between
1389 successive tephra from the same volcanic source (as in the case of the Borrobol-
1390 type tephra discussed here); for greater discriminatory power, therefore, recourse to
1391 the analysis of trace (including rare-earth) elements should perhaps become more
1392 routine;
- 1393
1394 • The development of a (crypto-)tephrostratigraphy is best conducted in parallel with
1395 detailed litho-, bio- and climatostratigraphic investigations, particularly where these
1396 provide regionally consistent ‘zones’ which can aid in the interpretation and
1397 correlation of tephra;

2243
2244
2245
2246
2247
2248
2249
2250
2251
2252
2253
2254
2255
2256
2257
2258
2259
2260
2261
2262
2263
2264
2265
2266
2267
2268
2269
2270
2271
2272
2273
2274
2275
2276
2277
2278
2279
2280
2281
2282
2283
2284
2285
2286
2287
2288
2289
2290
2291
2292
2293
2294
2295
2296
2297
2298
2299
2300
2301

- 1399 • Where possible, tephra layers should be dated independently and all chronological
1400 information for individual isochrons integrated using a Bayesian age modelling
1401 procedure;
- 1402
- 1403 • The primary limitation in developing a regional (crypto-)tephrostratigraphic framework
1404 is the time needed to detect, extract, chemically fingerprint and independently date
1405 glass shards representing the individual tephra layers, and hence further
1406 experimental work that leads to significant paring of the laborious procedures
1407 involved would greatly augment the potential applications of (crypto-
1408)tephrochronology.

1410 The framework proposed here marks a major step in the consolidation of tephrostratigraphic
1411 data dating to the LGIT in NW Europe. The scheme is, however, a work in progress and we
1412 hence encourage efforts to further refine the scheme, if possible by adopting the above
1413 recommendations, in order to enhance its potency as an aid for the correlation and dating of
1414 events during the LGIT.

1415

1416

1417 **Acknowledgements**

1418 The authors would like to express their gratitude to the numerous researchers whose hard
1419 work over the past thirty years has formed the basis of this review. In particular we'd like to
1420 thank all those former MSc Quaternary Science students at Royal Holloway who have
1421 conducted exploratory tephrostratigraphic investigations at a number of sites in the British
1422 Isles and whose provisional results have been compiled here. A special note of thanks, must
1423 also go to Elaine Turton (RHUL), Katy Flowers (RHUL), Dr Sean Pyne-O'Donnell, Dr Mark
1424 Hardiman (Portsmouth), Dr Paul Lincoln (RHUL) and Dr Chris Hayward (Edinburgh), whose
1425 advice and technical assistance given to many researchers over the past few years has
1426 proved invaluable to the development of this tephrostratigraphic scheme. In addition, we
1427 would like to extend our thanks to Jonathan Moles (OU) for information on the Tindfjallajökull
1428 and Torfajökull volcanoes, and also to Professor David Lowe (Waikato) and Dr Peter Abbott
1429 (Bern/Cardiff) for agreeing to review the manuscript and for providing thorough and
1430 constructive comments. Some of the data compiled in this review was funded by the RAPID
1431 Climate Change research programme (NERC project number: NE/C509158/1) awarded in
1432 2005 and the RESET project (NERC project number: NE/E015905/1) awarded in 2007. RT
1433 would like to acknowledge funding from Royal Holloway University of London (RHUL) in the
1434 form of a Reid scholarship, and thank the Quaternary Research Association (QRA) for the
1435 receipt of a 'New Research Workers Award' which assisted in the collection and analysis of

2302
2303
2304 1436 Orcadian lake records reported here. IM completed the work on LAN1-325 while in receipt of
2305 1437 a Reid scholarship (RHUL) and funded by Archaeological Development Services Ltd. JL
2306 1438 acknowledges the Leverhulme Trust (project number: EM-2014-025) for financial support for
2307 1439 some of the field and laboratory results in Scottish sites presented herein. This paper is an
2308 1440 output of the EXTRAS project '*EXTending tephRAS as a global geoscientific research tool*
2309 1441 *stratigraphically, spatially, analytically, and temporally*' led by the International focus group
2310 1442 on tephrochronology and volcanism (INTAV) of the International Union for Quaternary
2311 1443 Research (INQUA).
2312 1444
2313 1445
2314 1446
2315 1447
2316 1448
2317 1449
2318 1450
2319 1451
2320 1452
2321 1453
2322 1454
2323 1455
2324 1456
2325 1457
2326 1458
2327 1459
2328 1460
2329 1461
2330 1462
2331 1463
2332 1464
2333 1465
2334 1466
2335 1467
2336 1468
2337 1469
2338 1470
2339 1471
2340 1472
2341 1473
2342 1474
2343 1475
2344 1476
2345 1477
2346 1478
2347 1479
2348 1480
2349 1481
2350 1482
2351 1483
2352 1484
2353 1485
2354 1486
2355 1487
2356 1488
2357 1489
2358 1490
2359 1491
2360 1492

2361
2362
2363
2364
2365
2366
2367
2368
2369
2370
2371
2372
2373
2374
2375
2376
2377
2378
2379
2380
2381
2382
2383
2384
2385
2386
2387
2388
2389
2390
2391
2392
2393
2394
2395
2396
2397
2398
2399
2400
2401
2402
2403
2404
2405
2406
2407
2408
2409
2410
2411
2412
2413
2414
2415
2416
2417
2418
2419

1473 **Figure Captions**

1474

1475 Figure 1

1476 Overview of the British Isles and location of volcanic centres discussed in text that contribute
1477 to the British and European tephra frameworks.

1478

1479 Figure 2

1480 Summary of LGIT tephrostratigraphic sites in the British Isles. Note: only sites where glass
1481 shards from tephtras have been chemically characterised are included here. Each site is
1482 represented by a segmented chart with the coloured sections corresponding to the presence
1483 of a particular tephtra. A coloured section affixed with a ? symbol indicates a degree of
1484 uncertainty with the correlation. A ? symbol overlapping several segments signifies a likely
1485 correlation to one of those tephtra, but at present a correlation is indeterminable. A
1486 complementary schematic is presented in Supplementary Figure S1 which includes
1487 individual site stratigraphic data, negative findings of glass shards and sites whereby tephtra
1488 have been assigned on the premise of stratigraphy. A tabulated summary of tephtra
1489 correlations and sampling strategies can be found in Supplementary Table S1. Glass-shard
1490 compositional analyses used to make these correlations can be accessed from
1491 Supplementary Table S2.

1492

1493 Figure 3

1494 Last Termination or Last Glacial to Interglacial Transition (LGIT) event stratigraphy for
1495 Greenland, NW Europe, and the British Isles. The Greenland event stratigraphy is divided
1496 into Stadials (GS: cold phase), and Interstadials (GI: warm phase), with comparable, but not
1497 necessarily synchronous phases identified in European and British climate archives. GI-1 is
1498 divided into seven subunits, with (GI-1d, GI-1c2, GI1b) reflecting short lived cold events
1499 punctuating an otherwise comparatively warm interval (GI-1e, GI-1c3, GI-1c1, GI-1a; Björck
1500 et al. 1998; Rasmussen et al. 2006). In the early Holocene a number of similar reversion
1501 episodes are also identified, most notably the 11.4 ka event (Pre-Boreal Oscillation), 9.3 ka
1502 event and the 8.2 ka event. The example stratigraphy (Loch Etteridge) shows how these
1503 climatic events can be expressed in the sedimentological record, a pattern which can be
1504 recognised in basin sediments across the British Isles (Walker and Lowe, 2017).

1505

1506 Figure 4

1507 Selected chemical bi-plots of non-normalised glass compositional data from Dimlington
1508 Stadial tephtras identified in Scottish sequences. Correlations can be made to the Dimna Ash
1509 (Koren et al., 2008) and the Borrobol-type tephtra series. Low CaO wt % values exhibited by

2420
2421
2422 1510 glass analyses of the Dimlington Borrobol-type tephra negates a correlation to the
2423
2424 1511 Greenland GS-2.1 Borrobol-type tephra identified by Cook et al. (2018). The Dimlington
2425 1512 Borrobol-type tephra is therefore given the provisional name of 'Tanera Tephra' after the
2426
2427 1513 island where this tephra is presently most clearly defined. The site-specific glass analytical
2428 1514 data used for this figure is included in Supplementary Table S2. References for the chemical
2429
2430 1515 envelopes are listed in Supplementary Table S3.

2431 1516
2432
2433 1517 Figure 5
2434 1518 Schematic showing the inconsistent stratigraphic interpretation of the Borrobol-type tephra
2435 1519 series at the site of Borrobol, NW Scotland. Records from: A) Turney et al., (1997); B) Pyne-
2436
2437 1520 O'Donnell, (2007); C) Lind et al., (2016).

2438 1521
2439
2440 1522 Figure 6
2441 1523 Selected chemical bi-plots of non-normalised glass compositional data showing the similarity
2442
2443 1524 between the basaltic component of the Penifiler Tephra identified at Loch Ashik and the
2444 1525 NGIP-1573m Tephra. These tephra have an overlapping age estimate and share
2445 1526 indistinguishable glass compositions that match with those of the Katla volcanic centre and
2446 1527 of the Vedde Ash-type tephra series. The Loch Ashik glass analyses used for this figure are
2447 1527 included in Supplementary Table S2. References for the chemical envelopes are listed in
2448 1528
2449 1528 Supplementary Table S3.

2450 1529
2451 1530
2452
2453 1531 Figure 7
2454 1532 Selected chemical bi-plots of non-normalised glass compositional data for tephtras identified
2455 1533 at Finglas River. Three glass compositional populations can be identified, group A matches
2456 1533 with the Glacier Peak G Tephra, shard B matches with the Mount St Helens J Tephra and
2457 1534 shard C matches with the Borrobol-type series. The Finglas River glass analyses used for
2458 1534
2459 1535 this figure are included in Supplementary Table S2. References for the chemical envelopes
2460 1536
2461 1536 are listed in Supplementary Table S3.

2462 1537
2463 1538
2464
2465 1539 Figure 8
2466 1540 Selected chemical bi-plots of non-normalised glass compositional data comparing the
2467 1541 Roddans Port and LAS-1 tephtras with regional marker horizons of equivalent Windermere
2468 1541
2469 1542 Interstadial (WI) age. Some similarity can be observed between the analyses of the Roddans
2470 1543 Port B and LAS-1(B) glass shards with those from North American centres (i.e. Glacier Peak
2471 1543 and Mount St Helens), however, this similarity is not consistent across all major and minor
2472 1544 elements. The Roddans Port and LAS-1 glass analyses used for this figure are included in
2473 1545
2474 1545

2475
2476
2477
2478

2479
2480
2481 1546 Supplementary Table S2. References for the chemical envelopes are listed in
2482
2483 1547 Supplementary Table S3.
2484 1548
2485
2486 1549 Figure 9
2487 1550 Selected chemical bi-plots of non-normalised glass compositional data from the Abernethy
2488
2489 1551 Tephra plotted against glass analyses of the Vedde Ash and Windermere Interstadial (WI)
2490 1552 Borrobol-type tephtras. It is clear that in two of the three sites where the Abernethy Tephra
2491
2492 1553 has been analysed, the layer in question has returned a bi-modal glass compositional
2493 1554 signature. The site-specific glass analyses used for this figure are included in Supplementary
2494
2495 1555 Table S2. References for the chemical envelopes are listed in Supplementary Table S3.
2496 1556
2497 1557 Figure 10
2498
2499 1558 Chemical bi-plot (MgO vs. TiO₂) of non-normalised glass analyses from tephtras originating
2500 1559 in the Torfajökull volcanic centre during the early Holocene. An enrichment in TiO₂, Al₂O₃,
2501
2502 1560 MgO and CaO is noted in postglacial rhyolitic rocks from this centre (McGarvie et al., 1990).
2503 1561 This trend seems to apply to a the majority of the Torfajökull-type tephtras identified in the
2504
2505 1562 British Isles, however, the An Druim-Høvðarhagi Tephra seems to partially reverse this,
2506 1563 exhibiting both a 'less-evolved' and 'more-evolved' bi-modal glass composition. The site
2507
2508 1564 specific glass analyses used for this figure are included in Supplementary Table S2.
2509 1565 References for the chemical envelopes are listed in Supplementary Table S3.
2510
2511 1566
2512 1567 Figure 11
2513 1568 Chemical bi-plot (CaO vs. MgO) of non-normalised glass analyses from tephtras correlated to
2514
2515 1569 the Saksunarvatn 10-ka series in the British Isles. The 'Saksunarvatn Ash' at Loch Ashik has
2516 1570 been reassigned to the Havn-3/ Havn-4 Tephra on the premise of characteristically 'low'
2517
2518 1571 MgO wt % values (Wastegård et al., 2018). The 'Saksunarvatn' Ash layer identified at
2519 1572 Crudale Meadow by Bunting (1994) exhibits a bi-modal glass composition, group A
2520
2521 1573 correlates to the Grímsvötn volcanic centre, whilst group B shows a greater affinity to glass
2522 1574 analyses of the Veiðivötn-Bárðarbunga system. The site specific glass analyses used for this
2523
2524 1575 figure are included in Supplementary Table S2. References for the chemical envelopes are
2525 1576 listed in Supplementary Table S3.
2526
2527 1577
2528 1578 Figure 12
2529 1579 Regional tephrostratigraphic scheme for the British Isles. A) GICC05 δ¹⁸O ‰, and regional
2530
2531 1580 event stratigraphy (Rasmussen et al., 2006). B) Crudale Meadow sediment stratigraphy;
2532
2533 1581 note the three numbered minerogenic bands within the Interstadial marl sediments (Timms
2534 1582 et al., 2018). C) Tanera Mòr 1 sediment stratigraphy, note the absence of any

2538
2539
2540 1583 sedimentological change through the Interstadial sediments (Timms, 2016). D) Oxygen-
2541 1584 isotope record from Crudale Meadow (Whittington et al., 2015). E) Chironomid derived
2542 1584 isotope record from Crudale Meadow (Whittington et al., 2015). E) Chironomid derived
2543 1585 summer temperature reconstruction from Muir Park Reservoir (Brooks et al., 2016). F)
2544 1586 Regional tephrostratigraphic scheme for the British Isles, bar length denotes degrees of
2545 1586 confidence: (i) those considered to be based on the most robust glass analytical data, with
2546 1587 consistent stratigraphic positions and well-defined ages (n=6); (ii) those for which reasonably
2547 1588 robust glass analytical data are available, but questions remain about their precise origins or
2548 1588 age (n=9); and (iii) those most in need of further investigation, to test their potential to serve
2549 1589 as regional isochrons (n=11). Note: the alignment of the individual proxy series with the
2550 1590 GICC05 event stratigraphy is not intended to illustrate climatic synchronicity between the
2551 1590 records.
2552 1591
2553 1592
2554 1592
2555 1593
2556 1594
2557 1594

2558 1595 **Table Captions**

2559 1596
2560 1596
2561 1597 Table 1
2562 1598 Combined non-normalised glass-shard analytical data of tephtras identified in the British Isles
2563 1598 dating to the Last Glacial to Interglacial Transition (LGIT c. 16-8 ka BP). The value shown in
2564 1599 the 'Number of sites' row relates only to those locations where correlations are secure: see
2565 1600 Supplementary Table S1 for further details on the number of tentative correlations for each
2566 1601 tephtra. Mean glass data derived from: Roberts, (1997); Turney et al. (1997); Darville, (2011);
2567 1601 Davies et al. (2001); Mackie et al. (2002); Ranner et al. (2005); Pyne-O'Donnell, (2007),
2568 1602 Matthews, (2008); Pyne-O'Donnell et al. (2008); Matthews et al. (2011); Lane et al. (2012a);
2569 1603 Weston, (2012); MacLeod et al. (2015); Mithen et al. (2015); Lind et al. (2016); Timms,
2570 1603 (2016); Jones et al. (2017); Kelly et al. (2017); Lowe et al., (2017); Timms et al. (2017,
2571 1604 2018); Lowe et al. (in prep). Glass compositional data are available in full from
2572 1605 Supplementary Table S2.
2573 1605
2574 1606
2575 1607
2576 1607
2577 1608
2578 1609
2579 1609

2580 1610 Table 2
2581 1611 List of sites in the British Isles where the Borrobol (n=13), Penifiler (n=15) and CRUM1 597
2582 1612 tephtras have been proposed. Based on major and minor element analyses of glass shards,
2583 1612 13 sites are understood to contain the Borrobol Tephra, 15 sites the Penifiler Tephra and 2
2584 1613 sites the CRUM1 597 Tephra. A further 3 Borrobol, 4 Penifiler and 4 CRUM1 597 records
2585 1614 are tentatively proposed based on stratigraphic superposition and are indicated by a ?
2586 1614 symbol.
2587 1615
2588 1616
2589 1616
2590 1617

2591 1618 Table 3
2592 1618
2593
2594
2595
2596

2597
2598
2599 1619 Sites from which glass analyses have been obtained and used to claim the presence of the
2600 1620 'Abernethy Tephra'. In all cases except the Glen Turret Fan record, a mixed chemical
2602 1621 assemblage has been revealed, implicating the possibility of reworking and amalgamation of
2603 1622 older tephra deposits.
2604 1623
2605 1624
2606 1625 Table 4
2607 1626 Summary of tephra isochrons included, and those not yet considered suitable for inclusion,
2608 1627 within the British Isles tephrostratigraphic scheme (c. 16-8 ka BP). Also shown are reference
2609 1628 records for each tephra; these are the sites in the British Isles which each tephra is currently
2610 1629 best represented at. Categories i, ii and iii are explained in the text.
2611 1630
2612 1631
2613 1632 **Supplementary Files**
2614 1633
2615 1634
2616 1635
2617 1636
2618 1637
2619 1638
2620 1639
2621 1640
2622 1641
2623 1642
2624 1643
2625 1644
2626 1645
2627 1646
2628 1647
2629 1648
2630 1649
2631 1650
2632 1651
2633 1652
2634 1653
2635 1654
2636 1655
2637 1656
2638 1657
2639 1658
2640 1659
2641 1660
2642 1661
2643 1662
2644 1663
2645 1664
2646 1665
2647 1666
2648 1667
2649 1668
2650 1669
2651 1670
2652 1671
2653 1672
2654 1673
2655 1674

2656
2657
2658 1656 corresponding 'comments' column. A * symbol in association with the site co-ordinates
2659 1657 denotes an approximate position only and not the exact core location.
2661 1658
2662
2663 1659 Supplementary Table S2
2664 1660 Database of major and minor element analyses for glass shards reported from tephra
2665 1661 records in the British isles dating to the LGIT (c. 16-8 ka BP). Data presented as raw (un-
2667 1662 normalised) and normalised.
2668 1663
2669 1663
2670 1664 Supplementary Table S3
2671 1665 Reference list for analyses used to derive bi-plot figure envelopes.
2672 1666
2673 1666
2674 1667
2675 1667
2676 1668
2677 1669
2678 1669
2679 1670
2680 1671
2681 1671
2682 1672
2683 1673
2684 1673
2685 1674
2686 1675
2687 1675
2688 1676
2689 1677
2690 1677
2691 1678
2692 1679
2693 1680
2694 1680
2695 1681
2696 1682
2697 1682
2698 1683
2699 1684
2700 1684
2701 1685
2702 1686
2703 1686
2704 1687
2705 1688
2706 1688
2707 1689
2708 1690
2709 1691
2710 1691
2711 1692
2712
2713
2714

2715
2716
2717 1693
2718
2719 1694 **References**
2720 1695 Abbott, P.M. and Davies, S.M. 2012. Volcanism and the Greenland ice-cores: the tephra
2721 record. *Earth-Science Reviews* 115,173-191.
2722 1696
2723 1697
2724
2725 1698 Abbott, P.M., Griggs, A.J., Bourne, A.J., Chapman, M.R., Davies, S.M. 2018. Tracing marine
2726 cryptotephra in the North Atlantic during the last glacial period: Improving the North Atlantic
2727 marine tephrostratigraphic framework. *Quaternary Science Reviews* 189, 169-186.
2728 1700
2729 1701
2730 1702 Albert, P. 2007. *Tephrostratigraphical investigation of Loch Etteridge: stratigraphical*
2731 *uncertainties*. Unpublished MSc Thesis, University of London.
2732 1703
2733 1704
2734
2735 1705 Bakke, J., Lie, Ø., Heegaard, E., Dokken, T., Haug, G.H., Birks, H.H., Dulski, P. Nilsen, T.
2736 1706 2009. Rapid oceanic and atmospheric changes during the Younger Dryas cold period.
2737 *Nature Geoscience* 2, 202-205.
2738 1707
2739 1708
2740
2741 1709 Ballantyne, C.K. 2002. Paraglacial geomorphology. *Quaternary Science Reviews* 21, 1935-
2742 1710 2017.
2743
2744 1711
2745 1712 Ballantyne, C. K. 2010. Extent and deglacial chronology of the last British–Irish Ice Sheet:
2746 implications of exposure dating using cosmogenic isotopes. *Journal of Quaternary Science*
2747 1713 25, 515–34.
2748 1714
2749 1715
2750
2751 1716 Ballantyne, C.K. 2012. Chronology of glaciation and deglaciation during the Loch Lomond
2752 (Younger Dryas) Stade in the Scottish Highlands: implications of recalibrated 10Be exposure
2753 1717 ages. *Boreas* 41, 513-526.
2754 1718
2755 1719
2756
2757 1720 Ballantyne, C.K., Harris, C. 1994: *The Periglaciation of Great Britain*. Cambridge: Cambridge
2758 1721 University Press.
2759
2760 1722
2761 1723 Ballantyne, C.K., Small, D. 2018. The last Scottish ice sheet. *Earth and Environmental*
2762 *Science Transactions of the Royal Society of Edinburgh*, 1-39 (in First View:
2763 1724 doi.org/10.1017/S1755691018000038)
2764 1725
2765 1726
2766
2767 1727 Ballantyne, C.K., Schnabel, C., Xu, S. 2009. Readvance of the last British–Irish ice sheet
2768 1728 during Greenland interstade 1 (GI-1): the Wester Ross readvance, NW Scotland. *Quaternary*
2769 *Science Reviews* 28, 783-789.
2770 1729
2771
2772
2773

2774
2775
2776 1730
2777
2778 1731 Barber, K., Langdon, P., Blundell, A. 2008. Dating the Glen Garry tephra: a widespread late-
2779 1732 Holocene marker horizon in the peatlands of northern Britain. *The Holocene* 18, 31-43.
2780
2781 1733
2782 1734 Bennett, K.D., Boreham, S., Sharp, M.J., Switsur, V.R. 1992. Holocene history of
2783 environment, vegetation and human settlement on Catta Ness, Lunnasting, Shetland.
2784 1735 *Journal of Ecology* 80, 241-273.
2785 1736
2786
2787 1737
2788 1738 Bertrand, S., Daga, R., Bedert, R., Fontijn, K. 2014. Deposition of the 2011–2012 Cordón
2789 1739 Caulle tephra (Chile, 40°S) in lake sediments: Implications for tephrochronology and
2790 volcanology. *Journal of Geophysical Research: Earth Surface* 119, 2555-2573.
2791 1740
2792 1741
2793
2794 1742 Bickerdike, H.L., Evans, D.J.A., Stokes, C.R. Ó Cofaigh, C. 2018. The glacial
2795 1743 geomorphology of the Loch Lomond (Younger Dryas) Stadial in Britain: a review. *Journal of*
2796 *Quaternary Science* 33, 1-54.
2797 1744
2798 1745
2799
2800 1746 Birks, H.J. 1989. Holocene isochrone maps and patterns of tree-spreading in the British
2801 1747 Isles. *Journal of Biogeography* 503-540.
2802
2803 1748
2804 1749 Birks, H.H., Gulliksen, S., Hafliðason, H., Mangerud, J., Possnert, G. 1996. New radiocarbon
2805 1750 dates for the Vedde Ash and the Saksunarvatn Ash from western Norway. *Quaternary*
2806 *Research* 45,119-127.
2807 1751
2808 1752
2809
2810 1753 Björck, S., Walker, M.J., Cwynar, L.C., Johnsen, S., Knudsen, K.L., Lowe, J.J., Wohlfarth, B.
2811 1754 1998. An event stratigraphy for the Last Termination in the North Atlantic region based on
2812 the Greenland ice-core record: a proposal by the INTIMATE group. *Journal of Quaternary*
2813 1755 *Science* 13, 283-292.
2814 1756
2815
2816 1757
2817 1758 Björck, J., Wastegård, S. 1999. Climate oscillations and tephrochronology in eastern middle
2818 Sweden during the last glacial–interglacial transition. *Journal of Quaternary Science* 14 (5),
2819 1759 399-410.
2820 1760
2821 1761
2822
2823 1762 Björck, S., Muscheler, R., Kromer, B., Andresen, C.S., Heinemeier, J., Johnsen, S.J.,
2824 1763 Conley, D., Koç, N., Spurk, M., Veski, S. 2001. High-resolution analyses of an early
2825 Holocene climate event may imply decreased solar forcing as an important climate trigger.
2826 1764 *Geology* 29, 1107-1110.
2827 1765
2828
2829 1766
2830
2831
2832

2833
2834
2835 1767 Blackford J.J., Edwards K.J., Dugmore A.J., Cook G.T. Buckland P.C. 1992. Icelandic
2836 1768 volcanic ash and the mid-Holocene pollen decline in northern Scotland. *The Holocene* 2 (3),
2838 1769 260-265.
2839
2840 1770
2841 1771 Blockley, S.P.E., Pyne-O'Donnell, S.D.F., Lowe, J.J., Matthews, I.P., Stone, A., Pollard,
2842 1772 A.M., Turney, C.S.M., Molyneux, E.G. 2005. A new and less destructive laboratory
2844 1773 procedure for the physical separation of distal glass tephra shards from sediments.
2845 1774 *Quaternary Science Reviews* 24, 1952-1960.
2846
2847 1775
2848 1776 Blockley, S.P., Ramsey, C.B., Pyle, D.M. 2008. Improved age modelling and high-precision
2849 1777 age estimates of late Quaternary tephtras, for accurate palaeoclimate reconstruction. *Journal*
2850 1778 *of Volcanology and Geothermal Research* 177, 251-262.
2851
2852 1779
2853 1780 Blockley, S.P., Bourne, A.J., Brauer, A., Davies, S.M., Hardiman, M., Harding, P.R., Lane,
2854 1781 C.S., MacLeod, A., Matthews, I.P., Pyne-O'Donnell, S.D., Rasmussen, S.O, Wulf, S. and
2857 1782 Zanchetta, G. 2014. Tephrochronology and the extended intimate (integration of ice-core,
2858 1783 marine and terrestrial records) event stratigraphy 8–128 ka b2k. *Quaternary Science*
2860 1784 *Reviews* 106, 88-100.
2861
2862 1785
2863 1786 Bond, G.C., Mandeville, C., Hoffmann, S. 2001. Were rhyolitic glasses in the Vedde Ash and
2864 1787 in the North Atlantic's Ash Zone 1 produced by the same volcanic eruption?. *Quaternary*
2865 1788 *Science Reviews* 20, 1189-1199.
2867 1789
2868
2869 1790 Bondevik, S., Mangerud, J., Dawson, S., Dawson, A., Lohne, Ø. 2005. Evidence for three
2870 1791 North Sea tsunamis at the Shetland Islands between 8000 and 1500 years ago. *Quaternary*
2871 1792 *Science Reviews* 24, 1757–1775.
2872
2873 1793
2874
2875 1794 Bourne, A.J., Lowe, J.J., Trincardi, F., Asioli, A., Blockley, S., Wulf, S., Matthews, I.P., Piva,
2876 1795 A., Vigliotti, L. 2010. Distal tephra record for the last ca 105,000 years from core PRAD 1-2
2877 1796 in the central Adriatic Sea: implications for marine tephrostratigraphy. *Quaternary Science*
2879 1797 *Reviews* 29, 3079-3094.
2880
2881 1798
2882 1799 Bourne, A.J., Albert, P.G., Matthews, I.P., Trincardi, F., Wulf, S., Asioli, A., Blockley, S.P.E.,
2883 1800 Keller, J., Lowe, J.J. 2015a. Tephrochronology of core PRAD 1-2 from the Adriatic Sea:
2884 1801 insights into Italian explosive volcanism for the period 200–80 ka. *Quaternary Science*
2885 1802 *Reviews* 116, 28-43.
2886
2887 1803
2888
2889
2890
2891

2892
2893
2894 1804 Bourne, A.J., Cook, E., Abbott, P.M., Seierstad, I.K., Steffensen, J.P., Svensson, A., Fischer,
2895 1805 H., Schüpbach, S. Davies, S.M. 2015b. A tephra lattice for Greenland and a reconstruction
2896 1806 of volcanic events spanning 25–45 ka b2k. *Quaternary Science Reviews* 118, 122-141.
2897
2898
2899 1807
2900 1808 Boygle, J. 1999. Variability of tephra in lake and catchment sediments, Svínavatn, Iceland.
2901 1809 *Global and Planetary Change* 21, 129–149.
2902
2903 1810
2904 1811 Bramham-Law, C.W.F., Theuerkauf, M., Lane, C.S., Mangerud, J. 2013. New findings
2905 1812 regarding the Saksunarvatn Ash in Germany. *Journal of Quaternary Science* 28, 248-257.
2906
2907 1813
2908
2909 1814 Brauer, A., Endres, C., Günter, C., Litt, T., Stebich, M. Negendank, J.F. 1999. High
2910 1815 resolution sediment and vegetation responses to Younger Dryas climate change in varved
2911 1816 lake sediments from Meerfelder Maar, Germany. *Quaternary Science Reviews*. 18, 321-329.
2912
2913 1817
2914
2915 1818 Bronk Ramsey, C. 2008. Deposition models for chronological records. *Quaternary Science*
2916 1819 *Reviews* 27, 42-60.
2917
2918 1820
2919 1821 Bronk Ramsey, C. 2009. Dealing with outliers and offsets in radiocarbon dating.
2920 1822 *Radiocarbon* 51, 1023-1045.
2921
2922 1823
2923
2924 1824 Bronk Ramsey, C., Lee, S. 2013. Recent and planned developments of the program OxCal.
2925 1825 *Radiocarbon* 55, 720-730.
2926
2927 1826
2928 1827 Bronk Ramsey, C., Albert, P.G., Blockley, S.P., Hardiman, M., Housley, R.A., Lane, C.S.,
2929 1828 Lee, S., Matthews, I.P., Smith, V.C. and Lowe, J.J. 2015. Improved age estimates for key
2930 1829 Late Quaternary European tephra horizons in the RESET lattice. *Quaternary Science*
2931 1830 *Reviews* 118, 18-32.
2932
2933 1831
2934
2935 1832 Brooks, S.J., Birks, H.J.B. 2000. Chironomid-inferred Late-glacial air temperatures at Whitrig
2936 1833 Bog, Southeast Scotland. *Journal of Quaternary Science* 15, 759-764.
2937
2938 1834
2939
2940 1835 Brooks, S.J., Matthews, I.P., Birks, H.H., Birks, H.J.B. 2012. High resolution Lateglacial and
2941 1836 early-Holocene summer air temperature records from Scotland inferred from chironomid
2942 1837 assemblages. *Quaternary Science Reviews* 41, 67-82.
2943
2944 1838
2945 1839 Brooks, S.J., Davies, K.L., Mather, K.A., Matthews, I.P., Lowe, J.J. 2016.
2946 1840 Chironomid-inferred summer temperatures for the Last Glacial–Interglacial Transition from a
2947
2948
2949
2950

2951
2952
2953 1841 lake sediment sequence in Muir Park Reservoir, west-central Scotland. *Journal of*
2954 1842 *Quaternary Science* 31, 214-224.
2955 1843
2956 1844 Bryant, R.H. 1974. A late-Midlandian section at Finglas River, near Waterville, Kerry.
2957 1845 *Proceedings of the Royal Irish Academy. Section B: Biological, Geological, and Chemical*
2958 1846 *Science* 161-178.
2959 1847
2960 1848 Bunting, M.J. 1994. Vegetation history of Orkney, Scotland: Pollen records from two small
2961 1849 basins in west Mainland. *New Phytologist* 128, 771-792.
2962 1850
2963 1851 Callicott, R. 2013. *Tephrochronology, ice survival of the Lateglacial Interstadial and the*
2964 1852 *timing of the deglaciation of the Loch Lomond Readvance of Eilen Fada Mor, Summer Isles.*
2965 1853 Unpublished BSc Thesis, University of London.
2966 1854
2967 1855 Callicott, R. 2015. *Tephrostratigraphy of a Lateglacial sequence at the Loons, Orkney.*
2968 1856 Unpublished MSc Thesis, University of London.
2969 1857
2970 1858 Candy, I., Abrook, A., Elliot, F., Lincoln, P., Matthews, I.P., Palmer, A. 2016. Oxygen Isotope
2971 1859 evidence for high magnitude, abrupt climatic events during the Late-Glacial Interstadial in
2972 1860 northwest Europe: Analysis of a lacustrine sequence from the site of Tirinie, Scottish
2973 1861 Highlands. *Journal of Quaternary Science* 31, 607-621.
2974 1862
2975 1863 Carrivick, J.L., Russell, A.J., Rushmer, E.L., Tweed, F.S., Marren, P.M., Deeming, H. Lowe,
2976 1864 O.J., 2009. Geomorphological evidence towards a de-glacial control on volcanism. *Earth*
2977 1865 *Surface Processes and Landforms* 34, 1164-1178.
2978 1866
2979 1867 Cook, E., Davies, S.M., Guðmundsdóttir, E.R., Abbott, P.M., Pearce, N.J. 2018. First
2980 1868 identification and characterization of Borrobol-type tephra in the Greenland ice cores: new
2981 1869 deposits and improved age estimates. *Journal of Quaternary Science*. 33, 212-224.
2982 1870
2983 1871 Cook, E., Portnyagin, M., Ponomareva, V., Bazanova, L., Svensson, A., Garbe-Schönberg,
2984 1872 D. 2018b. First identification of cryptotephra from the Kamchatka Peninsula in a Greenland
2985 1873 ice core: Implications of a widespread marker deposit that links Greenland to the Pacific
2986 1874 northwest. *Quaternary Science Reviews* 181, 200-206.
2987 1875
2988
2989
2990
2991
2992
2993
2994
2995
2996
2997
2998
2999
3000
3001
3002
3003
3004
3005
3006
3007
3008
3009

3010
3011
3012 1876 Cooper, R., 1999. *Lithostratigraphy and tephrochronology of sediments spanning the time*
3013 1877 *interval of the Last Glacial-Interglacial Transition at Muir Park Reservoir, Scotland and*
3014 1878 *Sluggan Moss, Ireland*. Unpublished MSc Thesis, University of London.
3015
3016
3017 1879
3018 1880 Clark, C.D., Hughes, A.L., Greenwood, S.L., Jordan, C. Sejrup, H.P. 2012. Pattern and
3019 1881 timing of retreat of the last British-Irish Ice Sheet. *Quaternary Science Reviews*. 44, 112-146.
3020
3021 1882
3022 1883 Clynne, M.A., Calvert, A.T., Wolfe, E.W., Evarts, R.C., Fleck, R.J., Lanphere, M.A. 2008.
3023 1884 The Pleistocene eruptive history of Mount St. Helens, Washington, from 300,000 to 12,800
3024 1885 years before present. In: Sherrod, D.R., Scott, W.E., Stauffer, P.H. (Eds.) *A Volcano*
3025 1886 *Rekindled: the Renewed Eruption of Mount St. Helens, 2004-2006*. U.S. Geological Survey
3026 1887 Professional Paper 1750-28, 593-627.
3027
3028
3029 1888
3030 1889 Dahl, S.O., Nesje, A., Lie, Ø., Fjordheim, K. Matthews, J.A. 2002. Timing, equilibrium-line
3031 1890 altitudes and climatic implications of two early-Holocene glacier readvances during the
3032 1891 Erdalen Event at Jostedalsbreen, western Norway. *The Holocene* 12, 17-25.
3033
3034
3035 1892
3036 1893 Darvill, C.M. 2011. The Lateglacial at Star Carr: A Sedimentological and Stable Isotopic
3037 1894 Investigation of Palaeoenvironmental Change in Northeast England. Unpublished MSc
3038 1895 Thesis, University of London.
3039
3040 1896
3041 1897 Davies, L.J., Jensen, B.J.L., Froese, D.J., Wallace, K.L. 2016. Late Pleistocene and
3042 1898 Holocene tephrostratigraphy of interior Alaska and Yukon: Key beds and chronologies over
3043 1899 the past 30,000 years. *Quaternary Science Reviews* 146, 28-53.
3044
3045
3046 1900
3047 1901 Davies, S.M. 2003. *Extending the known distributions of micro-tephra layers of Last Glacial–*
3048 1902 *Interglacial Transition age in Europe*. Unpublished PhD Thesis, University of London.
3049
3050
3051 1903
3052 1904 Davies, S. M. 2015. Cryptotephra: the revolution in correlation and precision dating. *Journal*
3053 1905 *of Quaternary Science* 30, 114-130.
3054
3055 1906
3056 1907 Davies S.M., Turney C.S.M., Lowe JJ. 2001. Identification and significance of a visible,
3057 1908 basalt-rich Vedde Ash layer in a Late-glacial sequence on the Isle of Skye, Inner Hebrides,
3058 1909 Scotland. *Journal of Quaternary Science* 16, 99-104.
3059
3060
3061 1910
3062 1911 Davies, S.M., Branch, N.P., Lowe, J.J., Turney, C.S. 2002. Towards a European
3063 1912 tephrochronological framework for Termination 1 and the Early Holocene. *Philosophical*
3064
3065
3066
3067
3068

3069
3070
3071 1913 *Transactions of the Royal Society of London A: Mathematical, Physical and Engineering*
3072 *Sciences* 360, 767-802.
3073 1914
3074 1915
3075
3076 1916 Davies S.M., Wastegård, S. Wohlfarth, B. 2003. Extending the limits of the Borrobol Tephra
3077 1917 to Scandinavia and detection of new early Holocene tephra. *Quaternary Research* 59, 345-
3078 1918 352.
3079 1918
3080 1919
3081 1920 Davies, S.M., Wohlfarth, B., Wastegård, S., Andersson, M., Blockley, S., Possnert, G. 2004.
3082 1921 Were there two Borrobol Tephra during the early Lateglacial period: implications for
3083 1922 tephrochronology?. *Quaternary Science Reviews* 23, 581-589.
3084 1922
3085 1923
3086 1923
3087 1924 Davies, S.M., Elmquist, M., Bergman, J., Wohlfarth, B., Hammarlund, D. 2007. Cryptotephra
3088 1924 sedimentation processes within two lacustrine sequences from west central Sweden. *The*
3089 1925 *Holocene* 17, 319-330.
3090 1926
3091 1927
3092 1927
3093 1928 Davies, S.M., Larsen, G., Wastegård, S., Turney, C.S., Hall, V.A., Coyle, L. Thordarson, T.
3094 1929 2010. Widespread dispersal of Icelandic tephra: how does the Eyjafjöll eruption of 2010
3095 1929 compare to past Icelandic events?. *Journal of Quaternary Science* 25, 605-611.
3096 1930
3097 1931
3098 1931
3099 1932 Davies, S.M., Abbott, P.M., Pearce, N.J., Wastegård, S., Blockley, S.P. 2012. Integrating the
3100 1933 INTIMATE records using tephrochronology: rising to the challenge. *Quaternary Science*
3101 1933 *Reviews* 36, 11-27.
3102 1934
3103 1935
3104 1935
3105 1936 Davies, S.M., Abbott, P.M., Meara, R.H., Pearce, N.J., Austin, W.E., Chapman, M.R.,
3106 1937 Svensson, A., Bigler, M., Rasmussen, T.L., Rasmussen, S.O., Farmer, E.J. 2014. A North
3107 1937 Atlantic tephrostratigraphical framework for 130–60 ka b2k: new tephra discoveries, marine-
3108 1938 based correlations, and future challenges. *Quaternary Science Reviews*, 106, 101-121.
3109 1939
3110 1940
3111 1940
3112 1941 Dugmore, A. 1989. Icelandic volcanic ash in Scotland. *The Scottish Geographical Magazine*
3113 1941 105, 168-172.
3114 1942
3115 1943
3116 1943
3117 1944 Dugmore, A.J., Newton, A.J. 1992. Thin tephra layers in peat revealed by X-radiography.
3118 1945 *Journal of Archaeological Science* 19, 163-170.
3119 1945
3120 1946
3121 1947 Eden, D.N., Froggatt, P.C., McIntosh, P.D. 1992. The distribution and composition of
3122 1948 volcanic glass in late Quaternary loess deposits of southern South Island, New Zealand, and
3123 1948 some possible correlations. *New Zealand Journal of Geology and Geophysics* 35, 69-79.
3124 1949
3125
3126
3127

3128
3129
3130 1950
3131
3132 1951 Gehrels, M.J., Newnham, R.M., Lowe, D.J., Wynne, S., Hazell, Z.J., Caseldine, C. 2008.
3133 1952 Towards rapid assay of cryptotephra in peat cores: review and evaluation of various
3134 1953 methods. *Quaternary International* 178, 68-84.
3136 1954
3137
3138 1955 Griggs, A.J., Davies, S.M., Abbott, P.M., Coleman, M., Palmer, A.P., Rasmussen, T.L.,
3139 1956 Johnston, R. 2015. Visualizing tephra deposits and sedimentary processes in the marine
3140 1957 environment: The potential of X-ray microtomography. *Geochemistry, Geophysics,*
3142 1958 *Geosystems* 16, 4329-4343.
3143
3144 1959
3145 1960 Grönvold, K., Óskarsson, N., Johnsen, S.J., Clausen, H.B., Hammer, C.U., Bond, G. Bard,
3146 1961 E. 1995. Ash layers from Iceland in the Greenland GRIP ice core correlated with oceanic
3147 1962 and land sediments. *Earth and Planetary Science Letters* 135, 149-155.
3149 1963
3150
3151 1964 Gudmundsdóttir, E.R., Eiríksson, J., Larsen, G. 2011. Identification and definition of primary
3152 1965 and reworked tephra in Late Glacial and Holocene marine shelf sediments off North Iceland.
3153 1966 *Journal of Quaternary Science* 26, 589-602.
3155 1967
3156
3157 1968 Gudmundsdóttir, E.R., Larsen, G., Eiríksson, J. 2012: Tephra stratigraphy on the North
3158 1969 Icelandic shelf: extending tephrochronology into marine sediments off North Iceland. *Boreas*
3159 1970 41, 719-734.
3160
3161 1971
3162
3163 1972 Gudmundsdóttir, E.R., Larsen, G., Björck, S., Ingólfsson, Ó., Striberger, J. 2016. A new high-
3164 1973 resolution Holocene tephra stratigraphy in eastern Iceland: Improving the Icelandic and
3165 1974 North Atlantic tephrochronology. *Quaternary Science Reviews* 150, 234-249.
3166
3167 1975
3168 1976 Hardiman, M., 2007. *The Lateglacial sediment record in Loch Etteridge, Grampian*
3169 1977 *Highlands, Scotland: tephrostratigraphy and regional tephrocorrelation*. Unpublished BSc
3171 1978 Thesis, University of London.
3172
3173 1979
3174 1980 Harning, D.J., Thordarson, T., Geirsdóttir, Á., Zalzal, K., Miller, G.H. 2018. Provenance,
3175 1981 stratigraphy and chronology of Holocene tephra from Vestfirðir, Iceland. *Quaternary*
3177 1982 *Geochronology* 46, 59-76.
3178
3179 1983
3180 1984 Hayward, C. 2012. High spatial resolution electron probe microanalysis of tephtras and melt
3181 1985 inclusions without beam-induced chemical modification. *The Holocene*, 22, 119-125.
3182
3183 1986
3184
3185
3186

3187
3188
3189 1987 Housley, R.A., Lane, C.S., Cullen, V.L., Weber, M.J., Riede, F., Gamble, C.S., Brock, F.
3190
3191 1988 2012. Icelandic volcanic ash from the Late-glacial open-air archaeological site of Ahrenshöft
3192 1989 LA 58 D, North Germany. *Journal of Archaeological Science* 39, 708-716.
3193
3194 1990
3195 1991 Housley, R.A., MacLeod, A., Nalepka, D., Jurochnik, A., Masojć, M., Davies, L., Lincoln,
3196 P.C., Ramsey, C.B., Gamble, C.S. Lowe, J.J. 2013. Tephrostratigraphy of a Lateglacial lake
3197 1992 sediment sequence at Węgliny, southwest Poland. *Quaternary Science Reviews* 77, 4-18.
3198 1993
3199
3200 1994
3201 1995 Housley, R.A Lincoln, P.C., MacLeod, A. 2018. Tephrochronology of borehole 50a in the
3202 1996 Priest's Well basin. In Reindeer hunters at Howburn Farm, South Lanarkshire, A Late
3203 1997 Hamburgian settlement in southern Scotland - its lithic artefacts and natural environment. ed.
3204 1998 by Ballin, T.B., Saville, A., Tipping, R., Ward, T., Housely, R., Verrill, L., Bradley, M., Wilson,
3205 1999 C., Lincoln, P., MacLeod, A. Oxford: Archaeopress Archaeology: 90-96. ISBN
3208 2000 9781784919016.
3209
3210 2001
3211 2002 Hughes, A.L., Gyllencreutz, R., Lohne, O.S., Mangerud, J., Svendsen, J.I. 2016. The last
3212 2003 Eurasian ice sheets – a chronological database and time-slice reconstruction, DATED-1.
3213 2004 *Boreas* 45, 1-45.
3214 2005
3215 2006
3216 2007
3217 2008 Huntley, B. 1993. Rapid early-Holocene migration and high abundance of hazel (*Corylus*
3218 2009 *avellana* L.): alternative hypotheses. In Chambers, F.M. (ed.), *Climate Change and Human*
3220 2010 *Impact on the Landscape*, Springer, Dordrecht, 205-215.
3221 2011
3222 2012
3223 2013 Jennings, A.E., Grönvold, K., Hilberman, R., Smith, M., Hald, M. 2002. High-resolution study
3224 2014 of Icelandic tephra in the Kangerlussuaq Trough, southeast Greenland, during the last
3225 2015 deglaciation. *Journal of Quaternary Science* 17, 747-757.
3226 2016
3227 2017
3228 2018 Jennings, A., Thordarson, T., Zalzal, K., Stoner, J., Hayward, C., Geirsdóttir, Á., Miller, G.
3230 2019 2014. Holocene tephra from Iceland and Alaska in SE Greenland shelf sediments.
3231 2020 *Geological Society, London, Special Publications* 398, 157-193.
3232 2021
3233 2022
3234 2023
3235 2024 Jensen, B.J., Pyne-O'Donnell, S., Plunkett, G., Froese, D.G., Hughes, P.D., Sigl, M.,
3236 2025 McConnell, J.R., Amesbury, M.J., Blackwell, P.G., van den Bogaard, C. Buck, C.E. 2014.
3237 2020 Transatlantic distribution of the Alaskan white river ash. *Geology* 42, 875-878.
3238 2021
3239 2022
3240 2023 Jøhansen J. 1977. Outwash of terrestrial soils into Lake Saksunarvatn, Faroe Islands.
3241 2024 *Danmarks Geologiske Undersøgelse Årbog* 31–37.
3242 2025

3246
3247
3248
3249 2024
3250 2025 Jóhannesdóttir, G.E., Thordarson, T., Geirdóttir, Á., Larsen, G. 2005. The widespread ~10
3251 2026 ka Saksunarvatn tephra: a product of three large basaltic phreatoplinian eruptions. In:
3252
3253 2027 *Geophysical Research Abstracts* 7 (05991), 01607-0796.
3254 2028
3255
3256 2029 Jones, G., Davies, S.M., Farr, G.J., Bevan, J. 2017. Identification of the Askja-S Tephra in a
3257 2030 rare turlough record from Pant-y-Llyn, south Wales. *Proceedings of the Geologists'*
3258
3259 2031 *Association* 128 (4), 523-530.
3260 2032
3261 2033 Jones, G., Lane, C.S., Brauer, A., Davies, S.M., Bruijn, R., Engels, S., Haliuc, A., Hoek,
3262
3263 2034 W.Z., Merkt, J., Sachse, D. Turner, F. 2018. The Lateglacial to early Holocene
3264 2035 tephrochronological record from Lake Hämelsee, Germany: a key site within the European
3265
3266 2036 tephra framework. *Boreas* 47, 28-40.
3267 2037
3268
3269 2038 Jørgensen, K.A. 1980. The Thorsmörk ignimbrite: an unusual comenditic pyroclastic flow in
3270 2039 southern Iceland. *Journal of Volcanology and Geothermal Research* 8, 7-22.
3271
3272 2040
3273 2041 Kearney, R., Albert, P.G., Staff, R.A., Pál, I., Veres, D., Magyar, E., Ramsey, C.B. 2018.
3274
3275 2042 Ultra-distal fine ash occurrences of the Icelandic Askja-S Plinian eruption deposits in
3276 2043 Southern Carpathian lakes: New age constraints on a continental scale tephrostratigraphic
3277
3278 2044 marker. *Quaternary Science Reviews* 188, 174-182.
3279 2045
3280
3281 2046 Kelly, T.J., Hardiman, M., Lovelady, M., Lowe, J.J., Matthews, I.P., Blockley, S.P. 2017.
3282 2047 Scottish early Holocene vegetation dynamics based on pollen and tephra records from
3283
3284 2048 Inverlair and Loch Etteridge, Inverness-shire. *Proceedings of the Geologists' Association*
3285 2049 128, 125-135.
3286 2050
3287
3288 2051 Koren, J.H., Svendsen, J.I., Mangerud, J. Furnes, H. 2008. The Dimna Ash - a 12.8 14C ka-
3289 2052 old volcanic ash in Western Norway. *Quaternary Science Reviews* 27, 85-94.
3290
3291 2053
3292 2054 Kristjánsdóttir, G.B., Stoner, J.S., Jennings, A.E., Andrews, J.T., Grönvold, K 2007.
3293
3294 2055 Geochemistry of Holocene cryptotephra from the North Iceland Shelf (MD99-2269):
3295 2056 intercalibration with radiocarbon and palaeomagnetic chronostratigraphies. *The Holocene*
3296
3297 2057 17, 155-176.
3298 2058
3299
3300 2059 Kuehn, S.C., Froese, D.G., Carrara, P.E., Foit, F.F., Pearce, N.J., Rotheisler, P. 2009.
3301 2060 Major-and trace-element characterization, expanded distribution, and a new chronology for
3302
3303
3304

3305
3306
3307 2061 the latest Pleistocene Glacier Peak tephras in western North America. *Quaternary Research*.
3308 3309 2062 71, 201-216.
3310 2063
3311
3312 2064 Kylander, M.E., Lind, E.M., Wastegård, S., Löwemark, L. 2011. Recommendations for using
3313 2065 XRF core scanning as a tool in tephrochronology. *The Holocene* 22, 371-375.
3314 2066
3315 2067 Lacasse, C., Sugurdsson, H., Jóhannesson, H., Paterne, M., Carey, S. 1995. Source of Ash
3317 2068 Zone 1 in the North Atlantic. *Bulletin of Volcanology* 57, 18-32.
3318 2069
3319 2070 Lane, C.S., Andrič, M., Cullen, V.L., Blockley, S.P. 2011a. The occurrence of distal Icelandic
3320 2071 and Italian tephra in the Lateglacial of Lake Bled, Slovenia. *Quaternary Science Reviews*
3322 2072 30,1013-1018.
3323 2073
3324 2074 Lane, C. S., Blockley, S. P. E., Bronk Ramsey, C., Lotter, A. F. 2011b. Tephrochronology
3326 2075 and absolute centennial scale synchronisation of European and Greenland records for the
3327 2076 last glacial to interglacial transition: A case study of Soppensee and NGRIP. *Quaternary*
3328 2077 *International*. 246,145–156.
3329 2078
3330 2079 Lane, C.S., Blockley, S.P.E., Mangerud, J., Smith, V.C., Lohne, Ø., Tomlinson, E.L.,
3331 2080 Matthews, I.P., Lotter, A.F. 2012a. Was the 12.1ka Icelandic Vedde Ash one of a kind?.
3332 2081 *Quaternary Science Reviews* 33, 87-99.
3333 2082
3334 2083 Lane, C.S., De Klerk, P. and Cullen, V.L. 2012b: A tephrochronology for the Lateglacial
3335 2084 palynological record of the Enderburg Bruch (Vorpommern, north-east Germany). *Journal of*
3336 2085 *Quaternary Science*. 27, 141-149.
3337 2086
3338 2087 Lane, C.S., Brauer, A., Blockley, S.P. and Dulski, P. 2013. Volcanic ash reveals time-
3339 2088 transgressive abrupt climate change during the Younger Dryas. *Geology* 41, 1251-1254.
3340 2089
3341 2090 Lane, C.S., Lowe, D.J., Blockley, S.P.E., Suzuki, T. Smith, V.C. 2017. Advancing
3342 2091 tephrochronology as a global dating tool: Applications in volcanology, archaeology, and
3343 2092 palaeoclimatic research. *Quaternary Geochronology* 40, 1-7.
3344 2093
3345 2094 Lane, C.S., Martin-Jones, C.M., Johnson, T.C. 2018. A cryptotephra record from the Lake
3346 2095 Victoria sediment core record of Holocene palaeoenvironmental change. *The Holocene*,
3347 2096 p.0959683618798163.
3348 2097
3349
3350
3351
3352
3353
3354
3355
3356
3357
3358
3359
3360
3361
3362
3363

3364
3365
3366 2098 Lang, B., Brooks, S.J., Bedford, A., Jones, R.T., Birks, H.J.B., Marshall, J.D. 2010. Regional
3367 2099 consistency in Lateglacial chironomid-inferred temperatures from five sites in north-west
3368 2100 England. *Quaternary Science Reviews* 29, 1528-1538.
3370 2101
3371 2102
3372 2102 Larsen J.J. 2013. *Lateglacial and Holocene tephrostratigraphy in Denmark Volcanic ash in a*
3373 2103 *palaeoenvironmental context*. Unpublished PhD thesis, University of Copenhagen
3374 2104
3375 2104
3376 2105 Larsen, J.J., Noe-Nygaard, N., 2014. Lateglacial and early Holocene tephrostratigraphy and
3377 2106 sedimentology of the Store Slotseng basin, SW Denmark: a multi-proxy study. *Boreas* 43,
3378 2107 349-361.
3379 2108
3380 2109
3381 2108
3382 2109 Lilja, C., Lind, E.M., Morén, B., Wastegård, S. 2013. A Lateglacial–early Holocene
3383 2110 tephrochronology for SW Sweden. *Boreas* 42, 544-554.
3384 2111
3385 2111
3386 2112
3387 2112 Lincoln, P.C. 2011. *Tephrostratigraphic and Taphonomic study from Pulpit Hill, Western*
3388 2113 *Scotland*. Unpublished MSc Thesis, University of London.
3389 2114
3390 2114
3391 2115 Lind, E.M., Wastegård, S. 2011. Tephra horizons contemporary with short early Holocene
3392 2116 climate fluctuations: new results from the Faroe Islands. *Quaternary International* 246, 157-
3393 2117 167.
3394 2118
3395 2118
3396 2118
3397 2119 Lind, E.M., Wastegård, S., Larsen, J.J. 2013. A Late Younger Dryas–Early Holocene
3398 2120 tephrostratigraphy for Fosen, Central Norway. *Journal of Quaternary Science* 28, 803-811.
3399 2121
3400 2121
3401 2122 Lind, E.M., Lilja, C., Wastegård, S., Pearce, N.J. 2016. Revisiting the Borrobol tephra.
3402 2123 *Boreas* 45, 629-643.
3403 2124
3404 2124
3405 2125
3406 2125 Lohne Ø.S., Mangerud J., Birks H.H. 2014. IntCal13 calibrated ages of the Vedde and
3407 2126 Saksunarvatn ashes and the Younger Dryas boundaries from Kråkenes, western Norway.
3408 2127 *Journal of Quaternary Science* 29, 506-507.
3409 2128
3410 2128
3411 2129
3412 2129 Lowe, D.J. 2008. Globalization of tephrochronology: new views from Australasia. *Progress in*
3413 2130 *Physical Geography* 32, 311–335.
3414 2131
3415 2131
3416 2132 Lowe, D.J. 2011. Tephrochronology and its application: a review. *Quaternary Geochronology*
3417 2133 6 (2), 107-153.
3418 2134
3419 2134
3420
3421
3422

3423
3424
3425 2135 Lowe, D.J., Hunt, J.B. 2001. A summary of terminology used in tephra-related studies. Les
3426 2136 Dossiers de l'Archaéo-Logis 1, 17-22.
3427
3428 2137
3429
3430 2138 Lowe, D.J., Shane, P.A., Alloway, B.V. Newnham, R.M. 2008. Fingerprints and age models
3431 2139 for widespread New Zealand tephra marker beds erupted since 30,000 years ago: a
3432 2140 framework for NZ-INTIMATE. *Quaternary Science Reviews* 27, 95-126.
3433
3434 2141
3435 2142 Lowe, D.J., Blaauw, M., Hogg, A.G., Newnham, R.M. 2013. Ages of 24 widespread tephras
3436 2143 erupted since 30,000 years ago in New Zealand, with re-evaluation of the timing and
3437 2144 palaeoclimatic implications of the Lateglacial cool episode recorded at Kaipo bog.
3438 2145 *Quaternary Science Reviews* 74, 170-194.
3439
3440 2146
3441
3442 2147 Lowe, D.J., Pearce, N.J.G., Jorgensen, M.A., Kuehn, S.C., Tryon, C.A., Hayward, C.L.
3443 2148 2017. Correlating tephras and cryptotephras using glass compositional analyses and
3444 2149 numerical and statistical methods: Review and evaluation. *Quaternary Science Reviews*
3445 2150 175, 1-44.
3446
3447 2151
3448 2152 Lowe, J.J. 2001. Abrupt climatic changes in Europe during the last glacial–interglacial
3449 2153 transition: the potential for testing hypotheses on the synchronicity of climatic events using
3450 2154 tephrochronology. *Global and Planetary Change* 30, 73-84.
3451
3452 2155
3453 2156 Lowe, J.J., Lowe, S. 1989. Interpretation of the pollen stratigraphy of Late Devensian
3454 2157 lateglacial and early Flandrian sediments at Llyn Gwernan, near Cader Idris. North Wales.
3455 2158 *New Phytologist* 113, 391-408.
3456
3457 2159
3458 2160 Lowe, J.J., Turney, C.S.M. 1997. Vedde ash layer discovered in a small lake basin on the
3459 2161 Scottish mainland' *Journal of the Geological Society* 154, 605-612.
3460
3461 2162
3462 2163 Lowe, J.J., Walker, M.J.C. 1986. Lateglacial and early Flandrian environmental history of the
3463 2164 Isle of Mull, Inner Hebrides, Scotland. *Transactions of the Royal Society of Edinburgh Earth
3464 2165 Sciences*, 77, 1-30.
3465
3466 2166
3467 2167 Lowe, J.J. Roberts, S.J. 2003. Muir Park Reservoir. In: Evans, D.J.A (Ed.), *The Quaternary
3468 2168 of the Western Highland Boundary: Field Guide*. Quaternary Research Association, London
3469 2169 117-124.
3470
3471 2170
3472
3473
3474
3475
3476
3477
3478
3479
3480
3481

3482
3483
3484 2171 Lowe, J.J., Birks, H.H., Brooks, S.J., Coope, G.R., Harkness, D.D., Mayle, F.E., Sheldrick,
3485 3485 C., Turney, C.S.M., Walker, M.J.C. 1999. The chronology of palaeoenvironmental changes
3486 2172 during the Last Glacial-Holocene transition: towards an event stratigraphy for the British
3487 2173 Isles. *Journal of the Geological Society* 156, 397-410.
3488
3489 2174
3490 2175
3491
3492 2176 Lowe, J., Albert, P., Hardiman, M., MacLeod, A., Blockley, S. Pyne-O'Donnell, S. 2008.
3493 2177 Tephrostratigraphical investigations of the basal sediment sequence at Loch Etteridge. In:
3494 2178 *The Quaternary of Glen Roy and Vicinity Field Guide*. ed. by Palmer, A.P., Lowe, J.J., Rose,
3495 2178 J. Quaternary Research Association, 60-65.
3496 2179
3497 2180
3498
3499 2181 Lowe, J.J., Ramsey, C.B., Housley, R.A., Lane, C.S., Tomlinson, E.L., RESET Team.,
3500 2182 RESET Associates. 2015. The RESET project: constructing a European tephra lattice for
3501 2182 refined synchronisation of environmental and archaeological events during the last c. 100 ka.
3502 2183 *Quaternary Science Reviews* 118, 1-17.
3503 2184
3504 2185
3505 2185
3506 2186 Lowe, J., Pyne-O'Donnell, S.D.F., Timms, R. 2016. Tephra layers on Skye dating to the
3507 2187 Lateglacial-Early Holocene interval and their wider context. In: Ballantyne, C., Lowe,
3508 2187 J. (Eds.), *The Quaternary of Skye: Field Guide*. Quaternary Research Association.
3509 2188 Quaternary Research Association, London, 157-183.
3510 2189
3511 2190
3512 2190
3513 2191
3514 2191 Lowe, J.J., Palmer, A.P., Carter-Champion, A., MacLeod, A.M., Ramirez-Rojas, I., Timms,
3515 2192 R.G.O. 2017. Stratigraphy of a Lateglacial lake basin sediment sequence at Turret Bank,
3516 2193 Upper Glen Roy, Lochaber: implications for the age of the Turret Fan. *Proceedings of the*
3517 2193 *Geologists' Association* 128, 110–124.
3518 2194
3519 2195
3520 2195
3521 2196 Lowe, J.J., Matthews, I.P., Mayfield, R., Lincoln., P.C., Palmer, A., Timms, R.G.O. in prep.
3522 2197 On the timing of the last glaciers to occupy the SW Scottish Highlands and the impropriety of
3523 2197 the universal use of the term 'Younger Dryas'.
3524 2198
3525 2199
3526 2200
3527 2200 MacDonald, R., McGarvie, D. W., Pinkerton, H., Smith, R. L., Palacz, A. 1990. Petrogenetic
3528 2201 evolution of the Torfajökull Volcanic Complex, Iceland I. Relationship between the magma
3529 2201 types. *Journal of Petrology* 31, 429-459.
3530 2202
3531 2203
3532 2204
3533 2204 Mackay, H., Hughes, P.D.M., Jensen, B.J.L., Langdon, P.G., Pyne-O'Donnell, S.D.F.,
3534 2205 Plunkett, G., Froese, D.G., Coulter, S., Gardner, J.E. 2016. Mid to late Holocene
3535 2206 cryptotephra framework from eastern North America. *Quaternary Science Reviews* 132, 101-
3536 2206 113.
3537 2207
3538
3539
3540

3541
3542
3543 2208
3544
3545 2209 Mackie, E.A., Davies, S.M., Turney, C.S., Dobbyn, K., Lowe, J.J. Hill, P.G. 2002. The use of
3546 2210 magnetic separation techniques to detect basaltic microtephra in last glacial-interglacial
3547 2211 transition (LGIT; 15–10 ka cal. BP) sediment sequences in Scotland. *Scottish Journal of*
3548 2212 *Geology* 38, 21-30.
3549
3550
3551 2213
3552 2214 Maclennan, J., Jull, M., McKenzie, D., Slater, L., Grönvold, K. 2002. The link between
3553 2215 volcanism and deglaciation in Iceland. *Geochemistry, Geophysics, Geosystems* 3, 1-25.
3554
3555 2216
3556 2217 MacLeod, A. 2008. Tephrostratigraphy of the Loch Laggan East lake sequence. in *The*
3557 2218 *Quaternary of Glen Roy and Vicinity Field Guide*. ed by Palmer AP, Lowe JJ, Rose J.
3558 2219 Quaternary Research Association, London, 83-91.
3559
3560
3561 2220
3562 2221 MacLeod, A., Matthews, I.P., Lowe, J.J., Palmer, A.P., Albert, P.G. 2015. A second tephra
3563 2222 isochron for the Younger Dryas period in northern Europe: The Abernethy Tephra.
3564 2223 *Quaternary Geochronology* 28, 1-11.
3565
3566 2224
3567
3568 2225 Mangerud, J., Lie, S. E., Furnes, H., Kristiansen, I. L., Lømo, L. 1984. A Younger Dryas ash
3569 2226 bed in western Norway, and its possible correlations with tephra in cores from the Norwegian
3570 2227 Sea and the North Atlantic. *Quaternary Research* 21, 85-104.
3571
3572 2228
3573
3574 2229 Mangerud, J., Furnes, H., Jóhansen, J. 1986. A 9000-year-old ash bed on the Faroe Islands.
3575 2230 *Quaternary Research* 26, 262-265.
3576
3577 2231
3578 2232 Marshall, J.D., Jones, R.T., Crowley, S.F., Oldfield, F., Nash, S. Bedford, A. 2002. A high
3579 2233 resolution late-glacial isotopic record from Hawes Water, northwest England Climatic
3580 2234 oscillations: Calibration and comparison of palaeotemperature proxies. *Palaeogeography,*
3581 2235 *Palaeoclimatology, Palaeoecology* 185, 25-40.
3582
3583
3584 2236
3585 2237 Matthews, I.P. 2008. *The potential of tephrostratigraphy in the investigation of wetland*
3586 2238 *archaeological records*. Unpublished PhD thesis, University of London.
3587
3588 2239
3589
3590 2240 Matthews, I.P., Birks, H.H., Bourne, A.J., Brooks, S.J., Lowe, J.J., MacLeod, A.
3591 2241 Pyne-O'Donnell, S.D.F. 2011. New age estimates and climatostratigraphic correlations for
3592 2242 the Borrobol and Penifiler Tephtras: evidence from Abernethy Forest, Scotland. *Journal of*
3593 2243 *Quaternary Science* 26, 247-252.
3594
3595
3596 2244
3597
3598
3599

3600
3601
3602 2245 Matthews, I.P., Trincardi, F., Lowe, J.J., Bourne, A.J., MacLeod, A., Abbott, P.M., Anderson,
3603 N., Asioli, A., Blockley, S.P.E., Lane, C.S., Oh, Y.A., Satow, C.S., Staff, R.A., Wulf, S. 2015.
3604 2246 Developing a robust tephrochronological framework for Late Quaternary marine records in
3605 2247 the Southern Adriatic Sea: new data from core station SA03-11. *Quaternary Science*
3606 2248 *Reviews* 118, 84-104.
3607 2249
3608 2250
3609
3610
3611 2251 McGarvie, D.W., Macdonald, R., Pinkerton, H. Smith, R.L. 1990. Petrogenetic evolution of
3612 2252 the Torfajökull Volcanic Complex, Iceland II. The role of magma mixing. *Journal of Petrology*
3613 2253 31, 461-481.
3614 2254
3615 2255 McLean, D., Albert, P.G., Nakagawa, T., Suzuki, T., Staff, R.A., Yamada, K., Kitaba, I.,
3616 2256 Haraguchi, T., Kitagawa, J., Smith, V. 2018. Integrating the Holocene tephrostratigraphy for
3617 2257 East Asia using a high-resolution cryptotephra study from Lake Suigetsu (SG14 core),
3618 2258 central Japan. *Quaternary Science Reviews* 183, 36-58.
3619 2259
3620 2260 Mithen, S., Wicks, K., Pirie, A., Riede, F., Lane, C., Banerjea, R., Cullen, V., Gittins, M.
3621 2261 Pankhurst, N. 2015. A Lateglacial archaeological site in the far north-west of Europe at
3622 2262 Rubha Port an t-Seilich, Isle of Islay, western Scotland: Ahrensburgian-style artefacts,
3623 2263 absolute dating and geoarchaeology. *Journal of Quaternary Science* 30, 396-416.
3624 2264
3625 2265 Moles, J.D., McGarvie, D., Stevenson, J.A., Sherlock, S.C. 2018. Geology of Tindfjallajökull
3626 2266 volcano, Iceland. *Journal of Maps* 14, 22-31.
3627 2267
3628 2268 Moles, J.D., McGarvie, D., Stevenson, J.A., Sherlock, S.C., Abbott, P.M., Jenner, F.E.,
3629 2269 Halton, A.M. (in review) Widespread tephra dispersal and ignimbrite emplacement from a
3630 2270 subglacial volcano: the rhyolitic eruption of Torfajökull, Iceland, ~55 ka.
3631 2271
3632 2272 Moriwaki, H., Nakamura, N., Nagasako, T., Lowe, D.J., Sangawa, T. 2016. The role of
3633 2273 tephra in developing a high-precision chronostratigraphy for palaeoenvironmental
3634 2274 reconstruction and archaeology in southern Kyushu, Japan, since 30,000 cal. BP: an
3635 2275 integration. *Quaternary International* 397, 79-92.
3636 2276
3637 2277 Mortensen, A.K., Bigler, M., Grönvold, K., Steffensen, J.P., Johnsen, S.J. 2005. Volcanic ash
3638 2278 layers from the Last Glacial Termination in the NGRIP ice core. *Journal of Quaternary*
3639 2279 *Science* 20, 209-219.
3640 2280
3641
3642
3643
3644
3645
3646
3647
3648
3649
3650
3651
3652
3653
3654
3655
3656
3657
3658

3659
3660
3661 2281 Muschitiello, F. and Wohlfarth, B. 2015. Time-transgressive environmental shifts across
3662 Northern Europe at the onset of the Younger Dryas. *Quaternary Science Reviews* 109, 49-
3663 2282 56.
3664 2283
3665
3666 2284
3667 2285 Narcisi, B., Petit, J.R., Delmonte, B. 2010. Extended East Antarctic ice-core
3668 tephrostratigraphy. *Quaternary Science Reviews* 29, 21-27.
3669 2286
3670 2287
3671 2288 Neave, D.A., Maclennan, J., Thordarson, T., Hartley, M.E. 2015. The evolution and storage
3672 of primitive melts in the Eastern Volcanic Zone of Iceland: the 10 ka Grímsvötn tephra series
3673 2289 (i.e. the Saksunarvatn ash). *Contributions to Mineralogy and Petrology* 170, 1-23.
3674 2290
3675 2291
3676 2292 Newnham, R.M. Lowe, D.J. 1999. Testing the synchronicity of pollen signals using
3677 tephrostratigraphy. *Global and Planetary Change* 21, 113-128.
3678 2293
3679 2294
3680 2295 Noe-Nygaard A. 1951. Sub-fossil Hekla pumice from Denmark. *Medd fra Dansk Geol*
3681 *Forening* 12, 35–46.
3682 2296
3683 2297
3684 2298 Normand, S., Ricklefs, R.E., Skov, F., Bladt, J., Tackenberg, O, Svenning, J.C. 2011.
3685 Postglacial migration supplements climate in determining plant species ranges in Europe.
3686 2299 *Proceedings of the Royal Society, series B*, doi:10.1098/rspb.2010.2769.
3687 2300
3688 2301
3689 2302 Ott, F., Wulf, S., Serb, J., Słowiński, M., Obremaska, M., Tjallingii, R., Błaszkiwicz, M.
3690 2303 Brauer, A. 2016. Constraining the time span between the Early Holocene Häseldalen and
3691 Askja-S Tephra through varve counting in the Lake Czechowskie sediment record, Poland.
3692 2304 *Journal of Quaternary Science* 31, 103-113.
3693 2305
3694 2306
3695 2307 Palmer, A.P., Lowe, J.J. 2017. Dynamic landscape changes in Glen Roy and vicinity, west
3696 Highland Scotland, during the Last Termination: a synthesis. *Proceedings of the Geologists’*
3697 *Association* 128, 2-25.
3698 2309
3699 2310
3700 2311 Palmer, A.P., Rose, J., Lowe, J.J., MacLeod, A. 2010. Annually-resolved events of Younger
3701 2312 Dryas glaciation in Lochaber (Glen Roy and Glen Spean), Western Scottish Highlands.
3702 2313 *Journal of Quaternary Science* 25, 581-596.
3703 2314
3704 2315 Peacock, J.D. Rose, J. 2017. Was the Younger Dryas (Loch Lomond Stadial) icefield on
3705 Rannoch Moor, western Scotland, deglaciated as early as c. 12.5 cal ka BP?. *Proceedings*
3706 *of the Geologists’ Association* 128, 173-179.
3707 2317
3708
3709
3710
3711
3712
3713
3714
3715
3716
3717

3718
3719
3720 2318
3721
3722 2319 Pearce, N.J., Abbott, P.M., Martin-Jones, C. 2014. Microbeam methods for the analysis of
3723 2320 glass in fine-grained tephra deposits: a SMART perspective on current and future trends.
3724 2321 *Geological Society, London, Special Publications*, 398, SP398-1.
3725 2321
3726 2322
3727
3728 2323 Persson, C. 1966. Försök till tefrokronologisk datering av några svenska torvmossar.
3729 2324 *Geologiska Föreningens i Stockholm Förhandlingar* 88, 361-395.
3730 2325
3731
3732 2326 Phillips, W.M., Hall, A.M., Ballantyne, C.K., Binnie, S., Kubik, P.W., Freeman, S. 2008.
3733 2327 Extent of the last ice sheet in northern Scotland tested with cosmogenic ¹⁰Be exposure ages.
3734 2328 *Journal of Quaternary Science* 23, 101-107.
3735 2328
3736 2329
3737
3738 2330 Pilcher J.R., Hall V.A. 1992. Towards a tephrochronology for the Holocene of the north of
3739 2331 Ireland. *The Holocene* 2, 255-259.
3740 2331
3741 2332
3742 2333 Pilcher, J., Bradley, R.S., Francus, P., Anderson, L. 2005. A Holocene tephra record from
3743 2334 the Lofoten Islands, Arctic Norway. *Boreas* 34, 136-156.
3744 2334
3745 2335
3746 2336 Plunkett, G., Pilcher, J.R. 2018. Defining the potential source region of volcanic ash in
3747 2337 northwest Europe during the Mid-to Late Holocene. *Earth-Science Reviews* 179, 20-37.
3748 2337
3749 2338
3750
3751 2339 Pollard, A.M., Blockley, S.P.E., Ward, K.R. 2003. Chemical alteration of tephra in the
3752 2340 depositional environment: theoretical stability modelling. *Journal of Quaternary Science* 18,
3753 2341 385-394.
3754 2341
3755 2342
3756
3757 2343 Ponomareva, V., Portnyagin, M., Pendea, I.F., Zelenin, E., Bourgeois, J., Pinegina, T.,
3758 2344 Kozhurin, A. 2017. A full holocene tephrochronology for the Kamchatsky Peninsula region:
3759 2345 Applications from Kamchatka to North America. *Quaternary Science Reviews* 168, 101-122.
3760 2345
3761 2346
3762
3763 2347 Porter, S.C. 1978. Glacier Peak tephra in the North Cascade Range, Washington:
3764 2348 Stratigraphy, distribution, and relationship to late-glacial events. *Quaternary Research*. 10,
3765 2349 30-41
3766 2349
3767 2350
3768
3769 2351 Pyne-O'Donnell, S.D.F. 2005. *The factors affecting the distribution and preservation of*
3770 2352 *microtephra particles in Lateglacial and early Holocene lake sediments*. Unpublished PhD
3771 2353 thesis, University of London.
3772 2353
3773 2354
3774
3775
3776

3777
3778
3779 2355 Pyne-O'Donnell, S.D.F. 2007. Three new distal tephras in sediments spanning the Last
3780 2356 Glacial-Interglacial Transition in Scotland. *Journal of Quaternary Science* 22, 559-570.
3781 2357
3782 2358 Pyne-O'Donnell, S. 2011. The taphonomy of Last Glacial-Interglacial Transition (LGIT) distal
3783 2359 volcanic ash in small Scottish lakes. *Boreas* 40, 131-145.
3784 2360
3785 2361 Pyne-O'Donnell, S.D.F., Blockley, S.P.E., Turney, C.S.M. and Lowe, J.J. 2008. Distal
3786 2362 volcanic ash layers in the Lateglacial Interstadial (GI-1): problems of stratigraphic
3787 2363 discrimination. *Quaternary Science Reviews* 27, 72-84.
3788 2364
3789 2365 Pyne-O'Donnell, S.D., Cwynar, L.C., Jensen, B.J., Vincent, J.H., Kuehn, S.C., Spear, R.
3790 2366 Froese, D.G. 2016. West Coast volcanic ashes provide a new continental-scale Lateglacial
3791 2367 isochron. *Quaternary Science Reviews* 142, 16-25.
3792 2368
3793 2369 Pyne-O'Donnell, S., Jensen, B. 2018. The Glacier Peak ash in Scotland. INTAV International
3800 2370 Field Conference on Tephrochronology - Crossing New Frontiers, O 1.4.
3801 2371
3802 2372 Rach, O., Brauer, A., Wilkes, H., Sachse, D. 2014. Delayed hydrological response to
3803 2373 Greenland cooling at the onset of the Younger Dryas in western Europe. *Nature Geoscience*
3804 2374 7, 109-112.
3805 2375
3806 2376 Ranner, P.H., Allen, J.R.M., Huntley, B. 2005. A new early Holocene cryptotephra from
3807 2377 northwest Scotland. *Journal of Quaternary Science* 20, 201-208.
3808 2378
3809 2379 Rasmussen, S.O., Andersen, K.K., Svensson, A.M., Steffensen, J.P., Vinther, B.M.,
3810 2380 Clausen, H.B., Siggaard-Andersen, M.L., Johnsen, S.J., Larsen, L.B., Dahl-Jensen, D.,
3811 2381 Bigler, M., Röthlisberger, R., Fischer, H., Goto-Azuma, K., Hansson, M.E., Ruth, U. 2006. A
3812 2382 new Greenland ice core chronology for the last glacial termination. *Journal of Geophysical*
3813 2383 *Research D: Atmospheres* 111, D06102.
3814 2384
3815 2385 Reimer, P.J., Bard, E., Bayliss, A., Beck, J.W., Blackwell, P.G., Ramsey, C.B., Buck, C.E.,
3816 2386 Cheng, H., Edwards, R.L., Friedrich, M., Grootes, P.M. 2013. IntCal13 and Marine13
3817 2387 radiocarbon age calibration curves 0–50,000 years cal BP. *Radiocarbon* 55, 1869-1887.
3818 2388
3819 2389 Roberts, S.J. 1997. *The spatial and geochemical characteristics of Lateglacial tephra*
3820 2390 *deposits of Scotland and Northern England*. Unpublished MSc Thesis, University of London.
3821 2391
3822
3823
3824
3825
3826
3827
3828
3829
3830
3831
3832
3833
3834
3835

3836
3837
3838 2392 Roberts, S.J., Turney, C.C.M., Lowe, J. 1998. Icelandic Tephra in Late-glacial Sediments of
3839 2393 Scotland (14 - 9,000 14C BP). *Fróðskaparrit* 46, 335-339.
3841 2394
3842
3843 2395 Rose, J. 1985. The Dimlington Stadial/Dimlington Chronozone: a proposal for naming the
3844 2396 main glacial episode of the Late Devensian in Britain. *Boreas* 14, 225-230.
3845
3846 2397
3847 2398 Ruddiman, W.F., McIntyre, A. 1981. The North Atlantic Ocean during the last deglaciation.
3848 2399 *Palaeogeography, Palaeoclimatology, Palaeoecology* 35, 145-214.
3849
3850 2400
3851 2401 Sigmundsson, F., Pinel, V., Lund, B., Albino, F., Pagli, C., Geirsson, H., Sturkell, E. 2010.
3852 2402 Climate effects on volcanism: Influence on magmatic systems of loading and unloading from
3853 2403 ice mass variations, with examples from Iceland. *Philosophical Transactions of the Royal
3854 2404 Society A: Mathematical, Physical and Engineering Sciences* 368, 2519-2534.
3855
3856 2405
3857 2406
3858 2407 Sigvaldason, G.E. 2002. Volcanic and tectonic processes coinciding with glaciation and
3859 2408 crustal rebound: an early Holocene rhyolitic eruption in the Dyngjufjöll volcanic centre and
3860 2409 the formation of the Askja caldera, north Iceland. *Bulletin of Volcanology* 64, 192-205.
3861
3862 2410
3863 2411 Stevenson, J.A., Loughlin, S., Rae, C., Thordarson, T., Milodowski, A.E., Gilbert, J.S.,
3864 2412 Harangi, S., Lukács, R., Højgaard, B., Ártung, U., Pyne-O'Donnell, S., MacLeod, A., Whitney,
3865 2413 B., Cassidy, M. 2012. Distal deposition of tephra from the Eyjafjallajökull 2010 summit
3866 2414 eruption. *Journal of Geophysical Research: Solid Earth* 117, (B9).
3867
3868 2415
3869 2416 Stevenson, J.A., Loughlin, S.C., Font, A., Fuller, G.W., MacLeod, A., Oliver, I.W., Jackson,
3870 2417 B., Horwell, C.J., Thordarson, T., Dawson, I. 2013. UK monitoring and deposition of tephra
3871 2418 from the May 2011 eruption of Grímsvötn, Iceland. *Journal of Applied Volcanology* 2, 1-17.
3872
3873 2419
3874 2420 Swindles, G.T., Lawson, I.T., Savov, I.P., Connor, C.B., Plunkett, G. 2011. A 7000 yr
3875 2421 perspective on volcanic ash clouds affecting northern Europe. *Geology* 39, 887-890.
3876
3877 2422
3878 2423 Thordarson T. 2014. The widespread ~10 ka Saksunarvatn tephra is not a product single
3879 2424 eruption. *American Geophysical Union, Fall Meeting 2014*, V24B-04.
3880
3881 2425
3882 2426 Thornalley, D.J., McCave, I.N., Elderfield, H. 2011. Tephra in deglacial ocean sediments
3883 2427 south of Iceland: Stratigraphy, geochemistry and oceanic reservoir ages. *Journal of
3884 2428 Quaternary Science* 26, 190-198.
3885
3886
3887
3888
3889
3890
3891
3892
3893
3894

3895
3896
3897 2429 Timms, R.G.O. 2016. *Developing a refined tephrostratigraphy for Scotland, and constraining*
3898 2430 *abrupt climatic oscillations of the Last Glacial-Interglacial Transition (ca 16-8 ka BP) using*
3900 2431 *high resolution tephrochronologies*. Unpublished PhD thesis, University of London.
3901
3902 2432
3903 2433 Timms, R.G.O., Matthews, I.P., Palmer, A.P., Candy, I., Abel, L. 2017. A high-resolution
3904 2434 tephrostratigraphy from Quoyloo Meadow, Orkney, Scotland: implications for the
3906 2435 tephrostratigraphy of NW Europe during the Last Glacial-Interglacial Transition. *Quaternary*
3907 2436 *Geochronology* 40, 67-81.
3908
3909 2437
3910 2438 Timms, R.G.O., Matthews, I.P., Palmer, A.P., Candy, I. 2018: Toward a tephrostratigraphic
3911 2439 framework for the British Isles: a Last Glacial to Interglacial Transition (LGIT c. 16-8 ka) case
3912 2440 study from Crudale Meadow, Orkney. *Quaternary Geochronology* 46, 28-44.
3913
3914
3915 2441
3916 2442 Tipping, R. M. 1987. The prospects for establishing synchronicity in the early postglacial
3917 2443 pollen peak of *Juniperus* in the British Isles. *Boreas* 16, 155–163.
3918
3919 2444
3920
3921 2445 Tomlinson, E.L., Thordarson, T., Müller, W., Thirlwall, M., Menzies, M.A. 2010. Microanalysis
3922 2446 of tephra by LA-ICP-MS—strategies, advantages and limitations assessed using the
3923 2447 Thorsmörk Ignimbrite (Southern Iceland). *Chemical Geology* 279, 73-89.
3924
3925 2448
3926
3927 2449 Tomlinson, E.L., Thordarson, T., Lane, C.S., Smith, V.C., Manning, C.J., Müller, W. Menzies,
3928 2450 M.A. 2012. Petrogenesis of the Sólheimar ignimbrite (Katla, Iceland): Implications for
3929 2451 tephrostratigraphy. *Geochimica et Cosmochimica Acta* 86, 318-337.
3930
3931 2452
3932 2453 Tomlinson, E.L., Smith, V.C., Albert, P.G., Aydar, E., Civetta, L., Cioni, R., Cubukcu,
3933 2454 E., Gertisser, R., Isaia, R., Menzies, M.A., Orsi, G., Rosi, M., Zanchetta, G. 2015. The major
3935 2455 and trace element glass compositions of the productive Mediterranean volcanic sources:
3936 2456 tools for correlating distal tephra layers in and around Europe. *Quaternary Science Reviews*
3937 2457 118, 48-66.
3938
3939
3940 2458
3941 2459 Turney, C.S.M. 1998a. Extraction of rhyolitic component of Vedde microtephra from
3942 2460 minerogenic lake sediments. *Journal of Paleolimnology* 19, 199-206.
3943
3944 2461
3945 2462 Turney, C.S.M. 1998b. *Isotope stratigraphy and tephrochronology of the Last Glacial–*
3946 2463 *Interglacial Transition (14–9 ka ¹⁴C BP) in the British Isles*. Unpublished PhD thesis,
3947 2464 University of London.
3948
3949
3950 2465
3951
3952
3953

3954
3955
3956 2466 Turney, C.S., Harkness, D.D., Lowe, J.J. 1997. Rapid Communication: The use of
3957 2467 microtephra horizons to correlate Late-glacial lake sediment successions in Scotland.
3958 2468 *Journal of Quaternary Science* 12 (6), 525-531.
3960 2469
3961 2470 Turney C.S.M., Van Den Burg, K., Wastegård, S., Davies, S.M., Whitehouse, N.J., Pilcher,
3962 2471 J.R., Callaghan, C. 2006. North European last glacial–interglacial transition (LGIT; 15–9 ka)
3964 2472 tephrochronology: extended limits and new events. *Journal of Quaternary Science* 21, 335-
3966 2473 345.
3967 2474
3968 2475 Þórarinnsson, S. 1944: Tefrokronologiska studier pa Island. *Geografiska Annaler* 26, 1-217.
3970 2476
3971 2477 Valentine, H. 2015. *Constraining the timing of deglaciation on Priest Island, Summer Isles*
3972 2478 *using tephrostratigraphy*, Unpublished MSc thesis, University of London.
3973 2479
3974 2480 van Asch, N., Lutz, A.F., Duijkers, M.C., Heiri, O., Brooks, S.J., Hoek, W.Z. 2012. Rapid
3975 2481 climate change during the Weichselian Lateglacial in Ireland: Chironomid-inferred summer
3976 2482 temperatures from Fiddaun, Co. Galway. *Palaeogeography, Palaeoclimatology,*
3977 2483 *Palaeoecology* 315, 1-11.
3978 2484
3979 2485 Van der Bilt, W.G.M., Lane, C.S., Bakke, J. 2017. Ultra-distal Kamchatkan ash on Arctic
3980 2486 Svalbard: Towards hemispheric cryptotephra correlation. *Quaternary Science Reviews* 164,
3981 2487 230-235.
3982 2488
3983 2489 Van Vliet-Lanoë, B., Guðmundsson, Á., Guillou, H., Duncan, R.A., Genty, D., Ghaleb, B.,
3984 2490 Gouy, S., Récourt, P. Scaillet, S. 2007. Limited glaciation and very early deglaciation in
3985 2491 central Iceland: implications for climate change. *Comptes Rendus Geoscience* 339, 1-12.
3986 2492
3987 2493 Walker, M.J.C. 1984. Pollen analysis and Quaternary research in Scotland. *Quaternary*
3988 2494 *science reviews* 3, 369-404.
3989 2495
4000 2496 Walker, M.J.C. 1995. Climatic changes in Europe during the last glacial/interglacial
4001 2497 transition. *Quaternary International* 28, 63-76.
4002 2498
4003 2499 Walker, M., Lowe, J., 2017. Lateglacial environmental change in Scotland. *Earth and*
4004 2500 *Environmental Science Transactions of The Royal Society of Edinburgh* 1-26.
4005 2501
4006
4007
4008
4009
4010
4011
4012

4013
4014
4015 2502 Walker, M.J.C., Björck, S., Lowe, J.J., Cwynar, L.C., Johnsen, S., Knudsen, K.L., Wohlfarth,
4016 2503 B. INTIMATE Group. 1999. Isotopic 'events' in the GRIP ice core: a stratotype for the Late
4017 2504 Pleistocene. *Quaternary Science Reviews* 18, 1143-1150.
4018
4019
4020 2505
4021 2506 Wastegård, S. 2002. Early to middle Holocene silicic tephra horizons from the Katla volcanic
4022 2507 system, Iceland: new results from the Faroe Islands. *Journal of Quaternary Science* 17, 723-
4023 2508 730.
4024
4025
4026 2509
4027 2510 Wastegård, S., Turney, C.S.M., Lowe, J.J. Roberts, S.J. 2000. New discoveries of the Vedde
4028 2511 Ash in southern Sweden and Scotland. *Boreas* 29, 72-78.
4029
4030 2512
4031 2513 Wastegård, S., Veres, D., Kliem, P., Hahn, A., Ohlendorf, C., Zolitschka, B., The PASADO
4032 2514 SAcience Team. 2013. Towards a late Quaternary tephrochronological framework for the
4033 2515 southernmost part of South America – the Laguna Potrok Aike tephra record. *Quaternary
4034 2516 Science Reviews* 71, 81-90.
4035
4036 2516
4037 2517
4038
4039 2518 Wastegård, S., Gudmundsdóttir, E.R., Lind, E.M., Timms, R.G.O., Björck, S., Hannon, G.E.,
4040 2519 Olsen, J., Rundgren, M. 2018. Towards a Holocene tephrochronology for the Faroe Islands,
4041 2520 North Atlantic. *Quaternary Science Reviews* 195, 195-214.
4042
4043 2521
4044
4045 2522 Watson, J.E., Brooks, S.J., Whitehouse, N.J., Reimer, P.J., Birks, H.J.B. Turney, C. 2010.
4046 2523 Chironomid-inferred late-glacial summer air temperatures from Lough Nadourcan, Co.
4047 2524 Donegal, Ireland. *Journal of Quaternary Science*. 25, 1200-1210.
4048
4049 2525
4050 2526 Watson, E.J., Kołaczek, P., Słowiński, M., Swindles, G.T., Marcisz, K., Gałka, M.,
4051 2527 Lamentowicz, M. 2017. First discovery of Holocene Alaskan and Icelandic tephra in Polish
4052 2528 peatlands. *Journal of Quaternary Science* 32, 457-462.
4053
4054 2529
4055
4056 2530 Weston, D.J. 2012. *A tephrostratigraphic study of the Late Glacial to Interglacial Transition
4057 2531 on Tanera Mòr, Summer Isles, Northwestern Scotland*. Unpublished MSc thesis, University
4058 2532 of London.
4059
4060 2533
4061
4062 2534 Whittington, G., Edwards, K.J., Zanchetta, G., Keen, D.H., Bunting, M.J., Fallick, A.E.
4063 2535 Bryant, C.L. 2015. Lateglacial and early Holocene climates of the Atlantic margins of Europe:
4064 2536 Stable isotope, mollusc and pollen records from Orkney, Scotland. *Quaternary Science
4065 2537 Reviews* 122, 112-130.
4066
4067 2538
4068
4069
4070
4071

4072
4073
4074 2539 Williams, A.N., Lowe, J.J., Turney, C.S.M., Woodcock, P. 2007. *Preliminary*
4075
4076 2540 *tephrostratigraphical investigations at Traeth Mawr*. In: Quaternary of the Brecon Beacons
4077 2541 Field Guide. ed by. Carr, S.J., Coleman, C.G., Humpage, A.J., Shakesby, R.A., Quaternary
4078
4079 2542 Research Association, 151-158.
4080 2543
4081 2544 Wohlfarth, B., Blaauw, M., Davies, S.M., Andersson, M., Wastegard, S., Hormes, A.
4082
4083 2545 Possnert, G. 2006. Constraining the age of Lateglacial and early Holocene pollen zones and
4084
4085 2546 tephra horizons in southern Sweden with Bayesian probability methods. *Journal of*
4086 2547 *Quaternary Science* 21, 321-334.
4087 2548
4088
4089 2549 Wulf, S., Ott, F., Słowinski, M., Noryskiewicz, A. M., Dräger, N., Martin-Puertas, C., Czymzik,
4090 2550 M., Neugebauer, I., Dulski, P., Bourne, A. J., Błaszkiwicz, M., Brauer, A. 2013. Tracing the
4091
4092 2551 Laacher See Tephra in the varved sediment record of the Trzechowskie palaeolake in
4093 2552 central Northern Poland. *Quaternary Science Reviews* 76, 129–139.
4094
4095 2553
4096 2554 Wulf, S., Dräger, N., Ott, F., Serb, J., Appelt, O., Guðmundsdóttir, E., van den Bogaard, C.,
4097
4098 2555 Słowiński, M., Błaszkiwicz, M., Brauer, A. 2016. Holocene tephrostratigraphy of varved
4099 2556 sediment records from Lakes Tiefer See (NE Germany) and Czechowskie (N Poland).
4100
4101 2557 *Quaternary Science Reviews* 132, 1-14.
4102 2558
4103
4104 2559 Wulf, S., Hardiman, M.J., Staff, R.A., Koutsodendris, A., Appelt, O., Blockley, S.P., Lowe,
4105 2560 J.J., Manning, C.J., Ottolini, L., Schmitt, A.K. and Smith, V.C., Tomlinson, E.L.,
4106
4107 2561 Vakhrameeva, P., Knipping, M., Kotthoff, U., Milner, A.M., Müller, U.C., Christanis, K.,
4108 2562 Kalaitzidia, S., Tzedakis, P.C., Schmiedl, G., Pross, J. 2018. The marine isotope stage 1–5
4109 2563 cryptotephra record of Tenaghi Philippon, Greece: Towards a detailed tephrostratigraphic
4110
4111 2564 framework for the Eastern Mediterranean region. *Quaternary Science Reviews* 186, 236-
4112 2565 262.
4113
4114
4115
4116
4117
4118
4119
4120
4121
4122
4123
4124
4125
4126
4127
4128
4129
4130



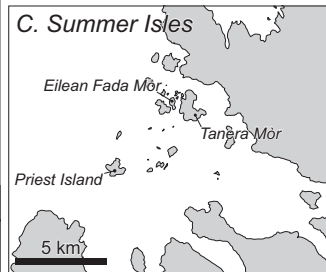
A. British Isles



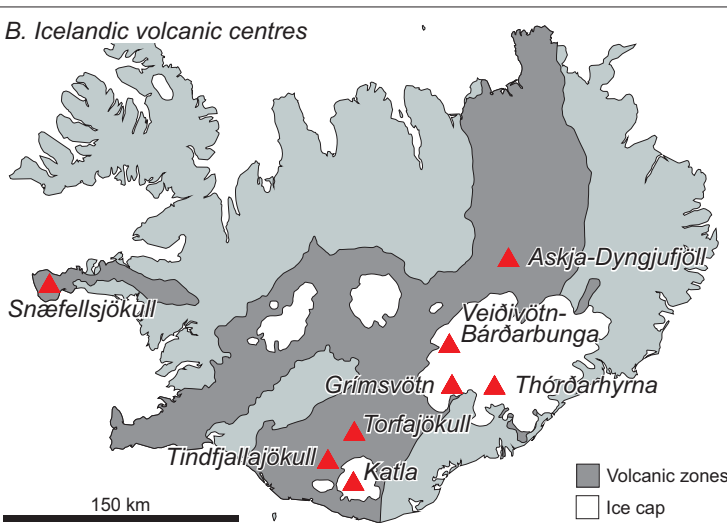
Proposed source of tephra reaching the British Isles during the LGIT

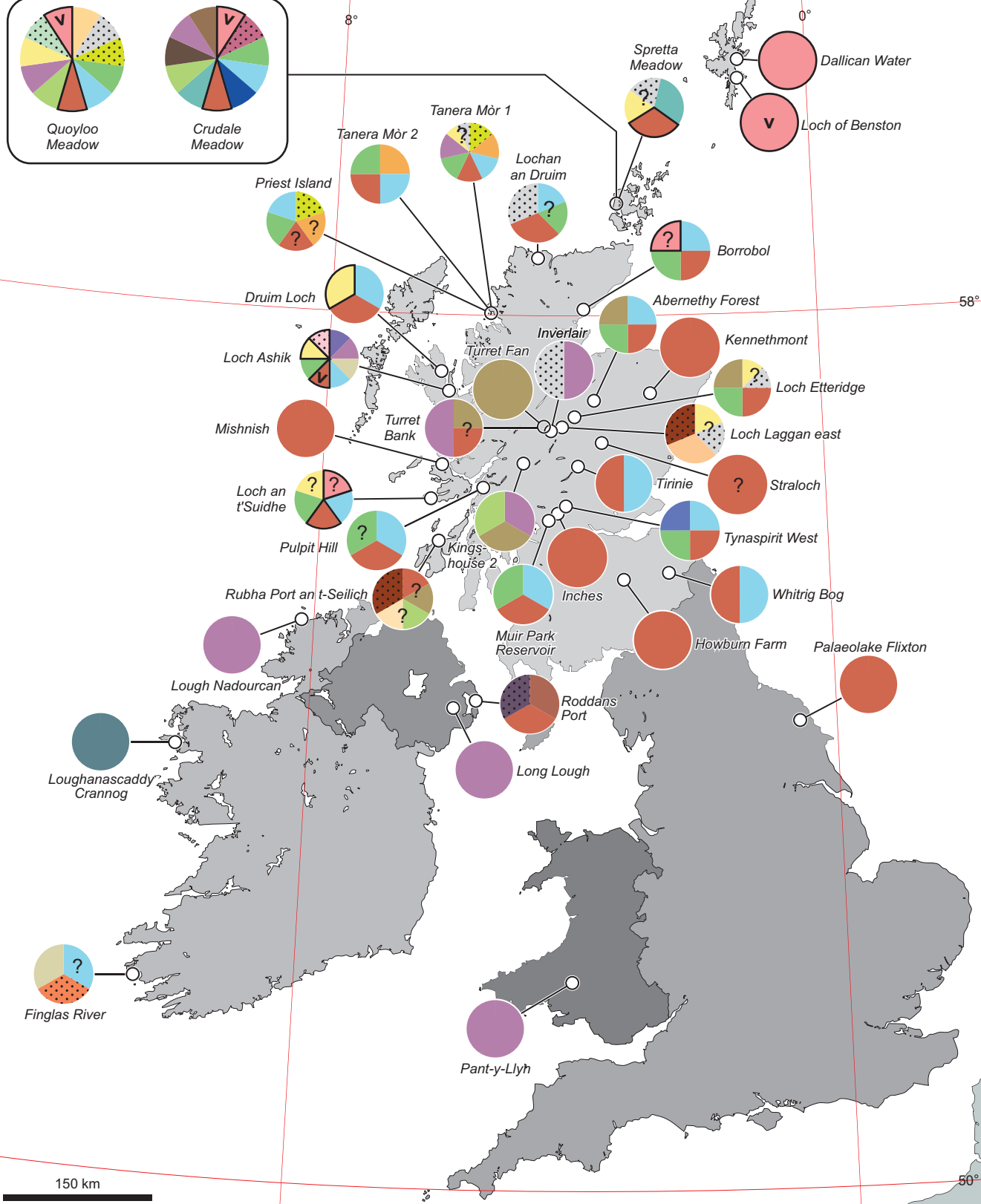
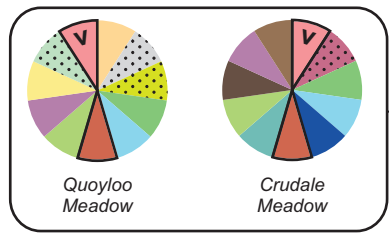
Other volcanic centres contributing to the European tephra framework (see Lowe et al., 2015)

C. Summer Isles

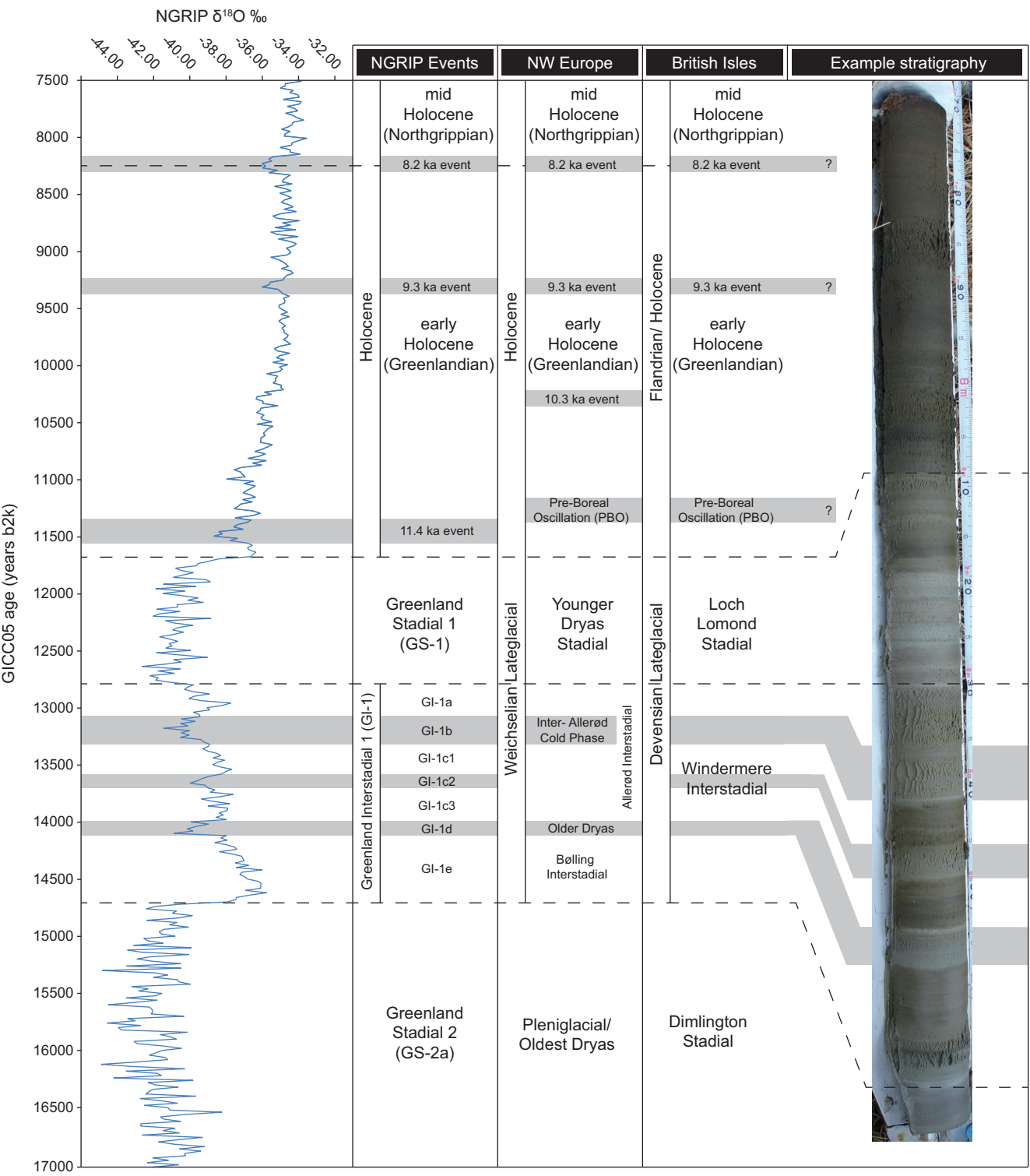


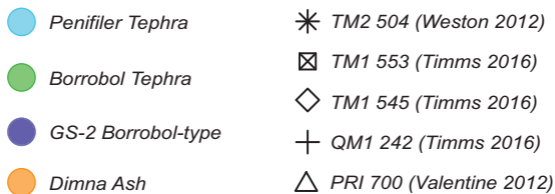
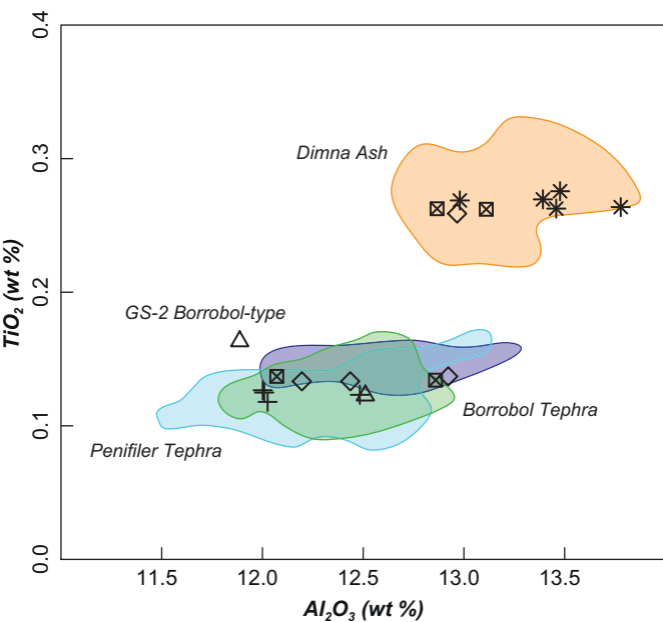
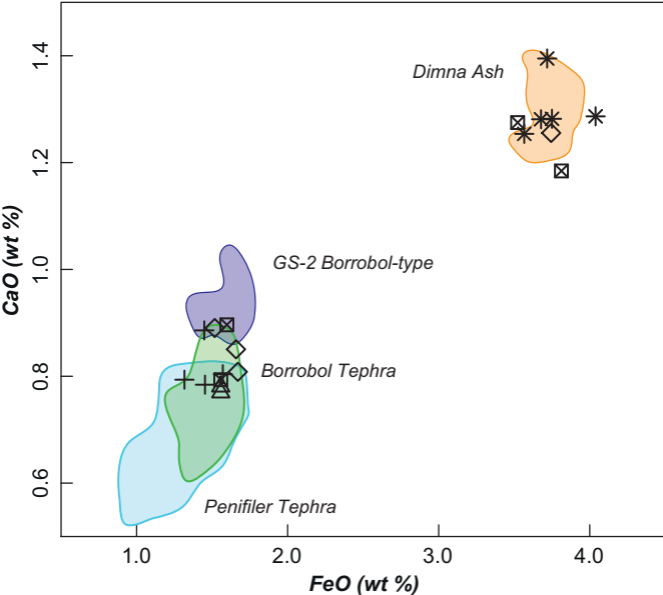
B. Icelandic volcanic centres

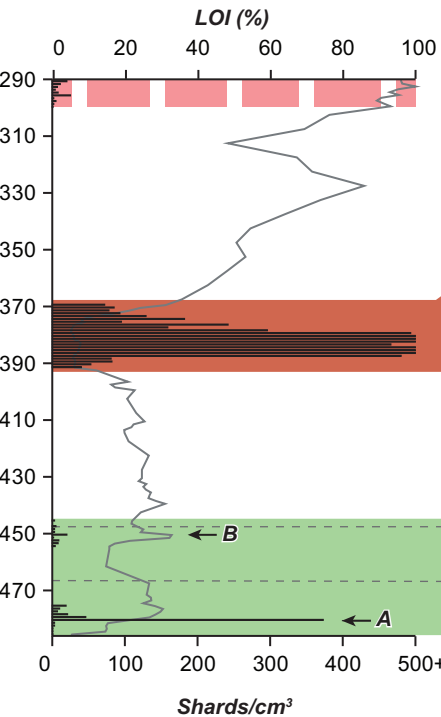
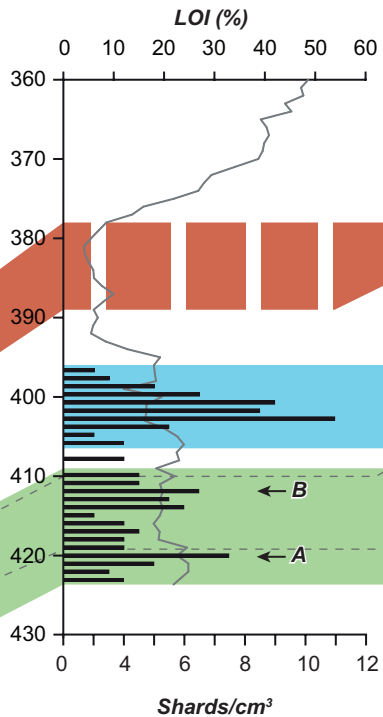
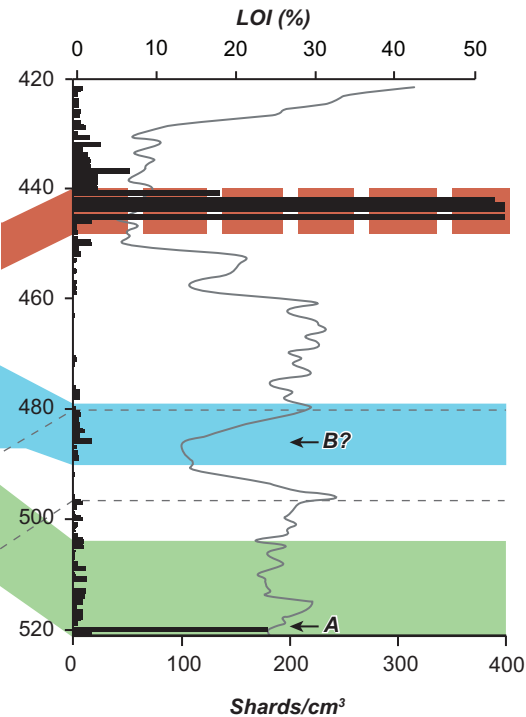






- | | | | |
|---|---|---|--|
| Breakish Tephra (unknown age) | Havn-3/ Havn-4 (10.3-10.4 ka/ 10.35-10.45 ka) | Hässeldalen Tephra (11,316 ± 124 cal. BP) | Glacier Peak (G & B) (13,710-13,410 cal. BP) |
| Suduroy Tephra (8073 ± 192 cal. BP) | CRUM1 444 Tephra (10,476 ± 254 cal. BP) | Crudale Tephra (12,111-11,174 cal. BP) | Mount St Helens J (13,800-12,800 cal. BP) |
| LAN1-325 Tephra (8434 ± 96 cal. BP) | Hovsdalur Tephra (10,475 ± 350 cal. BP) | Abernethy Tephra (11,462 ± 144 cal. BP) | Penifiler Tephra (13,939 ± 132 cal. BP) |
| An Druim Tephra (9648 ± 158 cal. BP) | Ashik Tephra (10,716 ± 230 cal. BP) | Vedde Ash (12,023 ± 86 cal. BP) | Borrobol Tephra (14,098 ± 94 cal. BP) |
| Fosen Tephra (10,139 ± 116 cal. BP) | Askja-S Tephra (10,824 ± 97 cal. BP) | CRUM1 597 Tephra (12,457 ± 896 cal. BP) | Dimna Ash (15,100 ± 300 cal. BP) |
| Saksunarvatn Ash (10,210 ± 70 cal. BP) | CRUM1 510 Tephra (10,837 ± 148 cal. BP) | Roddans Port A (unknown age) | Tanera Tephra (unknown age) |
| Visible ash layer | Uncertain correlation | Roddans Port B (unknown age) | CRUM1 676 (unknown age) |
| Basaltic tephra or basaltic component present | | | |







A. Borrobol 1997**B. Borrobol 2007****C. Borrobol 2016**

 Tephra correlated by chemical analyses

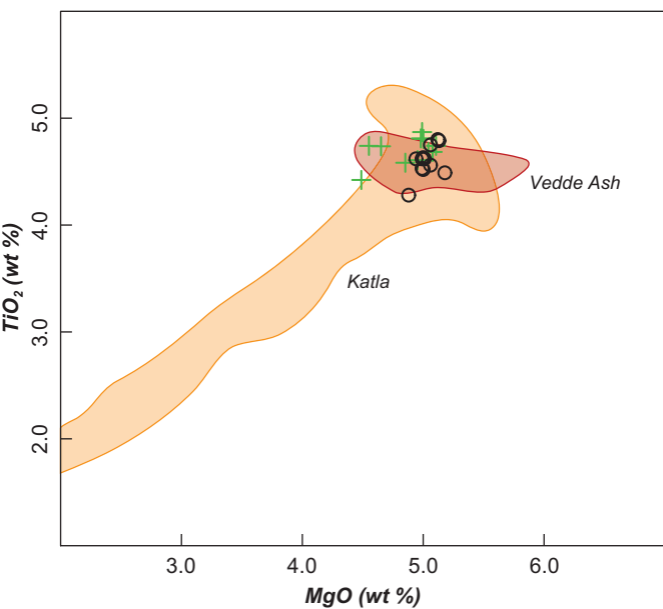
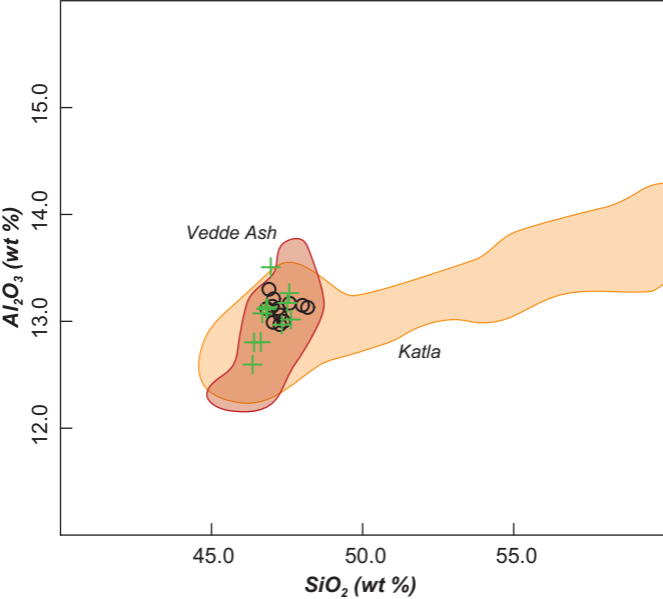
 Tephra correlated by stratigraphy

 Penifiler Tephra

 Borrobol Tephra

 Saksunarvatn Ash

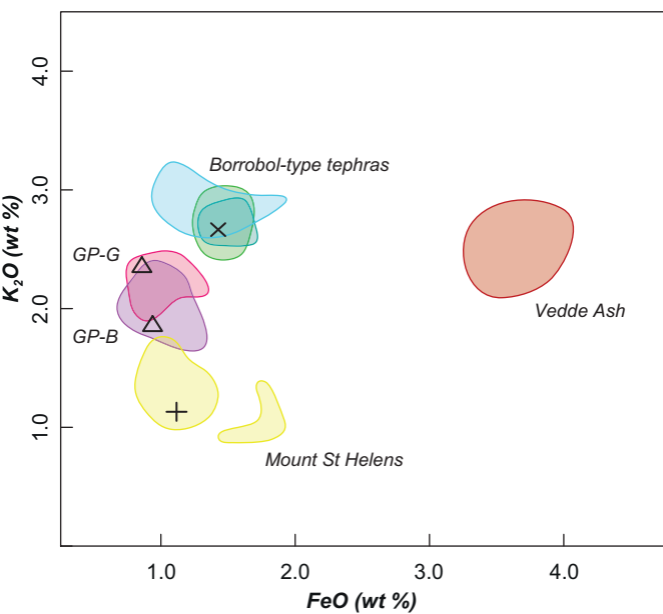
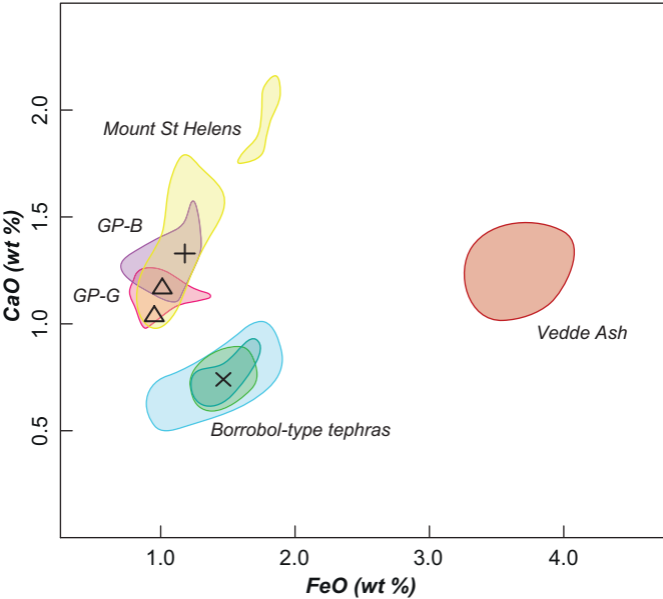
 Vedde Ash



● Vedde Ash (basaltic) ● Katla

○ Loch Ashik Isl-w 933 (Pyne-O'Donnell et al., 2008)

+ NGRIP 1573 m (Mortensen et al., 2005)



△ *Fin-53(A)* + *Fin-53(B)* × *Fin-53(C)* (*Turney 1998b*)

● *Vedde Ash*

● *Glacier Peak G*

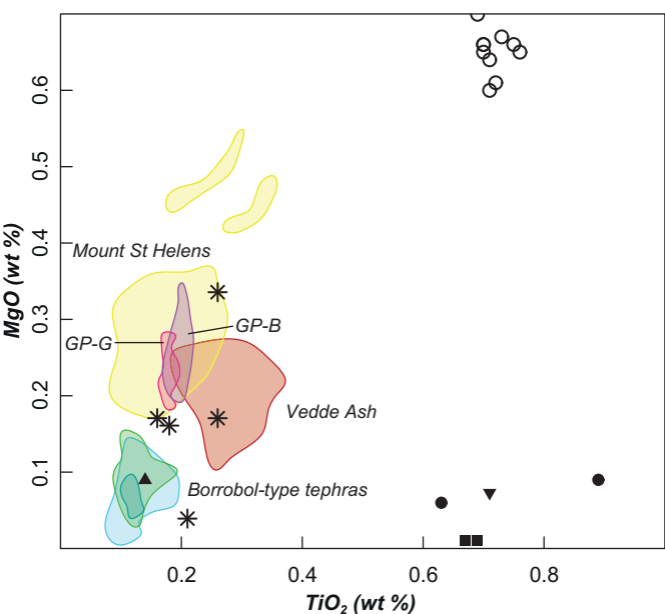
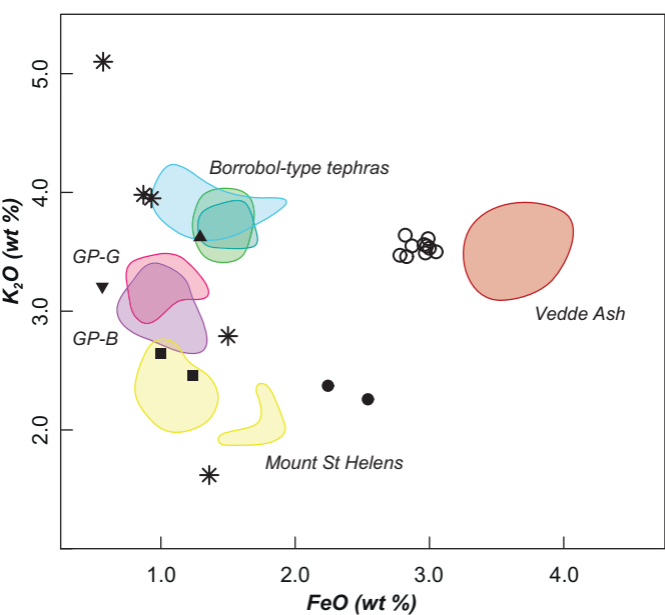
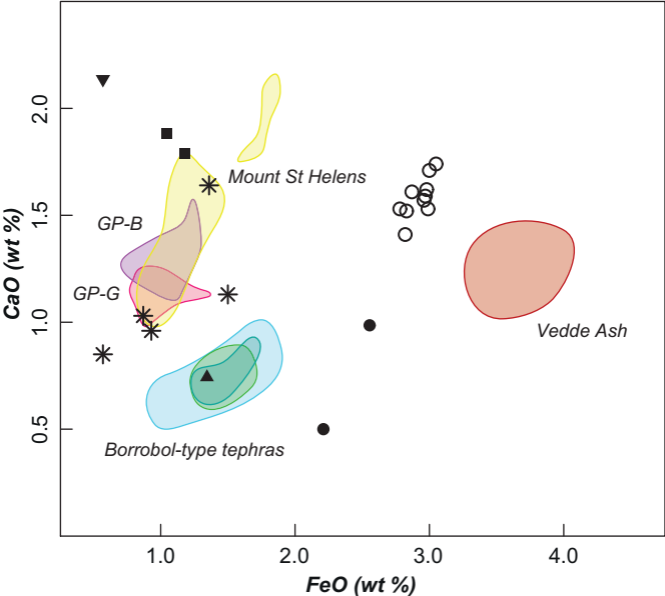
● *CRUM1 597 Tephra*

● *Glacier Peak B*

● *Penifiler Tephra*

● *Mount St Helens (Swift Creek)*

● *Borrobol Tephra*



● LAS-1(A) ■ LAS-1(B) ▲ LAS-1(C) ▼ LAS-1(D) (Davies, 2002)

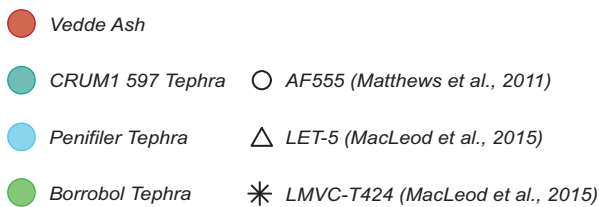
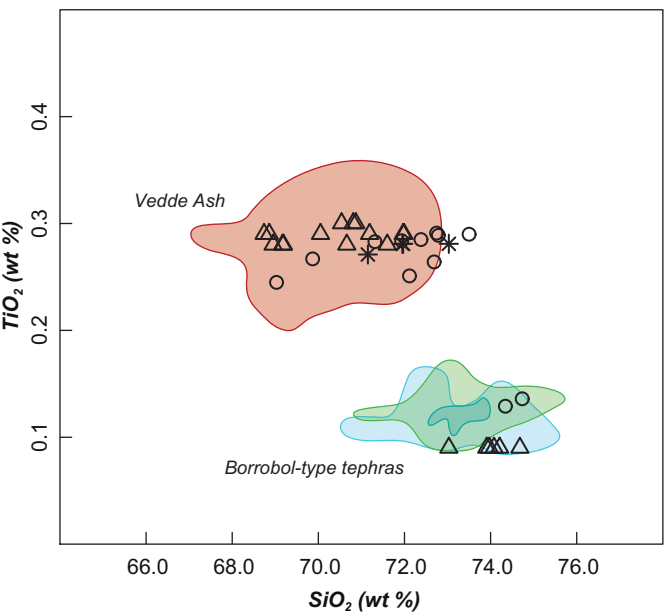
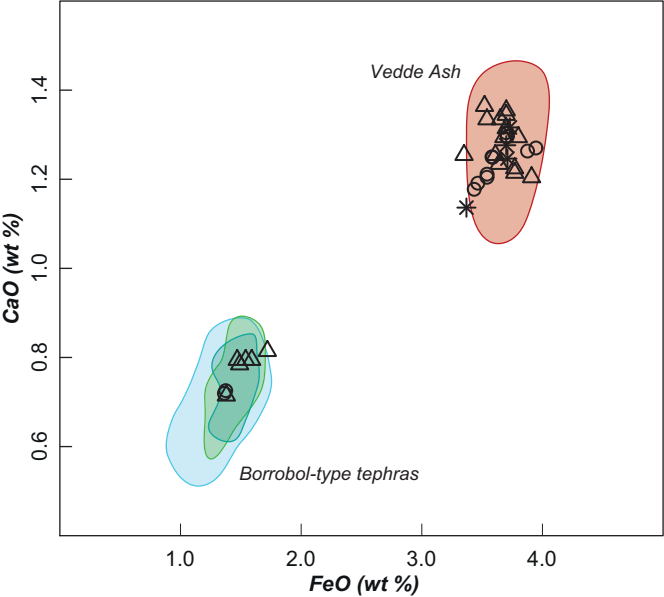
○ Roddans Port A * Roddans Port B (Turney et al., 2006)

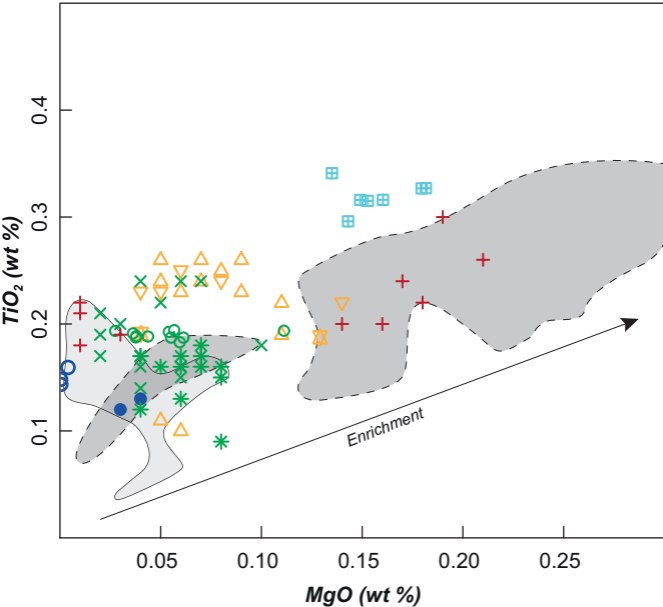
● Vedde Ash

● CRUM1 597 Tephra ● Glacier Peak G

● Penifiler Tephra ● Glacier Peak B

● Borrobol Tephra ● Mount St Helens (Swift Creek)





○ Torfajökull (Pleistocene)

● Torfajökull (Holocene)

LAN1-325 Tephra

■ Loughanascaddy Crannog (Matthews, 2008)

An Druim-Høvdarhagi Tephra

* Lochan An Druim S13 (Ranner et al., 2005)

× Inverlair B (Kelly et al., 2017)

○ Quoyloo Meadow 133 (Timms et al., 2017)

+ Høvdarhagi 217 (Lind and Wastegård, (2011))

Ashik Tephra

▽ Loch Ashik 882 (Pyne-O'Donnell, 2007)

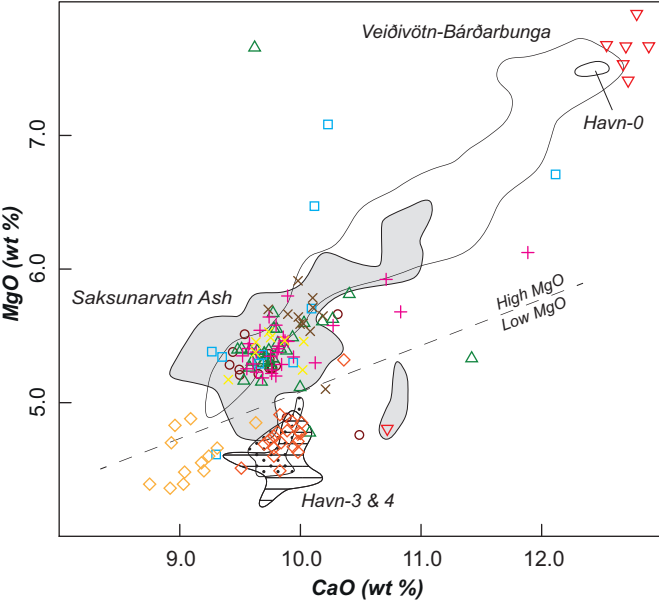
△ Druim Loch 1013 (Pyne-O'Donnell, 2007)

⊠ Quoyloo Meadow 187 (Timms et al., 2017)

Crudale Tephra

○ CRUM1 561 (Timms et al., 2018)

● Tynaspirit West 754 (Roberts, 1997)



- | | | | |
|---|------------------------------|---|--------|
| ○ | Veidivötn-Bárðarbunga | ◐ | Havn-4 |
| ● | Grímsvötn (Saksunarvatn Ash) | ◑ | Havn-3 |

Saksunarvatn 10-ka series (Grímsvötn)

- Quoyloo Meadow 163 (Bunting 1994)
- △ Quoyloo Meadow 160 (Timms et al., 2017)
- Crudale Meadow 386(A) (Bunting 1994)
- ✚ Crudale Meadow 394 (Timms et al., 2018)
- ✕ Crudale Meadow 444 (Timms et al., 2018)
- ✖ Loch of Benston (Bondevik et al., 2005)

Havn-3/ 4 correlations (Grímsvötn)

- ◇ Loch Ashik 865 (Pyne-O'Donnell 2007)
- ◇ Loch Ashik 865 (Kelly et al., 2017)

Havn-0 correlations (Veidivötn)

- ▽ Crudale Meadow 386(B) (Bunting 1994)

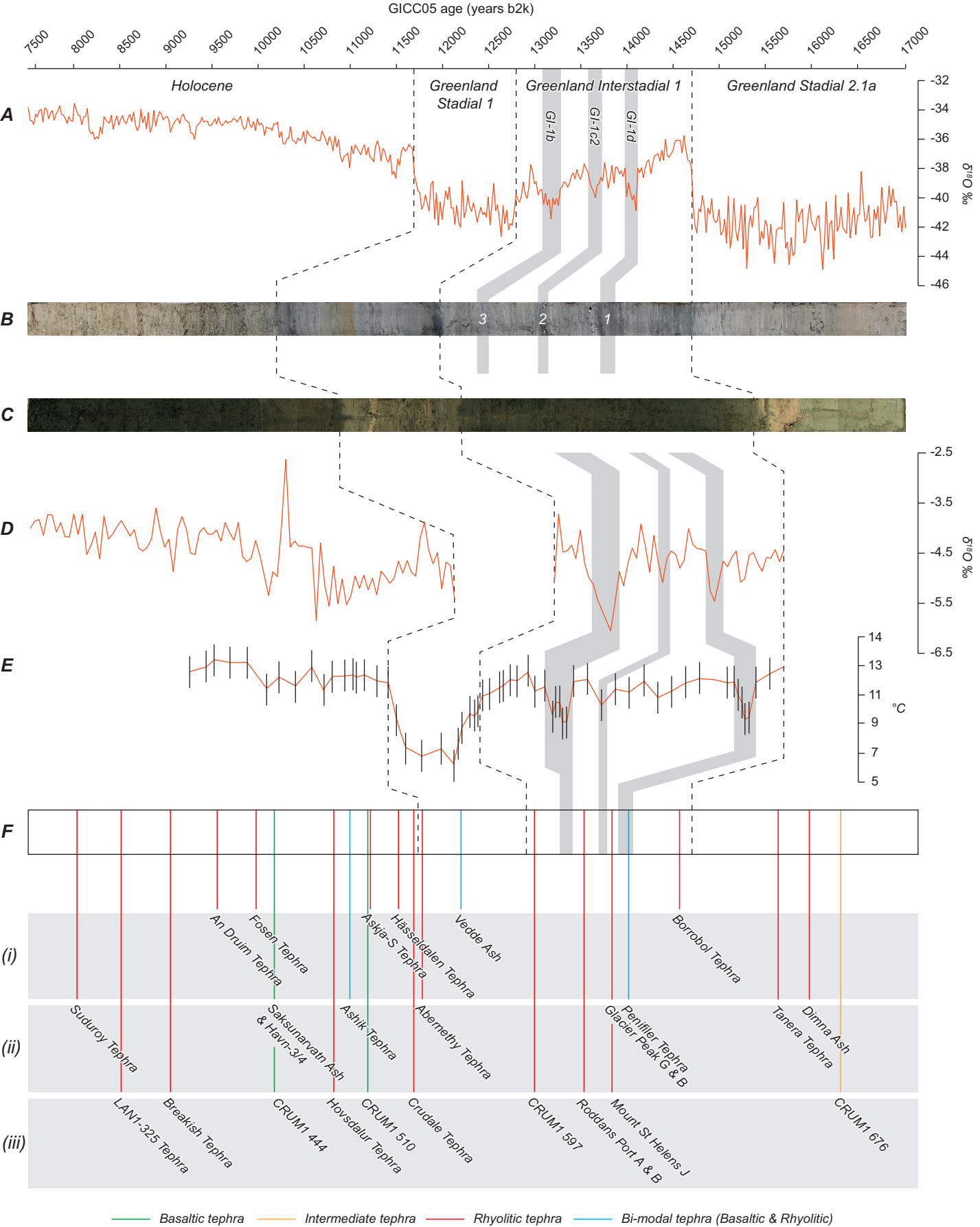


Table 1

Combined non-normalised glass-shard analytical data of tephra identified in the British Isles dating to the Last Glacial to Interglacial Transition (LGIT c. 16-8 ka BP). The value shown in the 'Number of sites' row relates only to those locations where correlations are secure: see Supplementary Table S1 for further details on the number of tentative correlations for each tephra. Mean glass data derived from: Roberts, (1997); Turney et al. (1997); Darville, (2011); Davies et al. (2001); Mackie et al. (2002); Ranner et al. (2005); Pyne-O'Donnell, (2007), Matthews, (2008); Pyne-O'Donnell et al. (2008); Matthews et al. (2011); Lane et al. (2012a); Weston, (2012); MacLeod et al. (2015); Mithen et al. (2015); Lind et al. (2016); Timms, (2016); Jones et al. (2017); Kelly et al. (2017); Lowe et al., (2017); Timms et al. (2017, 2018); Lowe et al. (in prep). Glass compositional data are available in full from Supplementary Table S2.

Tephra name	<i>CRUM1 676 Tephra</i>		<i>Dimna Ash</i>		<i>Tanera Tephra</i>		<i>Borrobol Tephra</i>		<i>Penifiler Tephra (R)</i>		<i>Penifiler Tephra (B)</i>	
Number of sites in British Isles	1		2		3		13		15		1	
Identified outside British Isles?	no		yes		uncertain		yes		uncertain		uncertain	
Current best age estimate	unknown		15,100 ± 300 cal. BP		unknown		14,098 ± 94 cal. BP		13,939 ± 132 cal. BP		13,939 ± 132 cal. BP	
Reference for age estimate	N/A		Koren et al. (2008)		N/A		Bronk Ramsey et al. (2015)		Bronk Ramsey et al. (2015)		Bronk Ramsey et al. (2015)	
Source	unknown		Katla, Iceland		unknown, Iceland		unknown, Iceland		unknown		Katla, Iceland	
Chemical composition	Dacite		Rhyolite		Rhyolite		Rhyolite		Rhyolite		Basaltic	
Major oxide (wt %)	n=1	2σ	n=8	2σ	n=11	2σ	n=243	2σ	n=177	2σ	n=12	2σ
SiO ₂	62.15	0.56	70.32	3.01	72.59	2.72	73.21	1.49	73.49	2.12	47.31	0.85
TiO ₂	1.24	0.02	0.27	0.01	0.13	0.02	0.12	0.04	0.11	0.04	4.60	0.29
Al ₂ O ₃	15.00	0.88	13.26	0.64	12.31	0.71	12.28	0.56	12.23	0.65	13.11	0.19
FeO	5.12	0.38	3.73	0.32	1.54	0.20	1.48	0.19	1.33	0.40	14.81	0.25
MnO	0.14	0.00	0.14	0.03	0.04	0.04	0.04	0.04	0.04	0.05	-	-
MgO	1.42	0.00	0.17	0.06	0.08	0.07	0.08	0.06	0.06	0.06	5.03	0.17
CaO	3.67	0.39	1.28	0.12	0.82	0.10	0.75	0.11	0.68	0.20	9.85	0.28
Na ₂ O	5.12	0.83	5.20	0.22	4.00	0.44	3.83	0.80	3.89	0.88	3.09	0.25

K2O	2.47	0.12	3.58	0.33	3.82	0.31	3.76	0.24	3.89	0.63	0.78	0.07
P2O5	0.93	0.15	0.18	0.01	0.02	0.02	0.01	0.01	0.02	0.12	-	-
Cl	-	-	0.03	0.00	0.13	0.03	0.06	0.12	0.13	0.02	-	-
Total	97.26	1.44	98.04	3.26	95.39	3.19	95.59	1.81	95.74	2.26	98.58	1.30
Tephra name	Mount St Helens J Tephra		Glacier Peak-G Tephra		Roddans Port A Tephra		Roddans Port B Tephra		CRUM1 597 Tephra		Vedde Ash (R)	
Number of sites in British Isles	1		2		1		1		2		23	
Identified outside British Isles?	yes		yes		no		no		no		yes	
Current best age estimate	13.86-12.80 cal. ka BP		13,710-13,410 cal. BP		unknown		unknown		12,457 ± 896 cal. BP		12,023 ± 86 cal. BP	
Reference for age estimate	Clynne et al. (2008)		Kuehn et al. (2009)		Turney et al. (2006)		Turney et al. (2006)		Timms et al. (2018)		Bronk Ramsey et al. (2015)	
Source	Mount St Helens		Glacier Peak, USA		unknown		unknown		unknown		Katla, Iceland	
Chemical composition	Rhyolite		Rhyolite		Rhyolitic		Rhyolitic		Rhyolitic		Rhyolitic	
Major oxide (wt %)	n=1	2σ	n=2	2σ	n=10	2σ	n=5	2σ	n=29	2σ	n=428	2σ
SiO2	72.88	-	73.03	2.67	68.99	2.23	75.08	2.71	73.32	0.73	70.36	2.58
TiO2	0.24	-	0.22	0.07	0.72	0.05	0.21	0.09	0.12	0.01	0.28	0.07
Al2O3	12.82	-	11.84	0.71	16.15	1.67	12.47	1.04	12.03	0.46	13.19	0.76
FeO	1.15	-	0.95	0.08	2.93	0.18	1.05	0.76	1.47	0.23	3.69	0.32
MnO	0.05	-	0.03	0.08	-	-	-	-	0.04	0.02	0.14	0.06
MgO	0.31	-	0.26	0.06	0.65	0.06	0.18	0.21	0.07	0.05	0.20	0.06
CaO	1.34	-	1.12	0.18	1.58	0.19	1.12	0.61	0.74	0.14	1.25	0.18
Na2O	3.76	-	3.10	0.03	4.97	0.49	3.24	1.59	4.11	0.28	4.73	1.19
K2O	2.09	-	3.12	0.55	3.54	0.12	3.49	2.65	3.73	0.20	3.50	0.27
P2O5	-	-	-	-	-	-	-	-	-	-	0.04	0.03
Cl	-	-	-	-	-	-	-	-	0.01	0.01	0.18	0.05
Total	94.64	-	93.66	3.18	99.54	1.26	96.83	3.39	95.64	1.08	97.42	3.34

Tephra name	Vedde Ash (B)		Abernethy Tephra (pop A)		Abernethy Tephra (pop B)		Crudale Tephra		Hässeldalen Tephra		Askja-S Tephra	
Number of sites in British Isles	5		4		3		2		3		10	
Identified outside British Isles?	yes		uncertain		uncertain		no		yes		yes	
Current best age estimate	12,023 ± 86 cal. BP		11,462 ± 144 cal. BP		11,462 ± 144 cal. BP		12,111 - 11,174 cal. BP		11,316 ± 124 cal. BP		10,824 ± 97 cal. BP	
Reference for age estimate	Bronk Ramsey et al. (2015)		Bronk Ramsey et al. (2015)		Bronk Ramsey et al. (2015)		Timms et al. (2018)		Wastegård et al. (2018)		Kearney et al. (2018)	
Source	Katla, Iceland		Katla, Iceland		Unknown, Iceland		Torfajökull, Iceland		Thórdarhyrna, Iceland		Askja-Dyngjufjöll, Iceland	
Chemical composition	Basaltic		Rhyolitic		Rhyolitic		Rhyolitic		Rhyolitic		Rhyolitic	
Major oxide (wt %)	n=106	2σ	n=33	2σ	n=8	2σ	n=5	2σ	n=23	2σ	n=177	2σ
SiO ₂	46.74	1.49	71.10	2.63	74.12	1.07	73.70	2.50	74.13	2.11	73.45	2.93
TiO ₂	4.55	0.31	0.27	0.02	0.09	0.04	0.15	0.04	0.08	0.01	0.30	0.04
Al ₂ O ₃	12.66	0.93	13.18	0.72	12.79	0.60	11.64	0.71	11.64	0.98	11.85	0.69
FeO	14.59	1.39	3.67	0.29	1.49	0.25	2.55	0.25	1.08	0.18	2.52	0.23
MnO	0.22	0.08	0.15	0.02	0.06	0.02	0.06	0.04	0.04	0.02	0.09	0.04
MgO	5.01	0.51	0.19	0.04	0.05	0.05	0.01	0.04	0.04	0.05	0.24	0.05
CaO	9.68	0.69	1.24	0.11	0.74	0.08	0.38	0.04	0.52	0.24	1.59	0.17
Na ₂ O	2.98	0.44	4.91	0.70	3.92	0.50	4.52	0.51	3.68	1.25	4.16	0.61
K ₂ O	0.73	0.12	3.50	0.23	4.82	1.33	4.09	0.38	4.10	0.42	2.49	0.20
P ₂ O ₅	0.51	0.09	0.05	0.14	0.06	0.17	0.01	0.01	0.01	0.01	0.04	0.02
Cl	-	-	0.01	0.04	0.00	0.01	-	-	-	-	-	-
Total	97.54	2.34	98.26	3.64	98.12	2.01	97.12	2.89	95.32	2.76	96.72	3.78
Tephra name	CRUM1 510 Tephra		Ashik Tephra (R)		Ashik Tephra (B)		Hovsdalur Tephra		CRUM1 444 Tephra		Havn-3/Havn-4 Tephra	
Number of sites in British Isles	1		3		1		1		1		1	
Identified outside British Isles?	uncertain		no		uncertain		yes		uncertain		yes	

Current best age estimate	10,837 ± 148 cal. BP		10,716 ± 230 cal. BP		10,716 ± 230 cal. BP		10,475 ± 350 cal. BP		10,476 ± 254 cal. BP		~10.37 and ~10.3 ka BP	
Reference for age estimate	Timms et al. (2018)		Timms et al. (2017)		Timms et al. (2017)		Wastegård, (2002)		Timms et al. (2018)		Wastegård et al. (2018)	
Source	Grímsvötn, Iceland		Torfajökull, Iceland		Grímsvötn, Iceland		Thordarhyrna, Iceland		Grímsvötn, Iceland		Grímsvötn, Iceland	
Chemical composition	Basaltic		Rhyolitic		Basaltic		Rhyolitic		Basaltic		Basaltic	
Major oxide (wt %)	n=27	2σ	n=19	2σ	n=6	2σ	n=4	2σ	n=8	2σ	n=31	2σ
SiO ₂	49.24	0.95	71.28	2.46	49.15	2.69	75.12	2.14	48.33	1.89	48.96	1.04
TiO ₂	3.05	0.12	0.22	0.09	3.34	1.50	0.10	0.01	3.04	0.17	3.39	0.80
Al ₂ O ₃	12.80	0.71	13.31	2.51	13.26	0.75	12.09	0.58	12.76	0.86	12.85	0.59
FeO	14.26	0.83	2.77	0.30	13.86	1.55	1.05	0.37	14.30	0.68	13.55	0.72
MnO	0.23	0.02	0.06	0.02		0.00	0.03	0.01	0.23	0.01	0.21	0.08
MgO	5.31	0.36	0.08	0.06	5.26	1.26	0.02	0.04	5.40	0.25	4.69	0.38
CaO	9.73	0.46	0.44	0.16	9.70	1.49	0.42	0.13	9.76	0.42	9.58	0.85
Na ₂ O	2.64	0.50	4.70	0.82	2.94	0.40	3.39	0.70	2.44	1.01	3.06	0.46
K ₂ O	0.47	0.05	4.14	0.39	0.64	0.42	5.30	1.78	0.49	0.08	0.64	0.48
P ₂ O ₅	0.30	0.05	0.02	0.01	-	0.00	0.01	0.01	0.53	0.93	-	-
Cl	-	-	-	-	-	0.00	-	-	-	-	-	-
Total	98.05	2.24	96.94	2.71	98.16	1.45	97.53	2.49	97.28	3.24	96.91	1.39
Tephra name	Saksunarvatn Ash		Fosen Tephra		An Druim Tephra		The LAN1-325 Tephra		The Suduroy Tephra		The Breakish Tephra	
Number of sites in British Isles	4		1		3		1		2		1	
Identified outside British Isles?	yes		yes		yes		uncertain		yes		no	
Current best age estimate	10,210 ± 35 cal. BP		10,139 ± 116 cal. BP		9648 ± 158 cal. BP		8245-8041 cal. BP		8073 ± 192 cal. BP		unknown	
Reference for age estimate	Lohne et al. (2014)		Timms et al. (2017)		Timms, (2016)		Matthews, (2008)		Wastegård, (2002)		Pyne-O'Donnell, (2007)	
Source	Grímsvötn, Iceland		unknown		Torfajökull, Iceland		Torfajökull, Iceland		Katla, Iceland		Askja-Dyngjufjöll, Iceland?	

Chemical composition	Basaltic		Rhyolitic		Rhyolitic		Rhyolitic		Rhyolitic		Rhyolitic	
Major oxide (wt %)	n=106	2 σ	n=10	2 σ	n=39	2 σ	n=7	2 σ	n=5	2 σ	n=4	2 σ
SiO ₂	49.28	1.55	73.36	0.74	70.82	1.85	70.12	1.41	71.43	0.33	71.44	0.96
TiO ₂	3.03	0.51	0.12	0.01	0.18	0.06	0.32	0.03	0.29	0.03	0.49	0.02
Al ₂ O ₃	12.92	2.38	11.92	0.33	11.90	0.78	12.38	0.77	13.64	0.14	12.74	0.25
FeO	14.13	1.88	1.52	0.19	2.79	0.35	2.16	0.40	3.82	0.12	3.59	0.20
MnO	0.23	0.06	0.04	0.01	0.08	0.07	0.13	0.04	0.12	0.02	0.08	0.04
MgO	5.42	0.96	0.07	0.06	0.05	0.04	0.16	0.04	0.20	0.02	0.42	0.04
CaO	9.87	0.98	0.71	0.04	0.37	0.14	0.55	0.12	1.30	0.12	2.32	0.11
Na ₂ O	2.70	0.56	4.11	0.29	5.12	0.44	4.09	1.03	5.40	0.27	3.55	0.17
K ₂ O	0.43	0.16	3.77	0.25	4.34	0.23	3.80	0.51	3.58	0.20	2.07	0.06
P ₂ O ₅	0.35	0.18	0.01	0.01	0.01	0.01	0.02	0.01	0.06	0.03	-	-
Cl	-	-	-	-	-	-	0.12	0.01	-	-	-	-
Total	98.39	2.09	95.62	1.04	95.64	2.12	93.95	1.59	99.77	0.68	96.67	1.47

Table 2

List of sites in the British Isles where the Borrobol (n=13), Penifiler (n=15) and CRUM1 597 tephtras have been proposed. Based on major and minor element analyses of glass shards, 13 sites are understood to contain the Borrobol Tephra, 15 sites the Penifiler Tephra and 2 sites the CRUM1 597 Tephra. A further 3 Borrobol, 4 Penifiler and 4 CRUM1 597 records are tentatively proposed based on stratigraphic superposition and are indicated by a ? symbol.

Site	Borrobol	Penifiler	CRUM1 597	Reference	Comment
The Loons	?	?	?	Callicott (2015)	A single Borrobol-type tephra was identified and chemically analysed within Windermere Interstadial sediments. It is not possible to confidently propose a correlation at present.
Quoyloo Meadow	x	x		Timms et al. (2017)	
Spretta Meadow			x	Timms (2016)	A Borrobol-type tephra has been identified at the Windermere Interstadial-Loch Lomond Stadial transition supporting the presence of the CRUM1 597 Tephra. Importantly no older sediments with earlier Windermere Interstadial tephtras are present at Spretta Meadow.
Crudale Meadow	x	x	x	Timms et al. (2018)	Site of first discovery for the CRUM1 597 Tephra
Lochan An Druim		?		Ranner et al. (2005)	A Borrobol-type tephra (S30 Tephra) was identified within Windermere Interstadial deposits and dated to 13.6 cal ka BP. It is uncertain as to which, if any, of the Borrobol-type tephtras the S30 correlates to.
Borrobol	x	x		Turney et al. (1997); Pyne-O'Donnell (2007); Lind et al. (2016)	Site of first discovery for the Borrobol Tephra
Tanera Mòr 1	x	x		Roberts (1997); Roberts et al. (1998); Timms (2016)	
Tanera Mòr 2	x	x	?	Weston (2012)	A tephra with Borrobol-type morphological properties lies at the boundary between the Windermere Interstadial and the Loch Lomond Stadial indicating a possible correlation with the CRUM1 597 Tephra.

Eilean Fada Mòr	?	?	?	Callicott, (2013)	Three peaks in glass shard concentration were identified within what is believed to be Windermere Interstadial sediments, although part of the sequence may be Dimlington in age. Shards in these peaks are typically Borrobol-type in morphology i.e. Blocky, cusped and inclusion rich. No chemical analyses have been obtained to date.
Priest Island	x	x		Valentine (2015)	
Druim Loch		x		Pyne O'Donnell (2007)	Site of first discovery for the Penifiler Tephra
Loch Ashik	x	x		Pyne O'Donnell (2007); Pyne O'Donnell et al. (2008; Brooks et al. (2012)	
Abernethy Forest	x	x		Matthews et al. (2011)	
Loch Etteridge	x		?	Albert (2007); Hardiman (2007); Lowe et al. (2008); MacLeod et al. (2015)	Glass shards positioned in the mid-Windermere Interstadial have previously been correlated to the Penifiler Tephra (Lowe et al., 2008), however, the major element chemistry of these does not support this correlation (see Supplementary Table S2). A tephra of low concentration has been noted at the Windermere Interstadial-Loch Lomond Stadial transition by Albert (2007) and Hardiman (2007). Crucially the shards comprising this tephra have been described as 'blocky' - characteristic of the Borrobol-type series.
Pulpit Hill	?	x		Lincoln (2011)	Stratigraphic evidence (a peak in glass shard concentrations) exists for the Borrobol Tephra, however, this has yet to be confirmed with chemical analyses.
Loch an t'Suidhe	x	x	?	Davies (2003); Pyne O'Donnell, (2007); Pyne O'Donnell et al. (2008)	The LAS-1 tephra was identified within Loch Lomond Stadial sediments by Davies (2003). Unfortunately, chemical analyses returned low analytical totals and a wide scatter in the data set. Whilst these analyses cannot be considered completely reliable, morphological analysis reveals some shards of a blocky and microlitic composition - characteristics of the Borrobol-type series.
Tirinie		x		Candy et al. (2016)	
Tynaspirit West	x	x		Turney et al. (1997); Pyne O'Donnell (2007); Pyne O'Donnell et al. (2008)	

Muir Park Reservoir	x	x		Roberts (1997); Cooper (1999); Lowe and Roberts (2003); Brooks et al. (2016)	
Whitrig Bog	x	x		Turney et al. (1997); Pyne O'Donnell et al. (2008)	
Traeth Mawr	?			Williams et al. (2007)	Borrobol Tephra correlated by stratigraphy.
Finglas River		?		Turney (1998b)	A single shard of a Borrobol-type composition have been identified alongside shards of the Glacier Peak and Mount St Helens J eruptions. Due to stratigraphic position it is likely this shard relates to the Penifiler Tephra, although this is not certain.

Table 3

Sites from which glass analyses have been obtained and used to claim the presence of the 'Abernethy Tephra'. In all cases except the Glen Turret Fan record, a mixed chemical assemblage has been revealed, implicating the possibility of reworking and amalgamation of older tephra deposits.

Site	n.o. of analyses obtained	% Katla-type	% Borrobol-type	% Other	Abernethy Tephra declared present	Reference
Abernethy Forest	12	83	17	0	Yes	Matthews et al. (2011)
Loch Etteridge	20	70	30	0	Yes	MacLeod et al. (2015)
Glen Turret Fan	4	100	0	0	Yes	MacLeod et al. (2015)
Kingshouse 2	8	63	0	37	Yes	Lowe et al. (in prep)
Crudale Meadow	12	42	50	8	No	Timms et al. (2018)
Tanera Mòr	35	89	11	0	No	Timms (2016)

Table 4

Summary of tephra isochrons included, and those not yet considered suitable for inclusion, within the British Isles tephrostratigraphic scheme (c. 16-8 ka BP). Also shown are reference records for each tephra; these are the sites in the British Isles which each tephra is currently best represented at. Categories i, ii and iii are explained in the text.

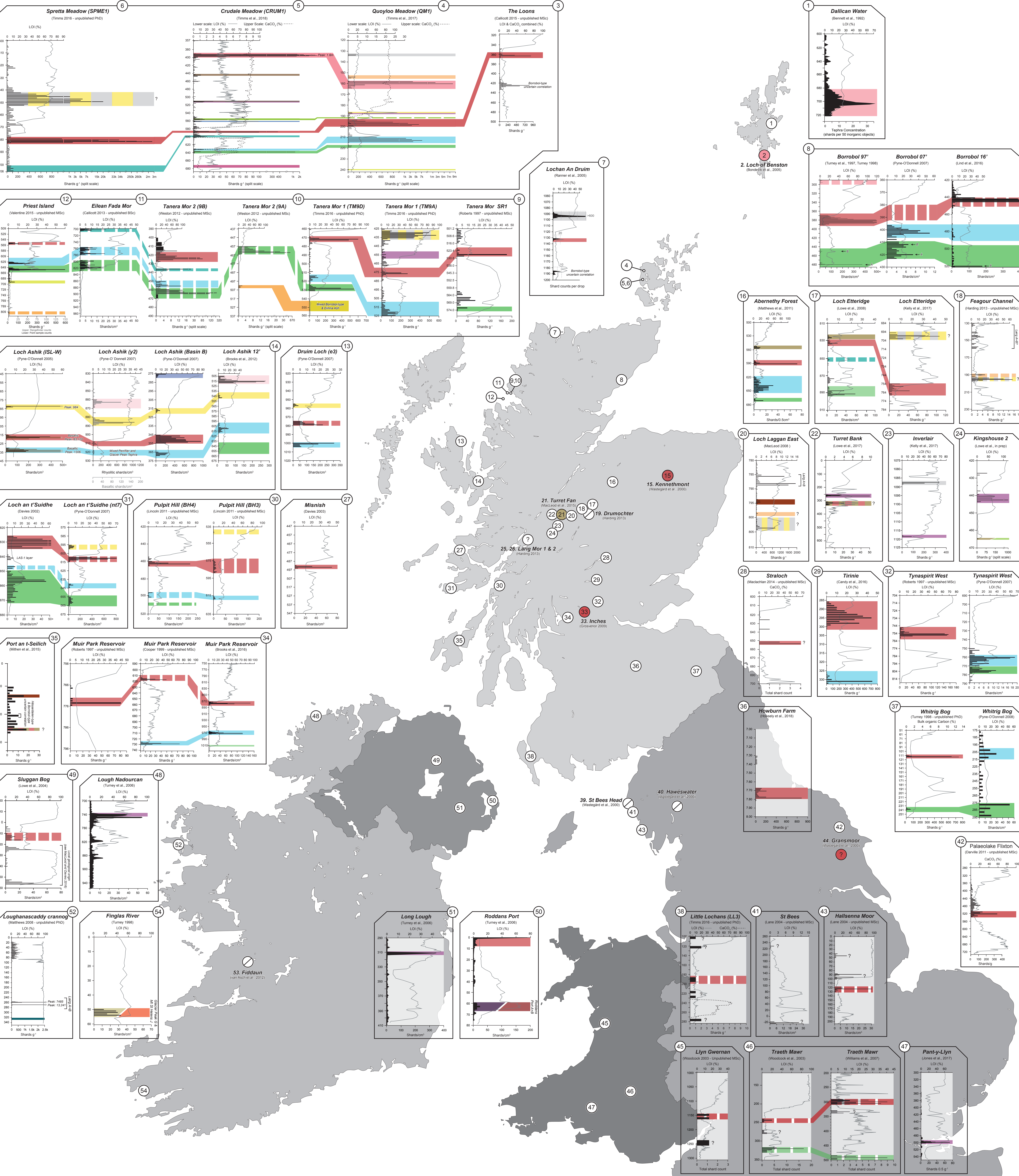
<i>Tephra included within the British Isles tephrostratigraphic framework</i>						
Tephra	Category	Age estimate	British Isles reference site	Reference source publication	Sites identified	Identified outside the British Isles?
Dimna Ash	ii	15,100 ± 300 cal. BP	Tanera Mòr 2	Weston (2012)	Tanera Mòr 1, Tanera Mòr 2, Priest Island	yes
Tanera Tephra	ii	unknown	Tanera Mòr 1	Timms (2016)	Quoyloo Meadow, Tanera Mòr 1, Priest Island	uncertain
Borrobol Tephra	i	14,098 ± 94 cal. BP	Abernethy Forest	Matthews et al. (2011)	Quoyloo Meadow, Crudale Meadow, Borrobol, Tanera Mòr 1, Tanera Mòr 2, Priest Island, Loch Ashik, Abernethy Forest, Loch Etteridge, Loch an t'Suidhe, Tynaspirit West, Muir Park Reservoir, Whitrig Bog	yes
Penifiler Tephra	ii	13,939 ± 132 cal. BP	Tirinie	Candy et al. (2016)	Quoyloo Meadow, Crudale Meadow, Borrobol, Tanera Mòr 1, Tanera Mòr 2, Priest Island, Druim Loch, Loch Ashik, Abernethy Forest, Tirinie, Pulpit Hill, Loch an t'Suidhe, Tynaspirit West, Muir Park Reservoir, Whitrig Bog	uncertain
Glacier Peak G & B	ii	13,710-13,410 cal. BP	Finglas River	this study	Finglas River, Loch Ashik	yes
Vedde Ash	i	12,023 ± 86 cal. BP	Loch Ashik	Davies et al. (2001); Pyne-O'Donnell (2011)	The Loons, Quoyloo Meadow, Crudale Meadow, Spretta Meadow, Lochan An Druim, Borrobol, Tanera Mòr 1, Tanera Mòr 2, Priest Island, Loch Ashik, Kennethmont, Abernethy Forest, Loch Etteridge, Mishnish, Tirinie, Pulpit Hill, Loch an t'Suidhe, Tynaspirit West, Inches (Lake of Menteith), Muir Park Reservoir, Howburn Farm, Whitrig Bog, Palaeolake Flixton	yes
Abernethy	ii	11,462 ± 144	Abernethy	Matthews et al.	Abernethy Forest, Loch Etteridge, Glen Turret Fan,	yes

Tephra		cal. BP	Forest	(2011)	Kingshouse 2	
Hässeldalen Tephra	i	11,316 ± 124 cal. BP	Crudale Meadow	Timms et al. (2018)	Quoyloo Meadow, Crudale Meadow, Kingshouse 2	yes
Askja-S Tephra	i	10,830 ± 114 cal. BP	Crudale Meadow	Timms et al. (2018)	Quoyloo Meadow, Crudale Meadow, Tanera Mòr 1, Loch Ashik, Glen Turret Bank, Inverlair, Kingshouse 2, Pant-y-Llyn, Lough Nadourcan, Long Lough	yes
Ashik Tephra	ii	10,716 ± 230 cal. BP	Loch Ashik	Pyne-O'Donnell (2007)	Quoyloo Meadow, Druim Loch, Loch Ashik	no
Saksunarvat n 10-ka series (Havn-3/4)	ii	~10.37 and ~10.3 ka BP	Loch Ashik	Pyne-O'Donnell (2007)	Loch Ashik	yes
Saksunarvat n 10-ka series (Saksunarvat n Ash <i>sensu stricto</i>)	ii	10,210 ± 35 cal. BP	Crudale Meadow	Timms et al. (2018)	Dallican Water, Loch of Benston, Quoyloo Meadow, Crudale Meadow	yes
Fosen Tephra	i	10,139 ± 116 cal. BP	Quoyloo Meadow	Timms et al. (2017)	Quoyloo Meadow	yes
An Druim Tephra	i	9648 ± 158 cal. BP	Lochan An Druim	Ranner et al. (2005)	Quoyloo Meadow, Lochan An Druim, Inverlair	yes
Suduroy Tephra	ii	8073 ± 192 cal. BP	Loch Laggan East	MacLeod (2008)	Loch Laggan East, Rubha Port an t-Seilich	yes
<i>Tephras not yet included within the British Isles tephrostratigraphic framework</i>						
CRUM1 676	iii	unknown	Crudale Meadow	Timms et al. (2018)	Crudale Meadow	no
Mount St Helens J	iii	13.860-12.800 cal. BP	Finglas River	Turney (1998b); this study	Finglas River	yes
Roddans Port A	iii	unknown	Roddans Port	Turney et al. (2006)	Roddans Port	no
Roddans Port B	iii	unknown	Roddans Port	Turney et al. (2006)	Roddans Port	no
CRUM1 597	iii	12,457 ± 896 cal. BP	Crudale Meadow	Timms et al. (2018)	Crudale Meadow, Spretta Meadow	no
Crudale	iii	c. 12,111-	Crudale	Timms et al.	Crudale Meadow, Tynaspirit West	uncertain

Tephra		11,174 cal. BP	Meadow	(2018)		
CRUM1 510 Tephra	iii	10,837 ± 148 cal. BP	Crudale Meadow	Timms et al. (2018)	Crudale Meadow	no
Hovsdalur Tephra	iii	10,475 ± 350 cal. BP	Quoyloo Meadow	Timms et al. (2017)	Quoyloo Meadow	yes
Saksunarvatn 10-ka series (CRUM1 444)	iii	10,476 ± 254 cal. BP	Crudale Meadow	Timms et al. (2018)	Crudale Meadow	uncertain
Breakish Tephra	iii	unknown	Loch Ashik	Pyne-O'Donnell (2007)	Loch Ashik	no
LAN1-325	iii	8245-8041 cal. BP	Loughanascadd y crannog	Matthews (2008)	Loughanascaddy crannog	uncertain
Breakish Tephra	iii	unknown	Loch Ashik	Pyne-O'Donnell (2007)	Loch Ashik	no

Summary of LGIT tephrostratigraphic sites in the British Isles.

Supplementary Figure S1
Summary of LGIT tephrostratigraphic sites in the British Isles. Each site, where possible, is represented by a tephra concentration diagram and loss-on-ignition (LOI) or calcium carbonate (CaCO₃) signal. Where multiple investigations have been conducted at a site, those profiles which best represent the tephrostratigraphic results have been selected. A solid coloured bar denotes a correlation made using glass-based analyses, a dashed coloured bar signals a correlation made on the premise of stratigraphic superposition. A band featuring two alternating represents an uncertain correlation between two tephra with glass components of indistinguishable major and minor element chemistry. A ? symbol indicates a degree of uncertainty with the correlation. A list of references is provided in Supplementary Table S1. Glass compositional data used to make these correlations can be accessed from Supplementary Table S2. This figure is best viewed in its original A0 format.



- | | | | |
|--|---|---|--|
| Breakish Tephra (unknown age) | Havn-3/ Havn-4 (10.3-10.4 ka/ 10.35-10.45 ka) | Håsseldalen Tephra (11,316 ± 124 cal. BP) | Roddars Port B (unknown age) |
| Suduroy Tephra (8073 ± 192cal. BP) | CRUM1 444 (10,476 ± 254 cal. BP) | Crudale Tephra (12,111-11,174 cal. BP) | Glacier Peak (G & B) (13,710-13,410 cal. BP) |
| LAN1-325 Tephra (8434 ± 96 cal. BP) | Hovsdalur Tephra (10,475 ± 350 cal. BP) | Abernethy Tephra (11,462 ± 144 cal. BP) | Mount St Helens J (13,800-12,800 cal. BP) |
| An Druim Tephra (9648 ± 158 cal. BP) | Ashik Tephra (10,716 ± 230 cal. BP) | Vedde Ash (12,023 ± 86 cal. BP) | Penifiler Tephra (13,939 ± 132 cal. BP) |
| Fosen Tephra (10,139 ± 116 cal. BP) | CRUM1 510 Tephra (10,837 ± 148 cal. BP) | CRUM1 597 Tephra (12,457 ± 896 cal. BP) | Borrobol Tephra (14,098 ± 94 cal. BP) |
| Saksunarvatn Ash (10,210 ± 70 cal. BP) | Askja-S Tephra (10,824 ± 97 cal. BP) | Roddars Port A (unknown age) | Tanera Tephra (unknown age) |
| | | | Dimna Ash (15,100 ± 300 cal. BP) |
| | | | CRUM1 676 (unknown age) |

- | | | | |
|---|---|---|--|
| Tephra horizon correlated by chemical signature | Tephra horizon correlated by stratigraphic super-position | Uncertain correlation between two chemically identical tephra | Uncertain correlation between two chemically identical tephra (inferred by stratigraphy) |
| Tephra looked for, identified and chemically analysed | Tephra looked for and not identified | Tephra looked for, identified, but not chemically analysed | Uncertain correlation |